MODELING & DESIGN OF PANEL ANCHOR IN PRECAST CONCRETE CONSTRUCTION

BY

ISLAM SAYED ABOUHAMDAH

A Thesis Presented to the

DEANSHIP OF GRADUATE STUDIES

KING FAHD UNIVERSITY OF PETROLEUM & MINERALS

DHAHRAN, SAUDI ARABIA

In Partial Fulfillment of the

Requirements for the Degree of

MASTER OF SCIENCE

In

CIVIL ENGINEERING

November-2015

KING FAHD UNIVERSITY OF PETROLEUM & MINERALS

DHAHRAN- 31261, SAUDI ARABIA

DEANSHIP OF GRADUATE STUDIES

This thesis, written by **Islam Sayed AbouHamdah** under the direction of his thesis advisor and approved by his thesis committee, has been presented and accepted by the Dean of Graduate Studies, in partial fulfillment of the requirements for the degree of **MASTER OF SCIENCE IN CIVIL ENGINEERING.**

Dr. Mohammed Baluch
(Advisor)

Dr. Salah U. Al-Dulaijan
Department Chairman

Dr. Muhammad K. Rahman
(Member)

Dr. Salam A. Zummo
Dean of Graduate Studies

Dr. Mohammed A. Al-Osta
(Member)

13/12/15
Date

©Islam Sayed AbouHamdah

2015

DEDICATED TO

My BELOVED PARENTS

AND

MY BROTHER AND SISTER

ACKNOWLEDGMENTS

All praise and thanks are due to my Lord, ALLAH SUBHAN WA TAALA, for giving me the health, knowledge and patience to complete this work.

My sincerest gratitude goes to my advisor Dr. M.H.Baluch, who guided me with his dedicated attention, expertise and knowledge throughout this research, and had to come all the way on his personal expenses to examine my thesis work, also I would like to thank my committee members Dr. Muhammad K. Rahman, & special thanks to Dr.Mohammed A. Al-Osta who made a lot of effort and helped throughout this thesis work. Thanks are also due to the Civil Engineering department's Chairman and his secretary for providing aid, and to other faculty members and staff.

I also acknowledge the sincere and untiring efforts of Eng. David Yebes who had the hand of opening my mind to understand structures, also a lot of thanks to PRAINSA SAUDI ARABIA and Eng. Miguel Amadeu for their support. I would like to offer my acknowledgement to Mr.John from PRAINSA Production department for his assistance in the preparation of the samples.

Special thanks are due to my colleagues in the Civil Engineering Department, for their aid and support. Thanks are also due to all my friends for their support and encouragement.

My heartfelt gratitude is given to my beloved father, mother, who always supports me with their love, patience, encouragement and constant prayers. I would like to thank my mother and father for their emotional and moral support throughout my study.

TABLE OF CONTENTS

List of Tables

List of Figures

ABSTRACT

Full Name : Islam Sayed AbouHamdah

Thesis Title : MODELING & DESIGN OF PANEL ANCHOR IN PRECAST CONCRETE CONSTRUCTION

Major Field : Structural Engineering

Date of Degree : November 2015

The Cast-in C-channel is a small anchoring steel piece used to post-connect different type of elements in precast concrete members. The advantages of implementing the cast-in C-channel is its simplicity to attach to the connecting elements which gives more tolerance between the connected members , in addition to that; its use leads to safe and economical design. Other means of connecting to precast concrete members is by using either post-installed anchoring systems or by fixed steel embedment, which consequently needs drilling inside concrete and sometimes difficult to be performed due to the presence of steel reinforcement inside the concrete members. The proposed system is composed of a C-shaped channel that can be either cold-formed or hot-rolled, and a hammer shaped head bolts with nuts and washers to hold the connected piece. The C-channel is pre-installed in concrete before casting and its anchorage with concrete is done by various ways, such as welding or by using riveting studs connected to the channel, or by inserting a small piece of steel at the back of the channel. The objective of this study is to experimentally investigate the ultimate capacity of cast-in C-channel under uni-axial tension and compare its ultimate load capacity and failure mode with 3-D finite element modeling using plastic-damage constitutive model for concrete. The results of the finite element modeling are conducted using ABAQUS. The study has been motivated by the

need to assess the performance and damage propagation in connections in precast structures, an area that has not been addressed at any great length. This preliminary assessment relates to monotonic loading of the connection, with an anticipation to extend the study to cyclic loading of such connections that would result from seismic loading of the precast structure.

ملخص الرسالة

الاسم الكامل: إسلام سيد أبوحمده

عنوان الرسالة: نمذجة و تصميم الوصلة الانشائية الفولاذية ذات الشكل C المستخدمة لربط الواجهات الخرسانية المسبقة الصنع بالهيكل الإنشائي للمباني.

التخصص: الهندسة المدنية القسم الإنشائي

تاريخ الدرجة العلمية: تشرين الثاني 2015 م

وصلة ال C الفولاذية يتم وضعها قبل صب العنصر الخرساني , من مميزات الوصلة انها تسمح بربط الواجهات الخرسناية مسبقة الصنع بالهيكل الانشائي للمبنى باريحيه و سهولة اضافة الى انها اقتصادية و غير مكلفة و قوتها تضيف آمان و سلامة للعنصر الإنشائي.

هناك وسائل اخرى لربط العناصر الانشائية المسبقة الصنع و ذلك باستخدام مسامير تركب بعد صب العنصر الخرساني و ذلك عن طريق الثقب و هذه الطريقة ليست بفعالية وصلة ال C و ذلك لصعوبة ثقب العنصر الخرساني بسبب وجود حديد التسليح مما يؤدي لزيادة في وقت التركيب , احد الطرق الاخرى المتبعة هي بوضع صفيحة فولاذية في الخرسانة قبل الصب و عمل لحام بين الوصلة الرابطة و القطعة اثناء التركيب بالموقع و تلك الطريقة ايضا تؤدي الى تاخر في عملية التركيب مما يؤثر على ميزانية المشروع.

تتكون الوصلة من قطعة فولاذية على شكل حرف ال Cهذه القطعة يتم تشكيلها من صفائح فولاذية أو يتم تصنيعها , الوصلة يتم تثبيتها في الخرسانة بعدة وسائل اما بوصلها مع حديد تسليح و عمل لحام بينهما او باستخدام مسامير غير مسننه قصيرة يتم لحمها او ربطها بوسائل مختلفة , و اخيرا يتم وضع مسمار ذو رأس على شكل المطرقة داخل الوصلة.

الهدف من هذا البحث هو ايجاد قوة تحمل الوصلة لقوى الشد و ذلك بعمل اختبارات لعينات مختلفة و مقارنتها مع عمل محاكاة للوصلة باستخدام برنامج ABAQUS و مقارنتها ايضا بتطوير معادلات رياضية لحساب قوة تحمل

الوصلة , و لقد تم اختيار هذا الموضوع لقلة الأبحاث في مجال الخرسانة مسبقة الصنع و سيتم استكمال مثل هذا البحث ليشمل قوة تحمل الوصلة للأحمال الدورية و أحمال الزلازل التي قد يتعرض لها المنشأ المسبق الصنع.

CHAPTER 1

INTRODUCTION

1.1 History and Uses

The Cast-in C-channels (Figure 1-1) is a small anchoring steel piece used to post-connect different type of elements to concrete members, The advantages of implementing the cast-in C-channel its simplicity to attach to the connecting elements which gives more tolerance between the connected members , in addition to that; its use lead to safe and economical design. Other means of connecting to precast concrete members is either by using post-installed anchoring systems or by fixed steel embedment. The former method needs drilling inside concrete which is sometimes difficult to be performed due to the presence of steel reinforcement inside the concrete members, whereas the second method is do not give enough tolerance in construction. (Figure 1-1) shows different types of the cast-in C-channel with Hummer Head Bolt, and Hummer Bolt installation.

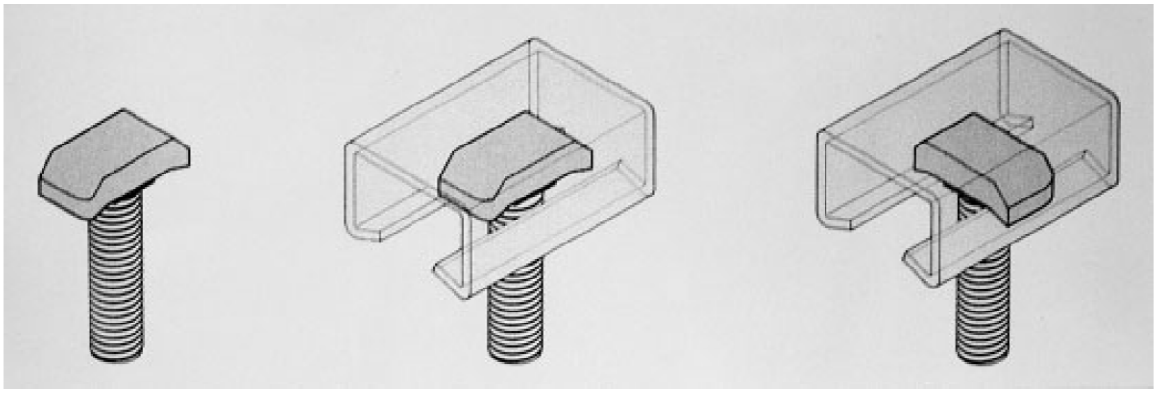

Figure 1-1: Cast in Channel with Hummer Head Bolt.

Cast-in channels was developed by Andreh Jordahl in 1913, a Norwegian civil engineer, a milestone in the history of connection systems and one of the best world's first ever anchor channels [1]. (Figure 1-2) shows a schematic of the first C-channel developed by Jordahl.

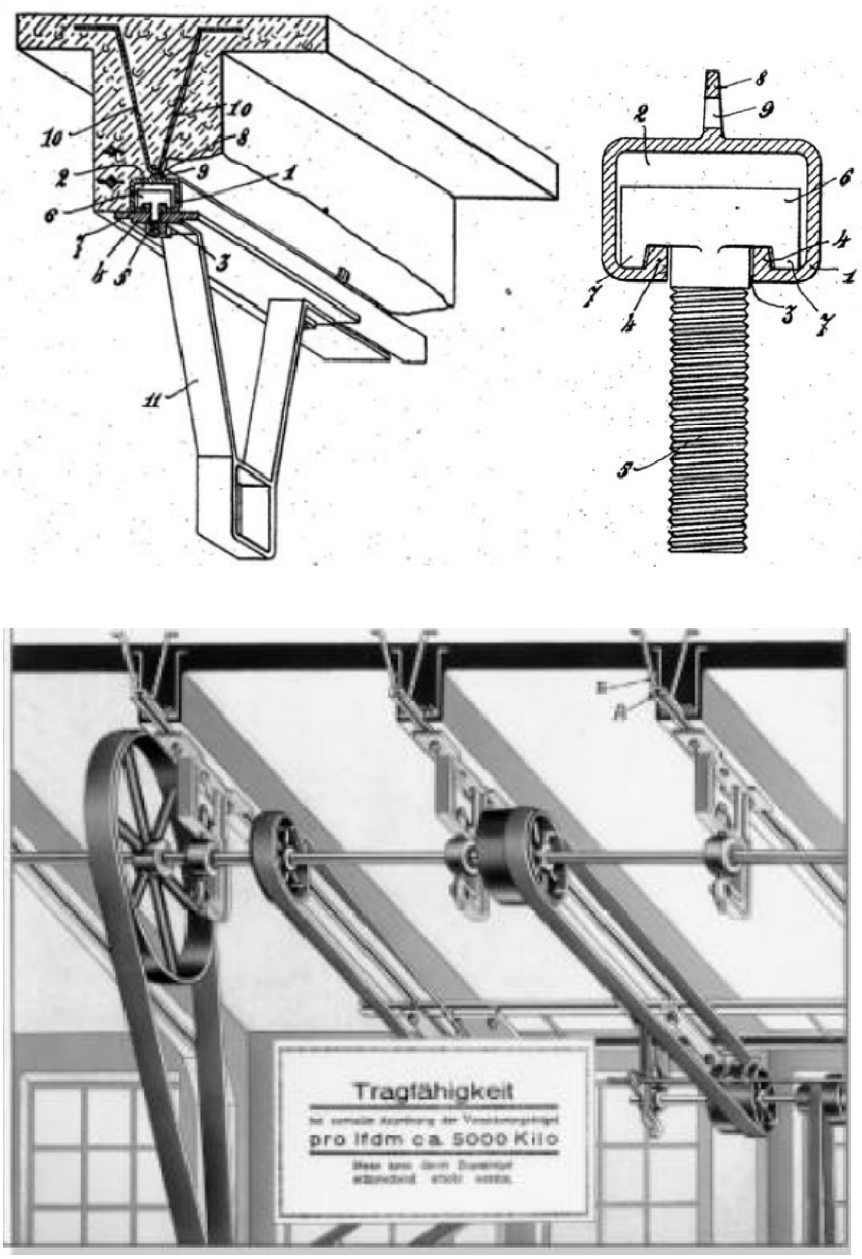

Figure 1-2: Sketch of the first c-channel by Jordahl [1].

The system is composed of a C-shaped channel that can be either cold-formed or hot-rolled, and a hummer shaped head bolts as shown in (Figure 1-3), with nuts and washers to hold the connected piece. The C-channel is preinstalled in concrete before casting and there are various ways of anchoring the channel to concrete, such as welding or by using riveting studs connected to the channel as shown in (Figure 1-4), inserting a small piece of steel at the back of the channel, or any other ways of anchoring to concrete (Figure 1-5), welding lifting hook type anchorage (Figure 1-6), and welding normal (straight, L-shape, J-shape, or studded) reinforcement bars to the channel as seen in (Figure 1-7)

Figure 1-3: Hummer Head Bolt.

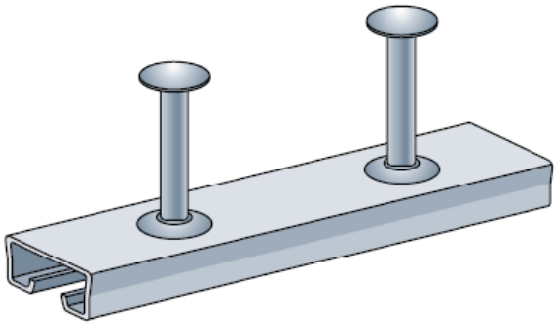

Figure 1-4: C-Channel with stud anchors.

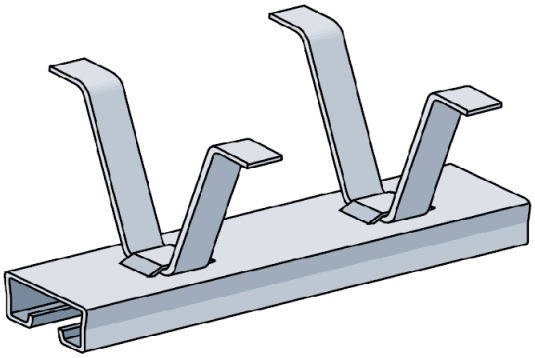

Figure 1-5: Anchorage using thin steel plates.

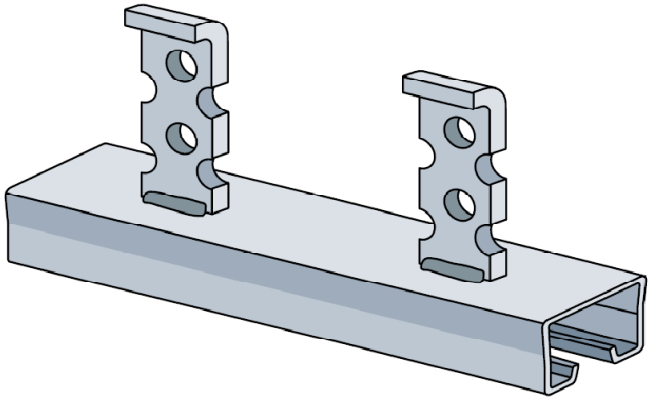

Figure 1-6: Hook type anchorage similar to that used in lifting precast elements.

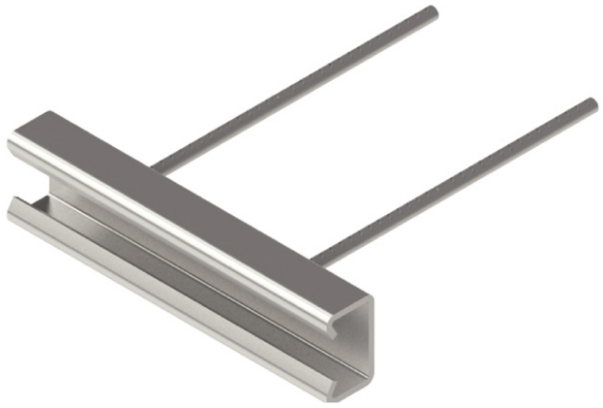

Figure 1-7: C-Channel anchored using normal reinforcement Bars.

1.2 Significance of Research

The cast-in channel have a wider use nowadays, and it is used a lot in precast construction like in fixing precast cladding panels to a the building main structure system (Figure 1-8) and (Figure 1-9), and to install electrical and mechanical utilities to the concrete member as shown in (Figure 1-10). There is no enough study available on finding the capacity of the cast-in channels, one of the available studies is about the anchorage failure but is not for the channel itself. The reason of such lack of study is due to manufacturers obsessive. Every manufacturer has his built in-house channel shape and design procedure. As a precast designer, this leads to face many questions about what is

the real capacity of such channels, and what is the procedure of calculating the ultimate capacity of such channels, without the need of relying on the manufacturer.

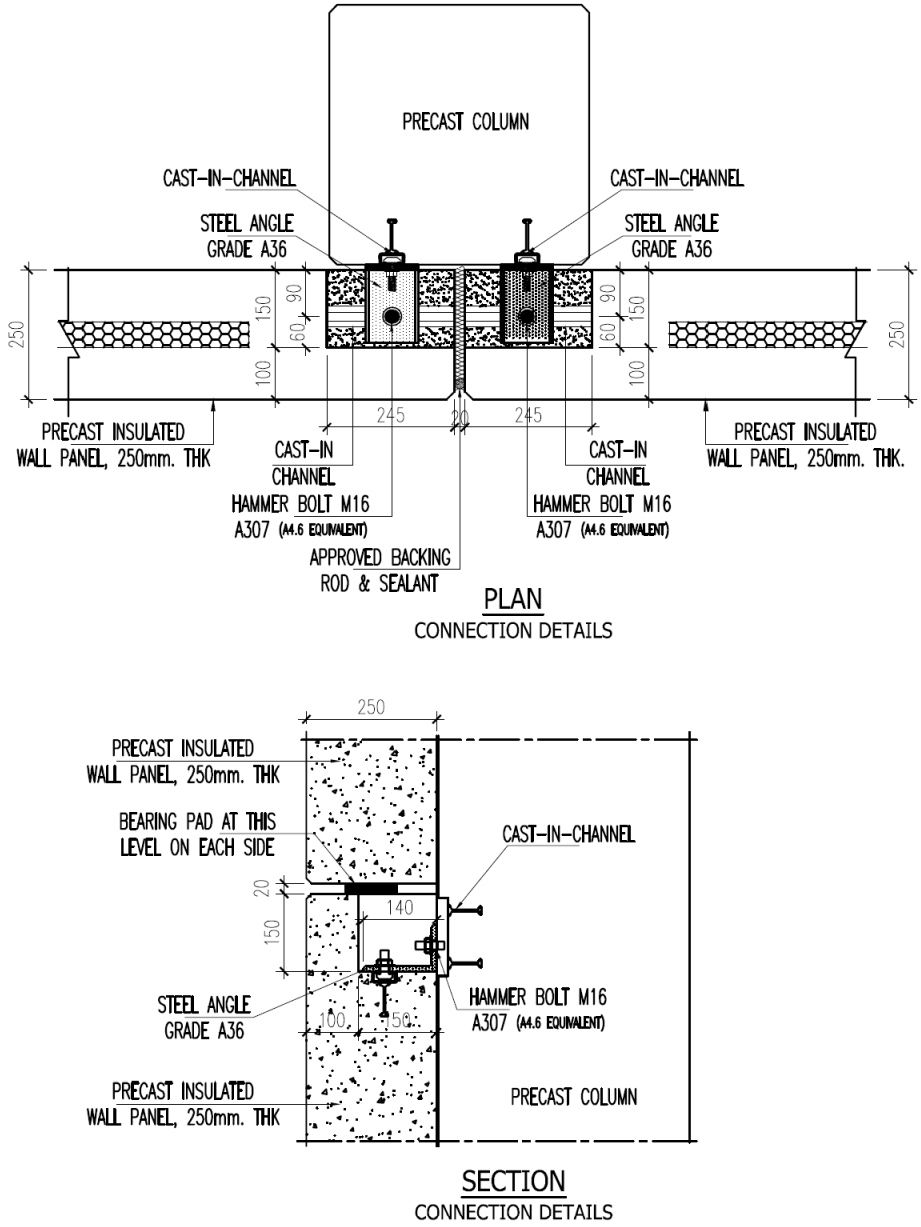

Figure 1-8: Cast in Channel use in precast cladding fixation.

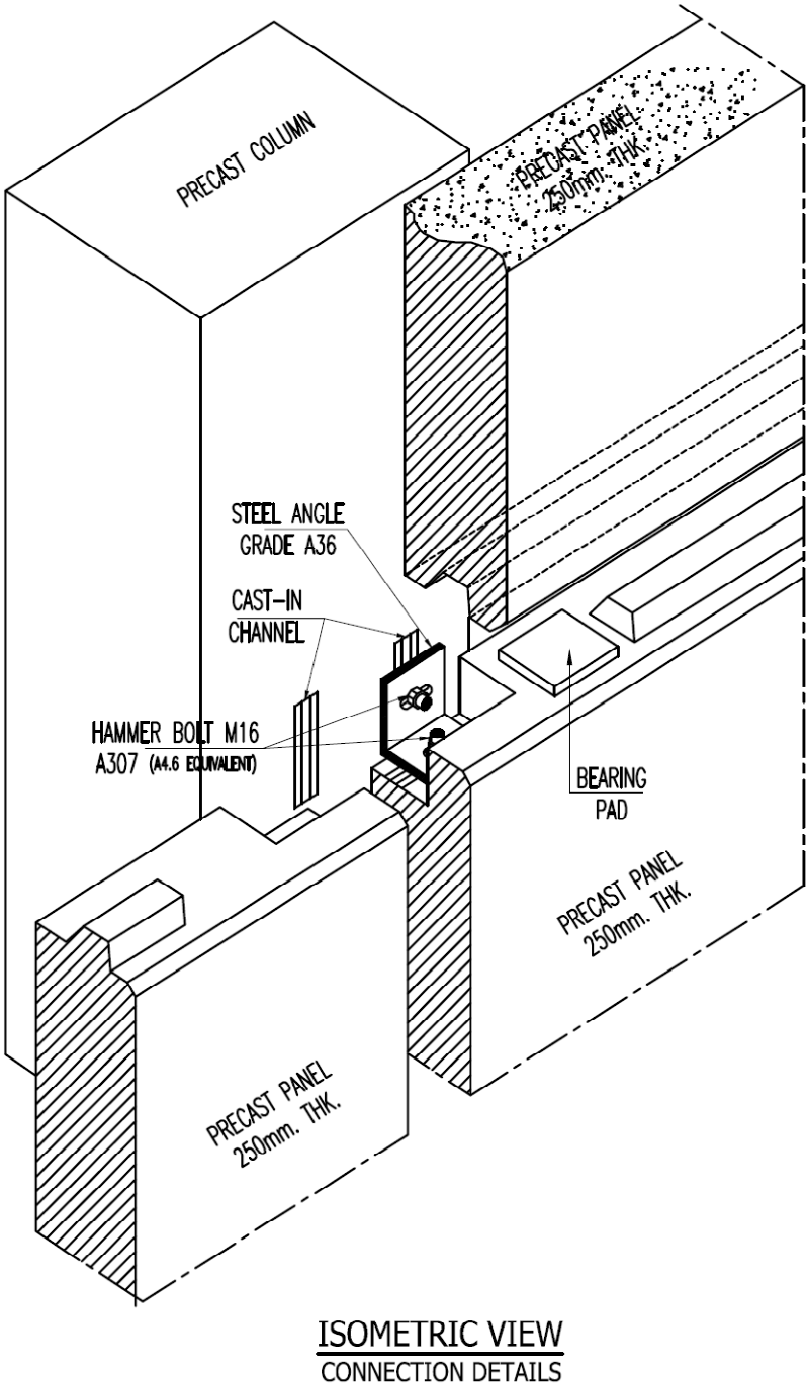

Figure 1-9: Isometric View of precast cladding fixation.

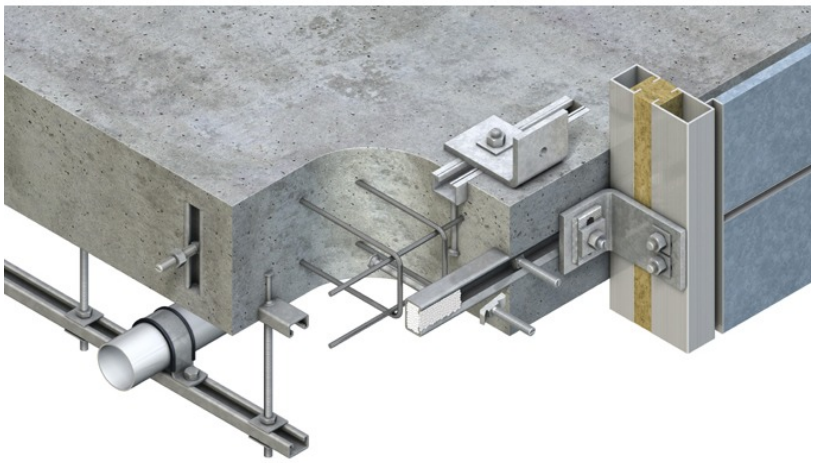

Figure 1-10: Different uses of the cast in c-channel

CHAPTER 2

LITERATURE REVIEW

2.1 Failure Modes

The cast-in channel is usually subjected to two types of loads, tension and shear as shown in (Figure 2-1). From observation of the cast-in channels, and as mentioned above, two main failure modes are assumed to happen, one mode is related to normal anchorage failure in concrete and the other is a local failures in the channel itself, a third failure that might be is in bolt itself. The failures were categorized in two main categorizes, steel related and concrete related failure modes.

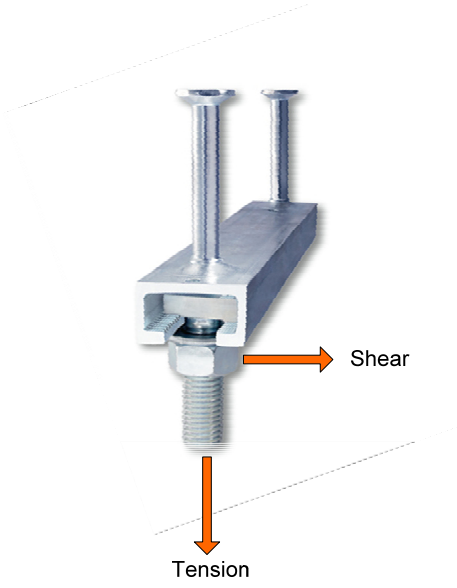

Figure 2-1: Type of forces acting on the cast in channel.

2.2 Steel Related Failure Mode

2.2.1 Tension

Due to a tension force applied on bolt; three failure modes are likely to happen channel section failure (Figure 2-3), bolts failure (Figure 2-4), and embedded anchor stud steel failure (Figure 2-5). Figure 2-2; show load vs. displacement relation of headed studs and how brittle the failure is if concrete failure mode governs compared to steel type of failure.

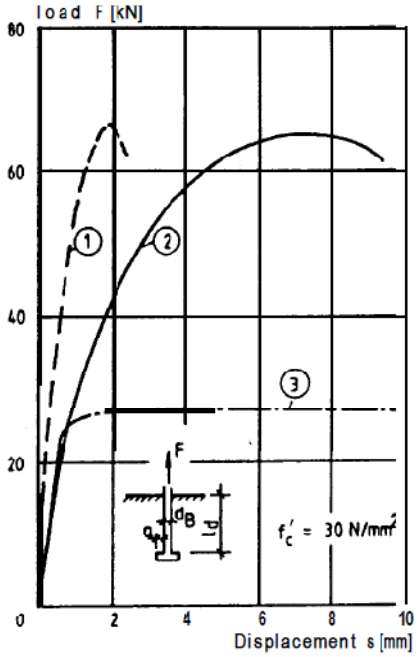

line	anchor type	d [mm]	d_h [mm]	a [mm]	ld [mm]	failure
①	headed	19	32	6,5	80	concrete
②	undercut	12	18	3,0	80	concrete
③	headed	9.5	19	4,8	68	steel

Figure 2-2: Typical Load-Displacement Relationship of headed and undercut anchor bolts [2].

2.2.1.1 Channel Section Flexure Failure

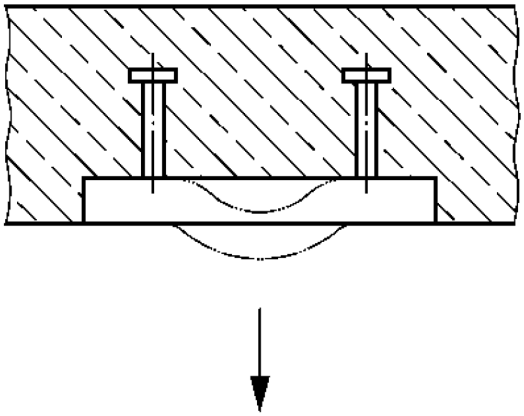

Figure 2-3: Local Flexure Failure of Channel. [3]

Such a failure can happen assuming the channel is simply supported and the anchor studs act like a hinged support, while neglecting the concrete resistance in tension under the channel.

2.2.1.2 Bolts and Embedded Stud Tension Failure

This is a common failure in tension for all kind of bolts, the nominal strength of an anchor in tension is governed by the steel, N_{sa}, shall be evaluated by calculations based on the properties of the anchor material. The nominal strength of a single or group of anchors in tension shall not exceed [4]:

$$N_{sa} = n\, A_{se,N}\, f_{uta} \qquad (2.1)$$

n: number of anchors in group.

$A_{se,N}$: effective cross sectional area of the threaded part.

f_{uta}: ultimate tensile strength.

The ultimate tension failure" f_{uta}" is used instead of the yield failure "f_{ya}" because the large majority of anchor materials do not exhibit a well-defined yield point [5].

Figure 2-4: Hummer head bolt tension failure.

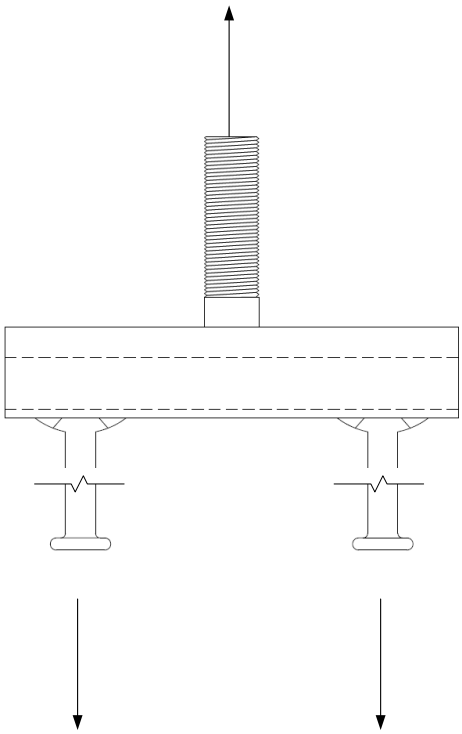

Figure 2-5: Embedded stud tension failure.

2.2.2 Shear

Shear failure will happen on the cast in channel system on the bolt (Figure 2-6).

2.2.2.1 Bolts Shear Failure

This is a common failure in tension for all kind of bolts, the nominal strength of an anchor in shear is governed by the steel, V_{sa}, shall be evaluated by calculations based on the properties of the anchor material and the physical dimensions of the anchor. The nominal strength of a single or group of anchors in shear shall not exceed [4]:

$$V_{sa} = n\ 0.6 A_{se,V}\ f_{uta} \qquad (2.2)$$

n: number of anchors in group.

$A_{se,N}$: effective cross sectional area of the threaded part.

f_{uta}: ultimate tensile strength.

The ultimate shear failure" f_{uta}" is used instead of the yield failure "f_{ya}" because the large majority of anchor materials do not exhibit a well defined yield point [5].

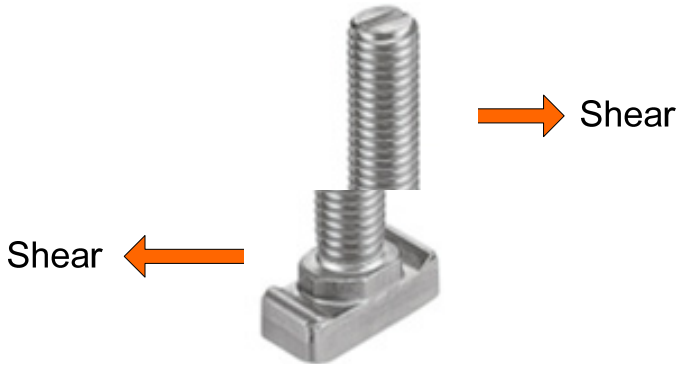

Figure 2-6: Hummer bolt shear failure.

2.3 Concrete Related Failure Mode

Such failure will have an effect on the concrete confining the channel, and can be addressed under to main load category, tension, & shear.

2.3.1 Tension

In case of studded head anchor, such failure will have a similar criteria as those mentioned in the literature [4].

2.3.1.1 Breakout (CONE) Failure

The concrete cone breakout failure mode is characterized by the formation of a cone-shaped fracture surface in the concrete (Figure 2-7)[6], the full tensile capacity of concrete is utilized and this failure is similar in shape to the punching shear failure. Cone failure have many factors affecting the capacity of the anchor bolts, such as concrete compressive strength, concrete condition (cracked or un-cracked), edge distance, anchor embedded length in concrete (h_{ef}) and spacing between the bolts[7].

The slope of the fracture surface is not constant as measured over the depth or the circumference and it varies from test to test. The slope as measured from the horizontal and

averaged over the circumference lies between 30° and 40°, and is on average about 35° (Figure 2-8)[6]. ACI recommend the use of angle of 35^{o}. [4]

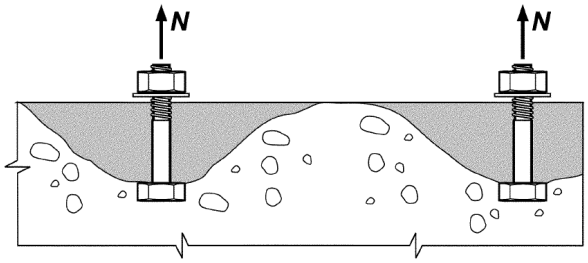

Figure 2-7: Breakout Failure. [4]

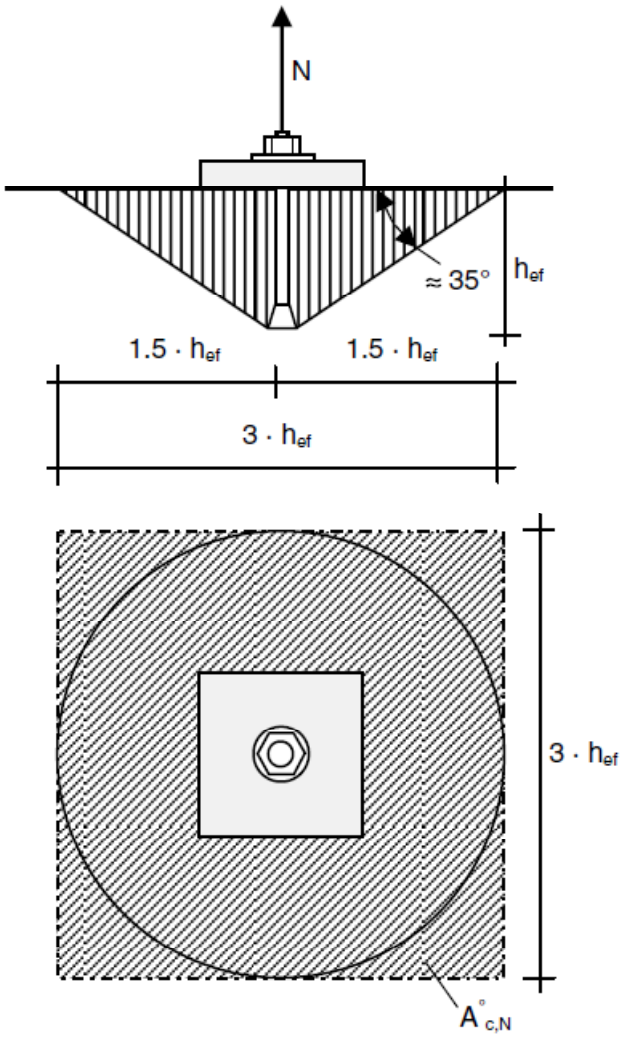

Figure 2-8: Concrete Breakout (Schematically). [7]

The nominal concrete breakout strength [4]:

For a single anchor:

$$N_{cb} = \frac{A_{Nc}}{A_{Nco}} \psi_{ed,N} \psi_{c,N} \psi_{cp,N} N_b \quad (2.3)$$

For a group of anchor :

$$N_{cbg} = \frac{A_{Nc}}{A_{Nco}} \psi_{ec,N} \psi_{ed,N} \psi_{c,N} \psi_{cp,N} N_b \quad (2.4)$$

A_{Nc} : projected concrete failure area of a single anchor or group of anchors (Figure 2-9).

A_{Nco} : projected concrete failure area of a single anchor with an edge distance $\geq 1.5\ h_{ef}$.

$\psi_{ec,N}$: modification factor for anchor groups loaded eccentrically in tension.

$\psi_{ed,N}$: modification factor for edge effects.

$\psi_{c,N}$: modification factor to account for cracked or un-cracked concrete.

$\psi_{cp,N}$: factor to consider and control splitting in concrete.

N_b : basic concrete breakout strength.

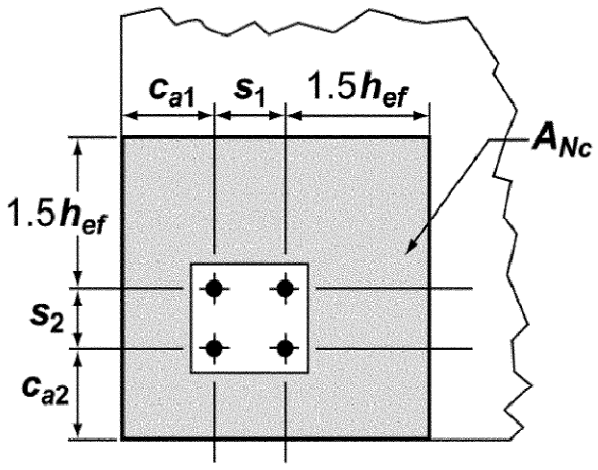

Figure 2-9: A_{Nc} definition. [4]

2.3.1.2 Pullout

This failure is more critical in post-installed anchor bolts due to the small bearing area between the head of the bolt and the concrete (Figure 2-10).

At the first peak the static friction is exceeded, whereupon the resistance drops and subsequent behavior is governed by sliding friction.[7]

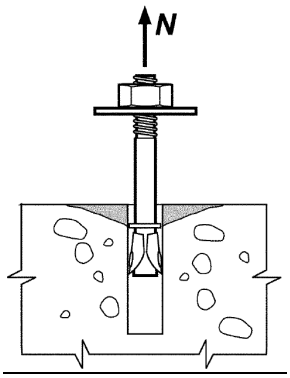

Figure 2-10: Pullout failure. [4]

The pullout strength of a single anchor in tension:

$$N_{pn} = \psi_{c,P} N_p \qquad (2.5)$$

$\psi_{c,P}$: modification factor to account for cracked or un-cracked concrete.

$N_p = 8\ A_{brg} f_c'$

A_{brg} : net bearing area of the head of stud.

f_c' : 28 days concrete (cylinder) strength.

2.3.1.3 Side Blowout

Side blow-out failure will govern the concrete capacity of studs having small edge distance (concrete cover) in combination with large embedment depth. Local concrete side blow-out failure is caused by the quasi-hydrostatic pressure in the region of the head of the stud which gives rise to a lateral bursting force F_b equal to α times the applied tension load N (Figure 2-12). [6]

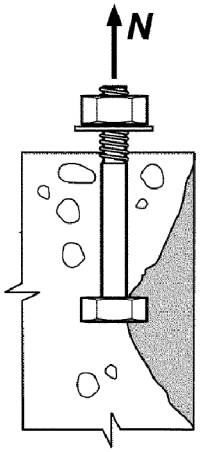

Figure 2-11: Side blow out failure [4].

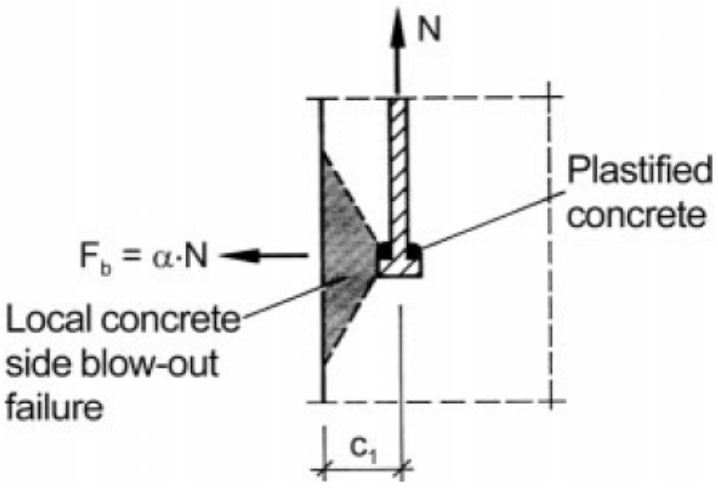

Figure 2-12: Side blowout burst force. [6]

Side blowout capacity: [4]

For single anchors:

$N_{sb} = (13\ c_{a1}\ \sqrt{A_{brg}}\ )\ \lambda \sqrt{f_c'}$ (2.6)

For group of anchors:

$N_{sbg} = (1 + \frac{s}{6\ c_{a1}})\ N_{sb}$ (2.7)

c_{a1} : (Figure 2-9)

s : outer distance between anchors along the edge (Figure 2-13).

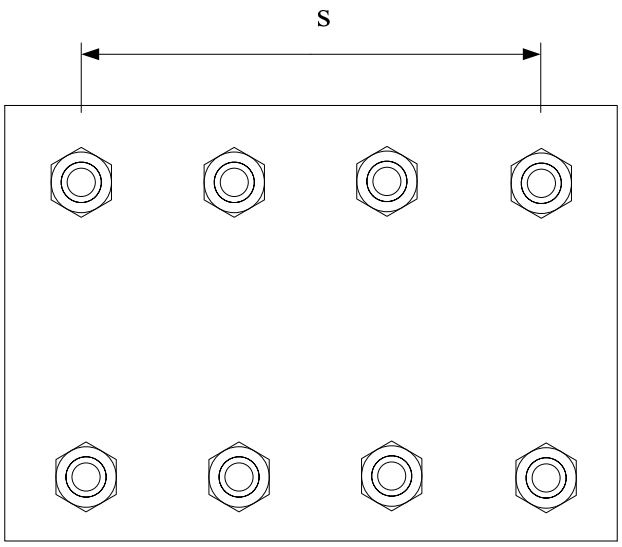

Figure 2-13: "s" definition.

2.3.2 Shear

In case of studded head anchor, such failure will have a similar criteria as those mentioned in the literature [4], such as edge breakout, and pryout.

2.3.2.1 Breakout

According to Wohlfahrt (1996) [8], the shear load is initially transferred into the concrete via the channel and the anchors. Owing to the edge distance from the front face of the channel closer to the edge, which is smaller than the edge distance of the anchor, a local

concrete failure starting at the front edge of the channel frequently occurs before the ultimate load is reached. Thereafter, the entire load is transferred to the concrete via the anchors.

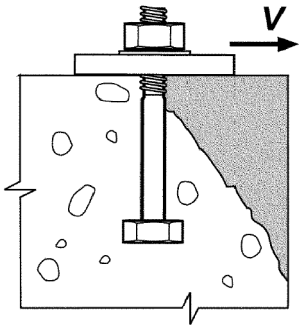

Figure 2-14: Shear edge breakout failure [4].

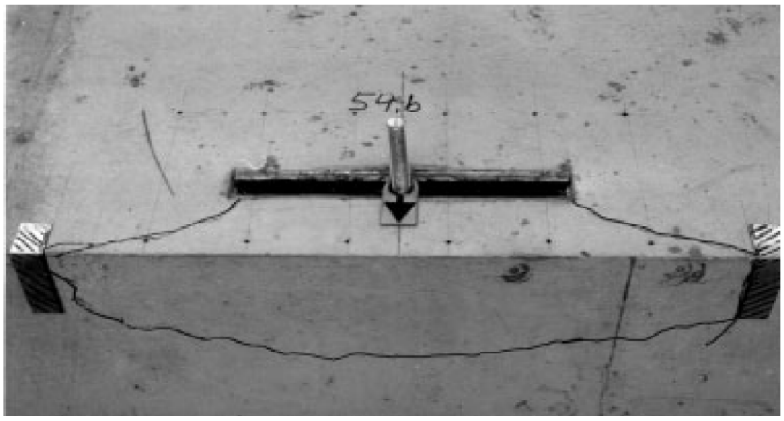

Figure 2-15: Photo of anchor channel after test, concrete edge failure. Shear load applied between anchors. [8]

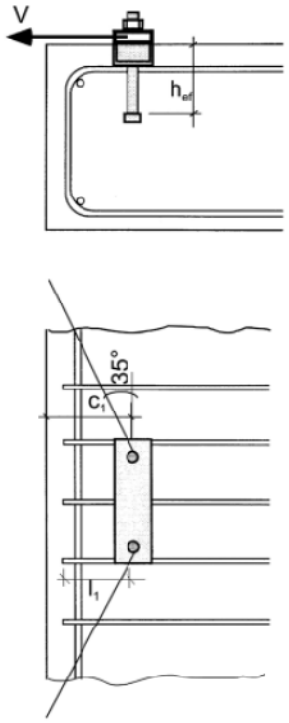

Figure 2-16: Breakout failure in cast in channel close to the edge. [7]

The nominal concrete breakout strength [4]:

For a single anchor:

$$V_{cb} = \frac{A_{Vc}}{A_{Vco}} \psi_{ed,V} \psi_{c,V} \psi_{h,V} V_b \quad (2.8)$$

For a group of anchor :

$$V_{cbg} = \frac{A_{Vc}}{A_{Vco}} \psi_{ec,V} \psi_{ed,V} \psi_{c,V} \psi_{h,V} V_b \quad (2.9)$$

A_{Vc} : projected concrete failure area of a single anchor or group of anchors at the edge side (Figure 2-17).

A_{Vco} : projected concrete failure area of a single anchor with an edge distance $\geq 1.5\ h_{ef}$ in the direction perpendicular to the shear force.

$\psi_{ec,V}$: modification factor for anchor groups loaded eccentrically in shear.

$\psi_{ed,V}$: modification factor for edge effects.

$\psi_{c,V}$: modification factor to account for cracked or un-cracked concrete.

$\psi_{h,V}$: factor to consider for anchors located in members where $h_a < 1.5\ c_{a1}$ (Figure 2-18).

V_b : basic concrete breakout strength in shear.

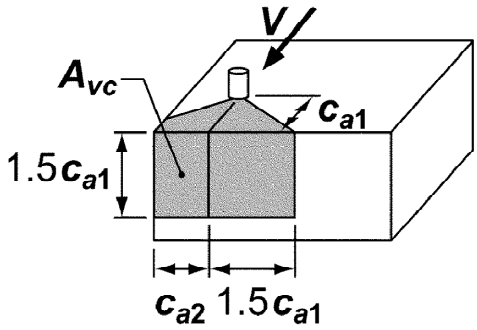

Figure 2-17: A_{VC} definition. [4]

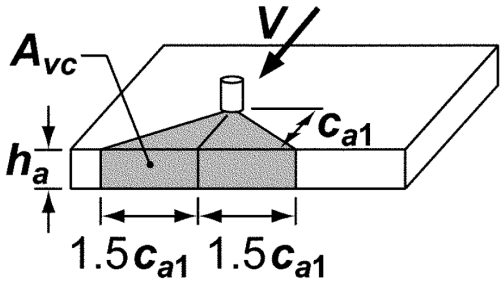

Figure 2-18: h_a and A_{vc} definition. [4]

2.3.2.2 Pryout

The pryout mechanism for cast-in anchors usually occurs with very short, stocky studs welded to a steel plate or beam flange. The studs are typically so short and stiff that under a direct shear load, they bend primarily in single curvature. The ensuing deformation results in the "heel" of the stud head "kicking back," which breaks out a crater of concrete behind the stud, as illustrated in (Figure 2-20). Internal bearing pressures develop in the concrete near the concrete surface at the stud weld and at the stud head due

to rotational restraint. This failure mechanism occurs away from all edge effects, when the anchorage is located “in-the-field” of the member. The behavior is somewhat analogous to a laterally loaded pile in earth. A longer and less stiff stud behaves differently. The longer and deeper embedded stud bends in double curvature and the deeply embedded head portion of the stud remains essentially stationary or fixed in the concrete. At the junction of the headed stud and plate or flange, the projected stud diameter in front of the stud bears directly on the concrete near the surface and induces a zone of concrete crushing. If the connection is close to an edge, the concrete anchorage assembly will likely break out a concrete section due to the edge effects. If the connection is located sufficiently away from the edge to preclude an edge breakout, the stud or studs will likely fail in a steel shear failure mode. [10]

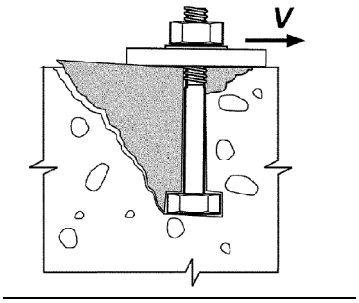

Figure 2-19: Pryout failure [4].

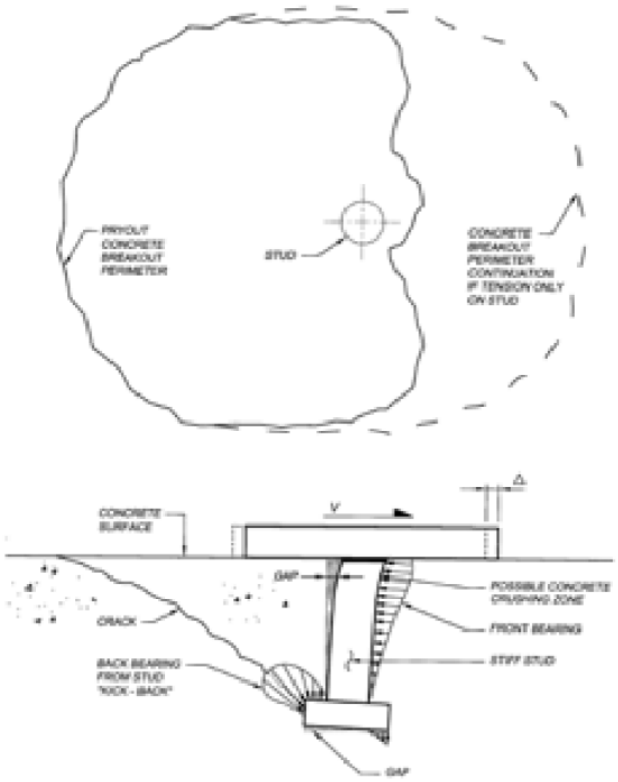

Figure 2-20: Pryout Mechanism. [9]

Concrete pryout strength: [4]

For a single anchor:

$$V_{cp} = k_{cp} N_{cb} \quad (2.10)$$

For a group of anchors:

$$V_{cpg} = k_{cp} N_{cbg} \quad (2.11)$$

2.4 Local Lip Failure

There may be other local or global failure modes that maybe observed during the experimental phase of this thesis and have not been addressed to in literature, such as local lip failure (Figure 2-21).

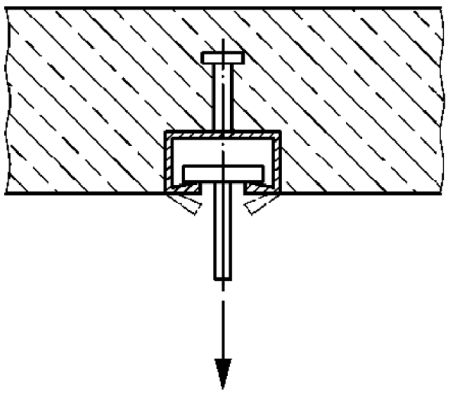

Figure 2-21: Local lip failure. [3]

CHAPTER 3

RESEARCH OBJECTIVES AND TASKS

3.1 Objectives

The objectives are to propose a method to calculate the capacity of cast-in C-channel and compare it with the experimental test results and finite element modeling. Specific objectives are:

i. Undertake an experimental work to generate substantive data;

ii. Develop theoretical prediction models using empirical approaches and finite element analysis in which failure is captured by modeling various effects;

iii. Verify of the proposed model using newly generated test data.

3.2 Scope

The Scope of this study is to make a small-scale concrete samples with cast-in C channel embedded as shown in (Figure 3-1). After that, the experimental test was conducted to investigate experimentally the actual behavior of the channel after, a finite element model has been made and a numerical procedure was generated to compare and validate all predicted results and develop a procedure of calculating the ultimate capacity of C channel embedded in concrete.

Figure 3-1: First sample

3.3 Approach

The research work is planned around the following eight tasks:

Task 1: Review of literature

Task 2: Casting and curing of test specimens

Task 3: Preparation for the experimental work

Task 4: Test more than one sample to observe the failures.

Task 5: Finite element modeling.

Task 6: Development of methods for calculating the capacity.

Task 7: Verification of the proposed method.

Task 8: Results and discussion and writing of dissertation.

CHAPTER 4

EXPERIMENTAL WORK

4.1 Experimental Program

The program was prepared to observe the different assumed main failures of the channel as mentioned in the literature review by pulling a hammer head bolt that is inserted in the cast in channel which is embedded in the concrete specimen shown in (Figure 4-1). The failures that are proposed to be monitored are as follow:

- Local channel lip failure.
- Channel concrete anchorage failure.
- Any other failures that could happen and are not citied in the literature review.

4.2 Details of Test Specimens

The first sample had a height of 42 cm x 20 cm width (Figure 4-1) that was not easy to observe the failures during the experimental test. Therefore, the size had been reduced to 20 cm x 20 cm (Figure 4-2) to be able to monitor the test. The concrete mix used in the experiment is the same mix used for precast columns prepared in PRAINSA SAUDI ARABIA factory. The reason is most of these cast in channels are embedded in the precast columns to connect precast cladding panels (Figure 1-8) and (Figure 1-9). The specified concrete 28 days compressive strength for such columns is 40 N/mm^2 (5,800 psi) according to ASTM cylinder.

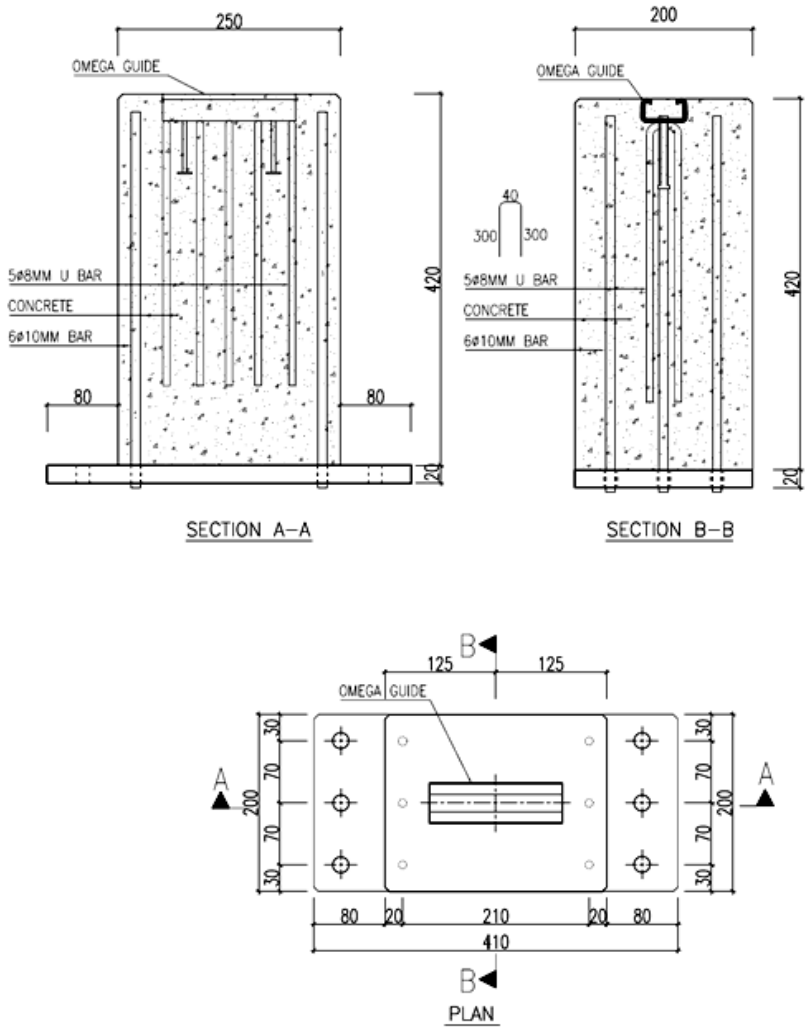

Figure 4-1: First Sample

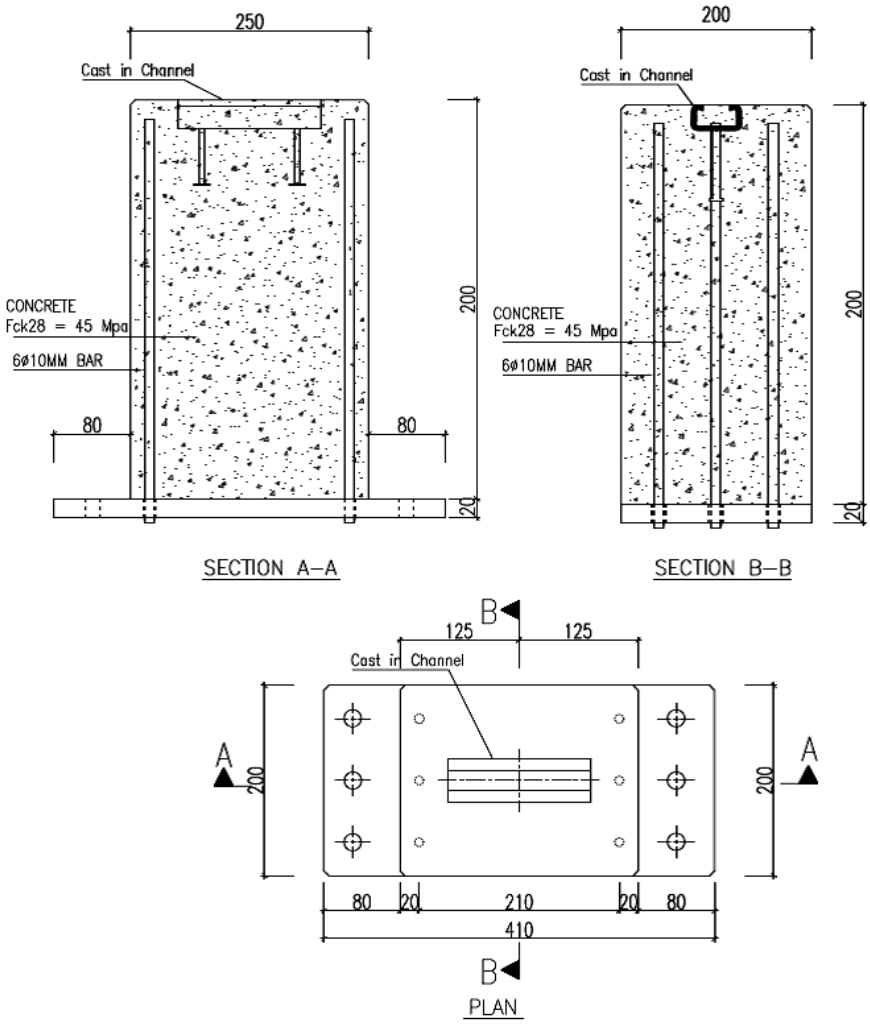

Figure 4-2:Reduced Sample

To fix the concrete part to the machine, a steel base plate (Figure 4-3), was used and cast with the concrete sample and was anchored to concrete using welded reinforcement bars, and the base plate with the sample was bolted to the test machine (Figure 4-5).

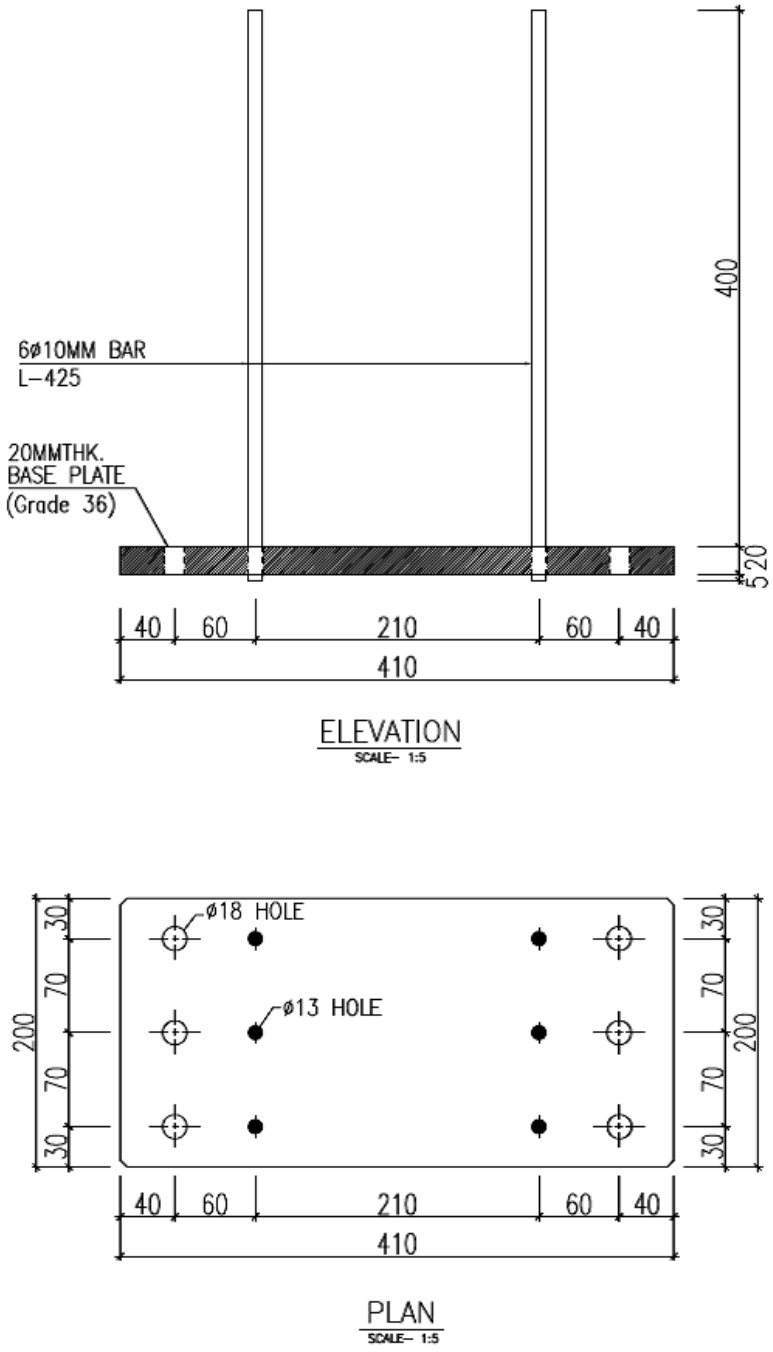

Figure 4-3: First Base Plate

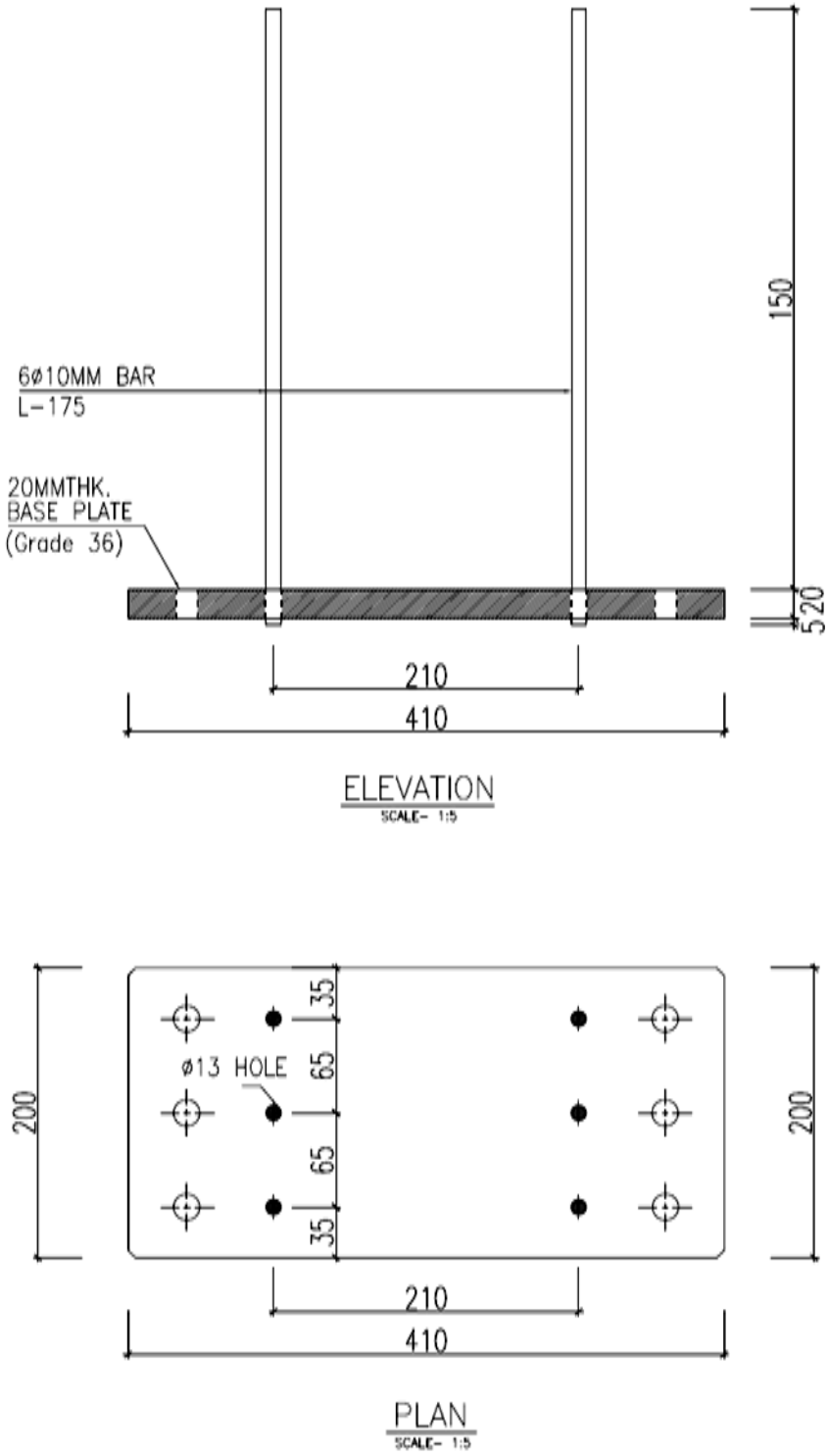

Figure 4-4: Modified Base Plate (Reduced development length)

The initial specimen (Figure 4-5) had a weight of 67.5 kg, the second reduced specimen (Figure 4-6) had a weight of 38.5 kg.

Figure 4-5: Concrete initial Sample Bolted to Test Device

Figure 4-6: Reduced Sample size

4.3 Sample Design

The sample was designed to replicate the use of the channel, and it was made in such a way to be easy to handle and placed on the test machine. The sample was designed to resist a tension load of 100 kN.

The size of the sample was determined based on the test machine; the test machine had 6 holes for screws/bolts that were used to bolt the base plate. The base plate was anchored to concrete specimen using normal reinforcement bars welded to the base plate. As show in Figure 4-7, three main components were designed for the sample:

1. Base Plate
2. Reinforcement Rebar
3. Bolts

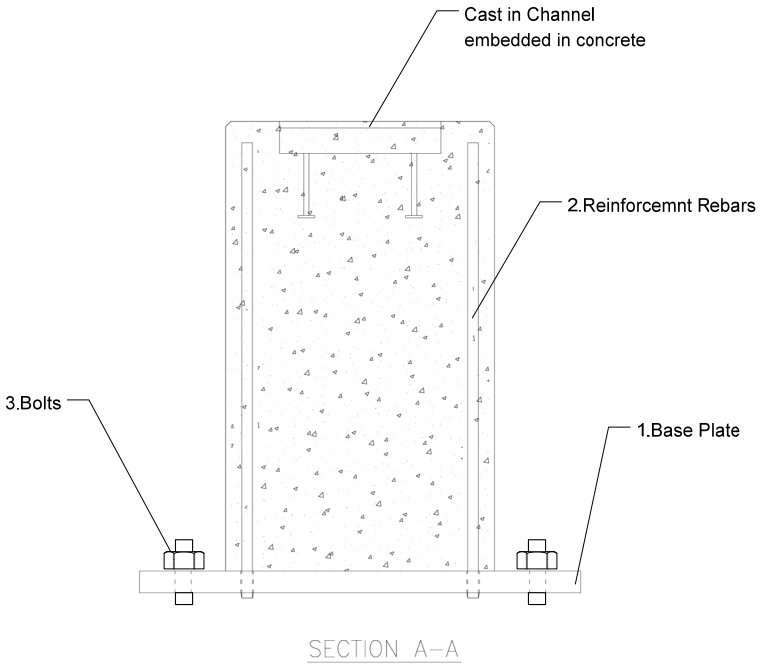

Figure 4-7: Sample main component

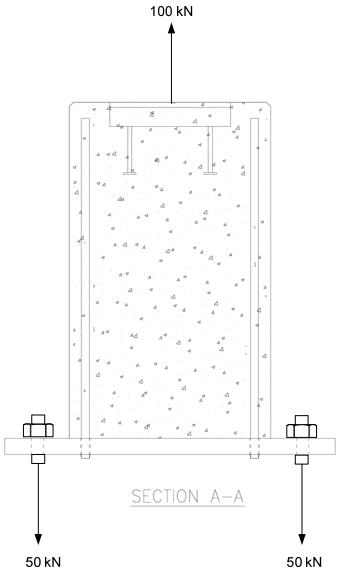

Figure 4-8: Tension load that sample designed to resist

4.3.1 Base Plate Design

The base plate thickness was designed to resist the bending moment due the bolts that is holding the sample to the testing machine. The lever arm is the distance between the center of the bolt and the reinforcement bar welded to the base plate [10], this distance is 40 mm + 20 mm = 60 mm (Figure 4-9), and the plate had a width of 200 mm as shown in (Figure 4-1) & (Figure 4-2).

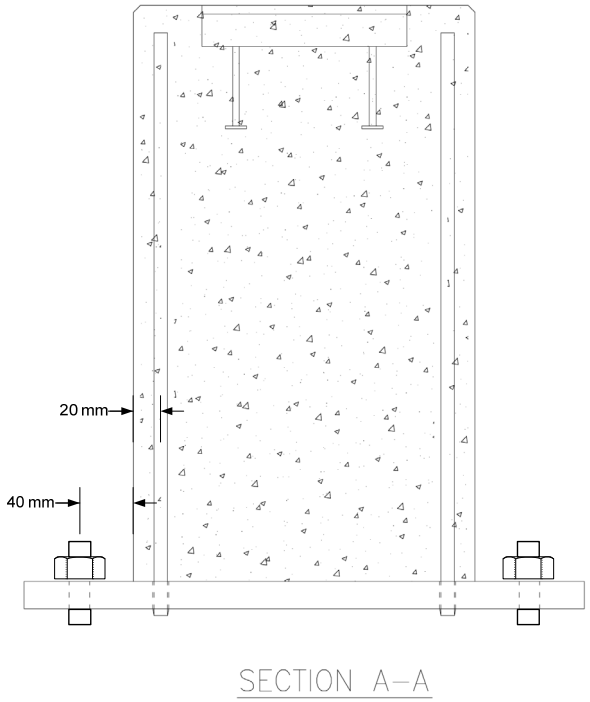

Figure 4-9: Lever arm for bending moment calculation

$M_u = 50 \times 0.06 = 3$ kNm (4.1)

The material used in the steel plate is grade A36 according to ASTM. The thickness of the plate has to be determined to avoid two failures that are likely to happen as per AISC [5], yielding and/or lateral torsion buckling.

First trial was by assuming that yielding of plate is governed to get the base plate thickness.

$\phi M_p = \phi F_y Z$ (4.2)

Where:

$\phi = 0.9$

F_y = yield strength = 248 N/mm^2 (36 ksi)

$$Z = \frac{b \times t^2}{4} \quad (4.3)$$

Z: plastic modulus of elasticity.

b: width of plate = 200 mm

t: thickness of plate

Substituting (4.3) into (4.2) and solving for "t" while equating to (4.1) will yield:

$$t = \sqrt{\frac{4 \times M_u}{\varphi F_y \times b}} = \sqrt{\frac{4 \times 3E6}{0.9 \times 248 \times 200}} = 17 \text{ mm} \quad (4.4)$$

Therefore, 20 mm was used that is available in the market.

Check the adequacy of thickness of base plate for the flexural capacity base plate as per AISC [5].

$$\frac{L_b d}{t^2} \leq \frac{0.08E}{F_y} \quad (4.5)$$

Where:

L_b : lever arm = 60 mm

d : thickness = 20 mm

t : width = 200 mm

E : modulus of elasticity = 200,000 N/mm2 (29,000 ksi)

F_y : yield strength = 248 N/mm2 (36 ksi)

Right side of equation (4.5)

$$\frac{L_b d}{t^2} = \frac{60 \times 20}{200^2} = 0.03$$

Left side of equation (4.5)

$$\frac{0.08E}{F_y} = \frac{0.08 \times 200{,}000}{248} = 64$$

Left hand side (0.03) < Right hand side (64), therefore only yielding is governed, and the lateral-torsional buckling will not likely to happen.

Using equation (4.2)

$\phi M_p = \phi F_y Z = 0.9 \times 248 \times 20{,}000 = 4{,}464{,}000$ N.mm x $10^{-6} = 4.46$ kNm

$Z = \frac{200 \times 20^2}{4} = 20{,}000$ mm^3

In addition, elastic flexural capacity needs to be checked as per AISC [5], equation (4.1)

$\leq 1.6\ \phi\ M_y$

$1.6\ \phi\ M_y = 1.6\ \phi F_y S$ (4.6)

Where:

$S = \frac{b \times t^2}{6} = \frac{200 \times 20^2}{6} = 13{,}333.33$ mm^3 (4.7)

$1.6\ \phi\ M_y = 1.6\ \phi F_y S = 1.6 \times 0.9 \times 248 \times 13{,}333.33 = 4{,}761{,}600$ N.mm x $10^{-6} = 4.76$ kNm

Since $\phi M_p \leq 1.6\ \phi\ M_y$, plastic capacity governs

$\phi M_n = \phi M_p = 4.46$ kNm > Mu = 3 kNm

4.3.2 Reinforcement Rebar

The rebars (Figure 4-7) must take the resisted tension force in the bolts that is equal to 50 kN, the rebar material grade used is grade 60 as per ASTM A615.

$$\phi T_n = \phi f_y A_s \quad (4.8)$$

Where:

ϕ: 0.75

f_y : rebar yield strength = 414 N/mm^2 (60 ksi)

A_s : Area of steel rebars.

Solving equation (4.8) in terms of A_s, yields:

$A_s = \frac{T_u}{\varphi f_y} = \frac{50}{0.75 \times 414000} = 0.0001610$ m^2 → use 3 bars of 10 mm diameter with A_s = 0.0002356 m^2

Development length:

As per ACI 318M-08 [4], the development length is calculated as follow:

$$l_d = \frac{f_y\, \psi_t\, \psi_e\, d_b}{2.1\, \lambda \sqrt{f_c'}} = \frac{414 \times 1 \times 1 \times 10}{2.1 \times 1 \times \sqrt{40}} = 312 \text{ mm (400 mm is provided)} \quad (4.9)$$

where:

f_y : rebar yield strength = 414 N/mm^2 (60 ksi)

$\psi_t = 1.0$

$\psi_e = 1.0$

$\lambda = 1.0$ (Normal weight concrete)

$f'_c = 40$ N/mm^2

4.3.3 Bolts

The bolts used are 16 mm diameter as per the holes available in the test machine (Figure 4-6), these bolts are of grade A36, and they are screwed to hold the whole test specimen to the testing machine. Six bolts was used, and the force per bolt is as follow:

100/6 = 16.7 kN/bolt

As per AISC [5], the bolts capacity in tension:

$$\phi R_n = \phi F_n A_b \quad (4.10)$$

$\phi R_n = 0.75 \times 300 \times 157 \times (1000^{-1}) = 35.33$ kN/bolt > 16.7 kN/bolt

where :

$\phi = 0.75$

$F_n = 0.75 F_u = 0.75 \times 400 = 300$ N/mm^2

$F_u = 400$ N/mm^2 (58 ksi)

$A_b = 157$ mm^2 (stress area of threaded part)

4.4 Materials Properties

4.4.1 Concrete

4.4.1.1 Concrete mix

Type I Portland cement (ASTM C150) was used in the preparation of concrete specimens. The coarse aggregate used in this study was crushed limestone processed from the quarries on Riyadh highway; two aggregate sizes were used 3/8" and 3/4". For mixing and curing of concrete, potable water was used; as well as super plasticizer admixture chemical.

The mix proportions used are as follows:

Water-cement ratio = 0.40

Cement content = 400 kg/m^3

The weights of constituent per cubic meter of concrete are given in (Table 4-1).

Table 4-1: Weight of component in one cubic meter of concrete mixture.

Constituent	Weight
Cement	400 (kg/m^3)
Water	160 (Liter/m^3)
Sand	640 (kg/m^3)
3/8" aggregate	535 (kg/m^3)
3/4" aggregate	675 (kg/m^3)
Additive	2.1 (Liter/m^3)

4.4.1.2 Concrete mechanical properties

Some tests related to compressive strength and tensile strength of concrete were conducted to simulate the experiment using computer modeling. For compressive strength parameters, cylinder samples were used, and for the tensile strength beam notch approach was used [11].

Compressive Strength:

Three cylinders were cast, the cylinder size was 3" x 6" (75 mm x 150 mm), according to ASTM [12].

The cylinders were tested under cyclic loading in order to get stress vs. strain curve and the slope of every cycle to get the damage factor that was used in the computer FEM model.

Figure 4-10: Molds of cylinder samples

Figure 4-11: Three concrete 3" x 6" cylinders

To assure the bottom and top side of the cylinders are leveled, caps were used, the caps were made using sulfate, the sulfate was melted and placed on a steel mold while the sample was placed on the steel mold, until the sulfate is dry (Figure 4-11).

Figure 4-12: Steps of preparing the cap for the 3" x 6" concrete cylinders

After 28 days, strain gauges specifically for concrete were attached on the concrete cylinders surfaces, those gauges are different than those used for steel, and the gauges were placed in a vertical and horizontal way.

Figure 4-13: Concrete cylinder with strain gauge

The gauge had a coefficient of 0.467, this value is important to input in the data logger.

The samples was tested under a maximum of 5 cycles, which means the cylinder was loaded up to a certain load then unloaded, then loaded again five times, this was done to capture the damage factor (d) (Figure 4-14).

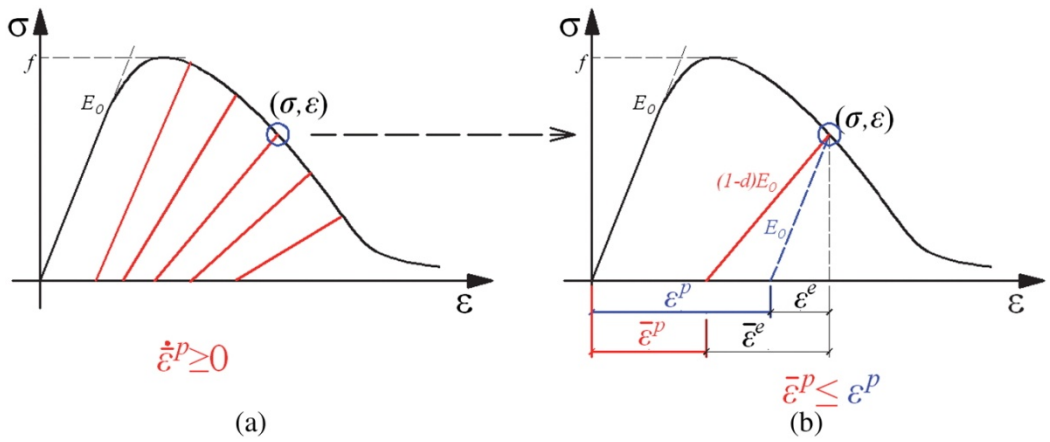

Figure 4-14: Damage plasticity model of concrete: (a) plastic strain degradation; (b) damage definition [13]

The test machine was connected to the data logger (Figure 4-15) and the recording of load was done manually every 2 kN, loading rate was at 0.2 mm/min. The stress vs. strain relationship is shown in Figure 4-16

Figure 4-15: Data logger connected to the compression test machine at KFUPM civil engineering lab

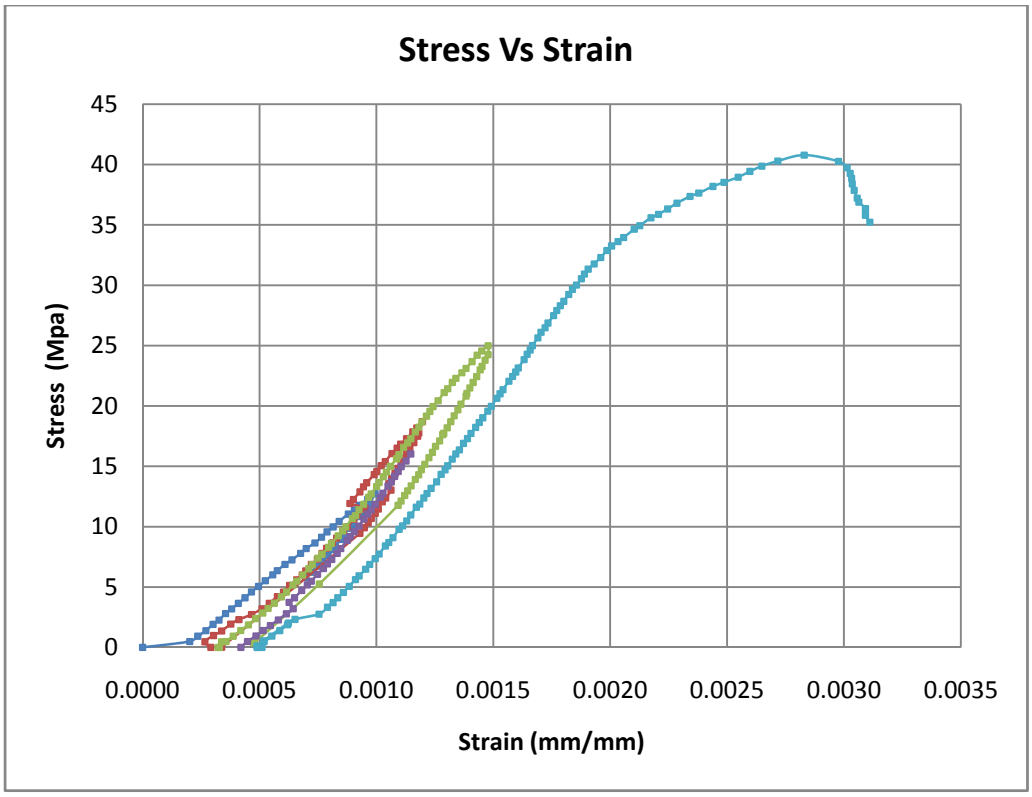

Figure 4-16: Cylinder Sample cyclic Stress Vs Strain diagram

Tensile Strength:

A beam with a notch in the middle of the beam was cast to measure the tensile strength of concrete [11]. The dimension and details of the beam are presented in Figure 4-17.

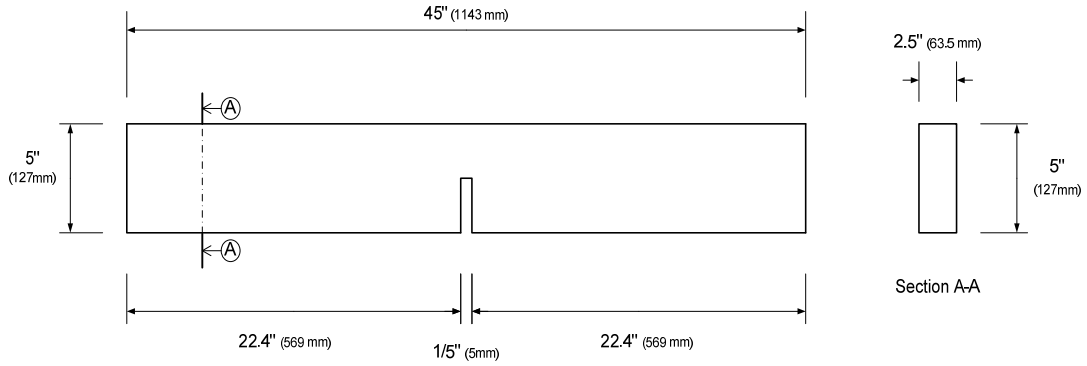

Figure 4-17: Beam notch dimension

The beam is un-reinforced, and it was loaded in the center with concentrated load as shown in Figure 4-20 and Figure 4-21 until the beam cracks. Gauges were placed around the notch to measure the displacement (Figure 4-19) while load increases opening size increases, the loading rate was very slow (0.5 mm/min) since there is no reinforcement in the beam.

The gauge was glued with epoxy resin around the notch at the center of the notch as shown in (Figure 4-19).

The load vs. displacement curve is shown in Figure 4-22. The beam failed at a load of 224 N, which is very low. Figure 4-22 shows the crack developed through the notch.

Figure 4-18: Steps of casting the beam notch specimen.

Figure 4-19: Strain gauge glued around notch.

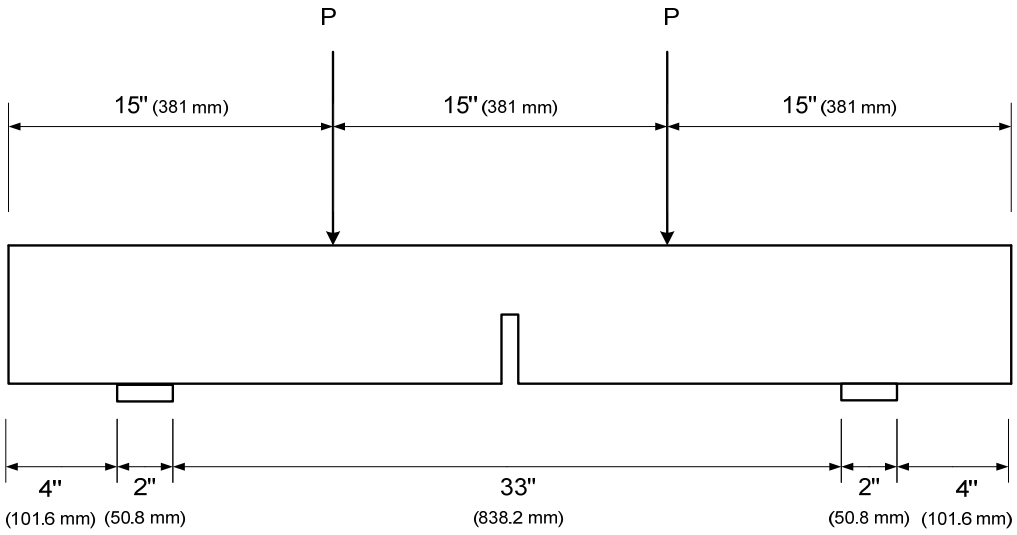

Figure 4-20: Beam notch loading schematic

Figure 4-21: Beam notch loading test.

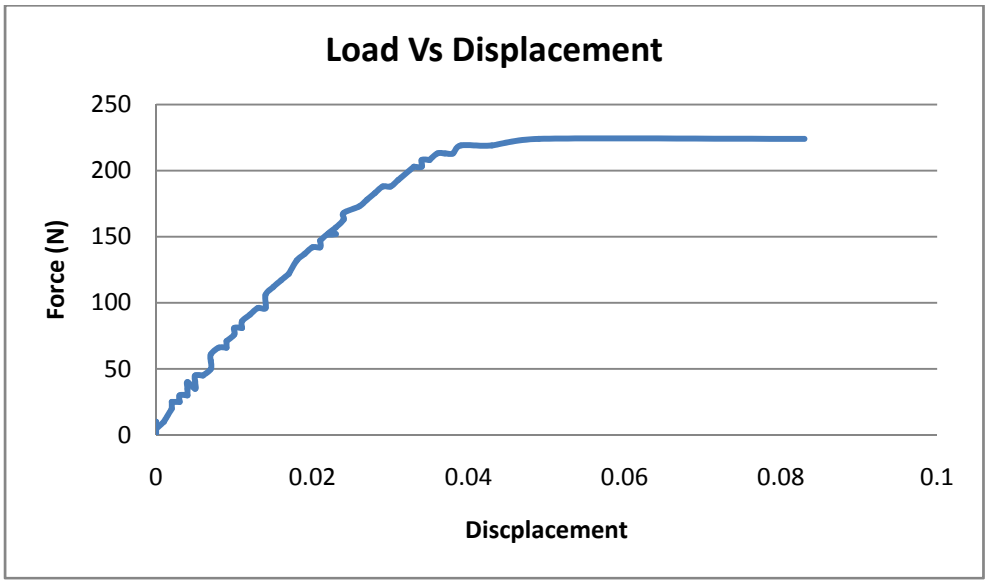

Figure 4-22: Beam notch Force Vs Displacement curve

Figure 4-23: Failure and crack of beam notch specimen.

4.4.2 Cast in Channel

The channel used in all the test specimens is of grade St-37-2 according to German material standard (DIN 17100), and it is equivalent to S235JR based on European standard (EN 10025-2:2004), Table 4-2 shows a comparison table between international steel grades.

The cast in channel is cold formed and its stress-strain curve is similar to that other ductile steel such as A36 or Grade 60 with the following mechanical characteristics:

Yield strength = 235 N/mm^2 (34 ksi)

Tensile strength = 360 N/mm^2 (52 ksi)

It is composed of 3 mm thick plate bended, and two stud bars riveted to the channel, the channel have the dimensions shown in (Figure 4-24).

Table 4-2: Non-alloy structural steels EN 10025-2:2004, steel grades Mechanical properties and approximate comparison with previous standard steels.

Yield strength [1] R_{eH} MPa	Tensile strength R_m MPa	Impact strength [1] KV J	t °C	EN 10025-2 2004	EN 10025:1990 +A1:1993	EN 10025: 1990	SFS 200 1986	SS xx xx xx-xx 1987	DIN 17100 1980	BS 4360 1986	NF A 35-501 1981
235	360-510	27	20	–	S235JR	Fe 360 B	–	14 13 11-00	St 37-2		E 24-2
235	360-510	27	20	S235JR	S235JRG2	Fe 360 B FN	Fe 37 B	14 13 12-00	RSt 37-2	40 B	–
235	360-510	27	0	S235J0	S235J0	Fe 360 C	–		St 37-3 U	40 C	E 24-3
235	360-510	27	-20	S235J2+N	S235J2G3	Fe 360 D1	Fe 37 D		St 37-3 N	40 D	E 24-4
235	360-510	27	-20	S235J2	S235J2G4	Fe 360 D2	–		–		
275	430-580	27	20	S275JR	S275JR	Fe 430 B	Fe 44 B	14 14 12-00	St 44-2	43 B	E 28-2
275	430-580	27	0	S275J0	S275J0	Fe 430 C	–		St 44-3 U	43 C	E 28-3
275	430-580	27	-20	S275J2+N	S275J2G3	Fe 430 D1	Fe 44 D	14 14 14-00	St 44-3 N	43 D	E 28-4
275	430-580	27	-20	S275J2	S275J2G4	Fe 430 D2	–	14 14 14-01	–		
355	510-680	27	20	S355JR	S355JR	Fe 510 B	–	(14 21 72-00)	–	50 B	E 36-2
355	510-680	27	0	S355J0	S355J0	Fe 510 C	Fe 52 C		St 52-3 U	50 C	E 36-3
355	510-680	27	-20	S355J2+N	S355J2G3	Fe 510 D1	Fe 52 D	(12 21 74-01)	St 52-3 N	50 D	
355	510-680	27	-20	S355J2	S355J2G4	Fe 510 D2	–		–		
355	510-680	40	-20	S355K2+N	S355K2G3	Fe 510 DD1	–		–	50 DD	E 36-4
355	510-680	40	-20	S355K2	S355K2G4	Fe 510 DD2	–		–		
185	310-540	–	–	S185	S185	Fe 310-0	Fe 33	14 13 00-00	St 33		A 33
295	490-660	–	–	E295	E295	Fe 490-2	Fe 50	14 15 50-00	St 50-2		A 50-2

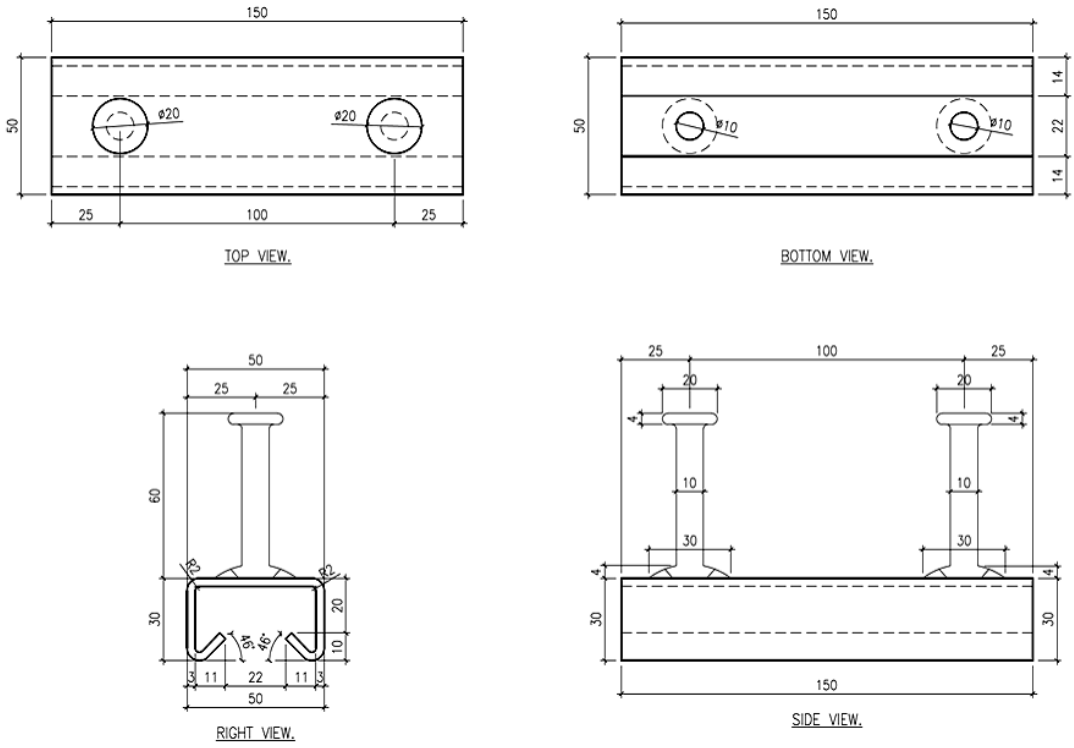

Figure 4-24: Cast in Channel Geometry.

4.4.3 Hammer Headed Bolt

The hammer headed bolt was used and inserted in the cast in channel to take the tension load and transfer it to the channel, The material grade is 4.6 European grade with following mechanical properties:

Yield strength = 240 N/mm^2 (34 ksi)

Tensile strength = 400 N/mm^2 (58 ksi)

Bolt had a diameter of 18 mm, and the geometry as show in (Figure 4-25).

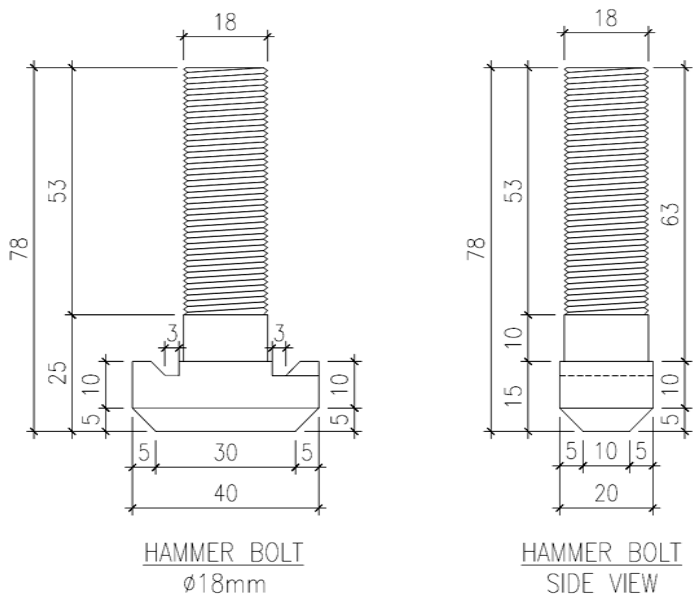

Figure 4-25: Hammer Headed Bolt.

4.5 Casting and Curing of Test Specimens

It is observed that most specimens reached the required compressive strength (40 N/mm^2 (5,800 psi)) at an early stage, before 28 days.

After base plate was fabricated (Figure 4-26), a steel mold or a wooden shuttering was placed around it, and the channel was connected to the mold to hold it before casting as shown in (Figure 4-27).

Figure 4-26: Steel Base Plate for concrete sample.

Figure 4-27: Steel Mold shuttering and positioning the cast in channel before casting.

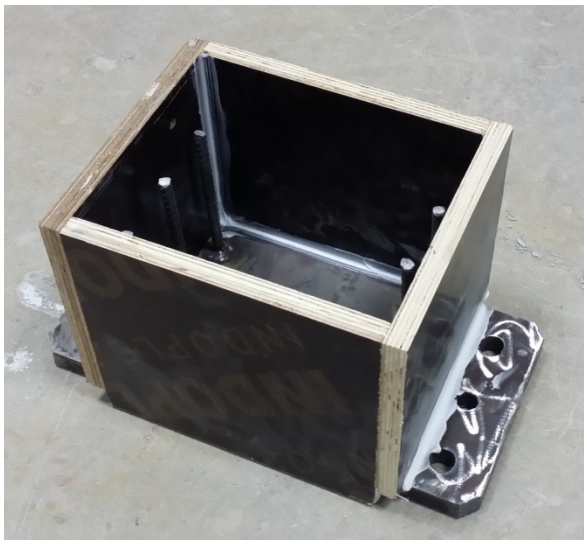

Figure 4-28: Wooden Shuttering used for sample casting

4.6 Experimental Techniques

In the beginning of the experimental work, it was not clear how many samples are needed since there is no sufficient literature covering this area as a whole. However, failures related to anchorage in concrete have a lot of research. Therefore, it was decided to concentrate on steel related local failures such as lip failure. The first sample had a reinforcement bars welded to the cast in channel to force the failure in the lip only without having any anchorage failure. At the end, the total numbers of samples tested are seven.

4.6.1 Sample 1

First test was to see how the failure would appear in the specimen Figure 4-31, Figure 4-32, Figure 4-33, & Figure 4-34, no strain gauges were attached, and load vs. displacement was recorder from hammer bolts elongation by the test machine.

Figure 4-29: Rebar welded to the cast in channel used in first test

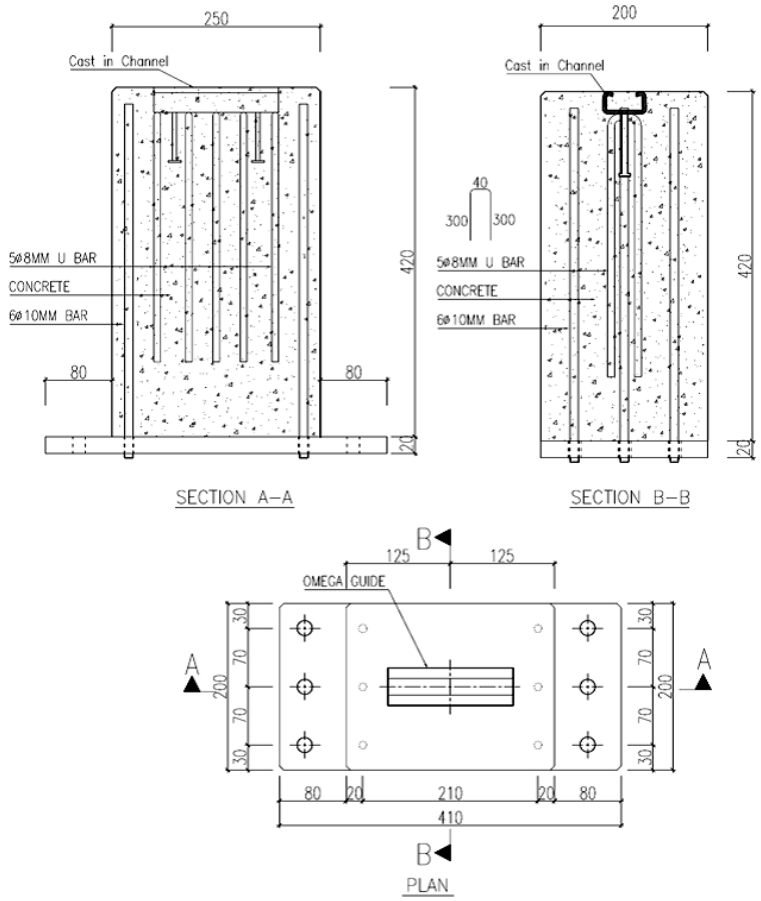

Figure 4-30: Drawing of the first sample showing the welded reinforcement bar to cast in channel.

The cast in channel had rebar welded to it (Figure 4-29) to assure no anchorage failure will appear.

Figure 4-31: First Sample after casting

Figure 4-32: First Sample Handling and placing on test machine

Figure 4-33: First Sample after placing on test machine and ready to be tested.

Figure 4-34: A close up on the machine grip that will pull the hammer head bolt.

The test was set to speed of 1 mm/min and the channel started to fail when the force reached 45 kN as shown in below force vs. displacement Figure 4-36 these points were recorded by computer that is connected to the test machine Figure 4-35.

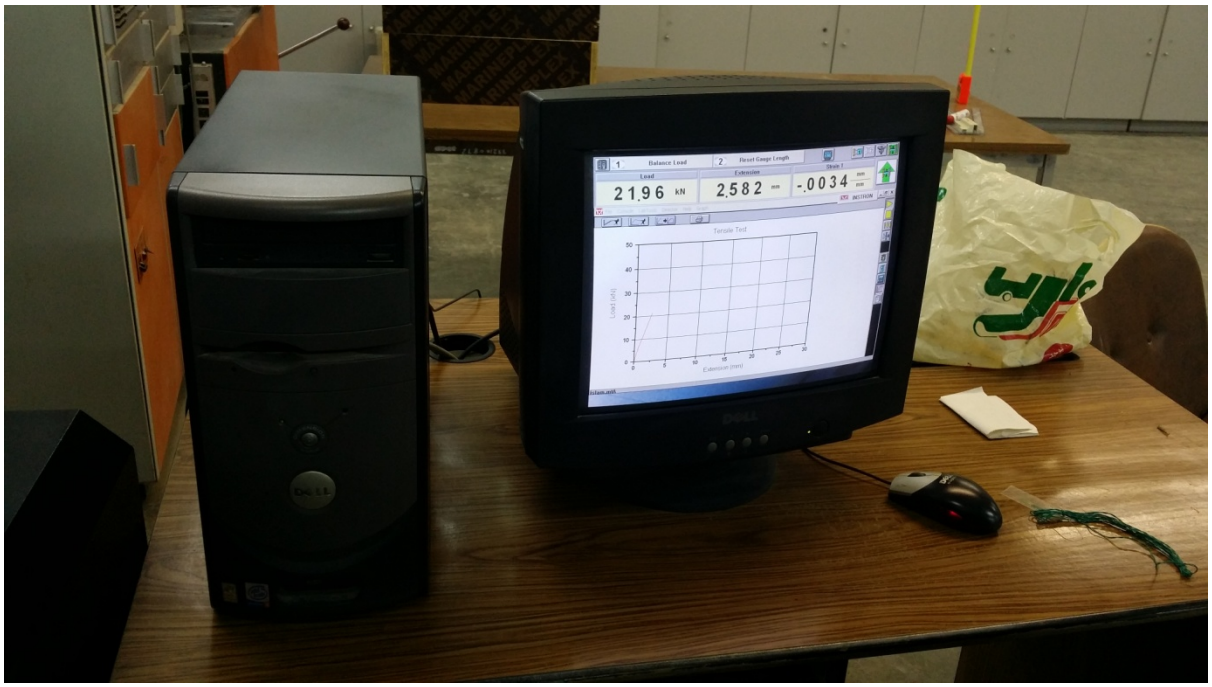

Figure 4-35: PC connected to the test machine to record force vs. displacement readings.

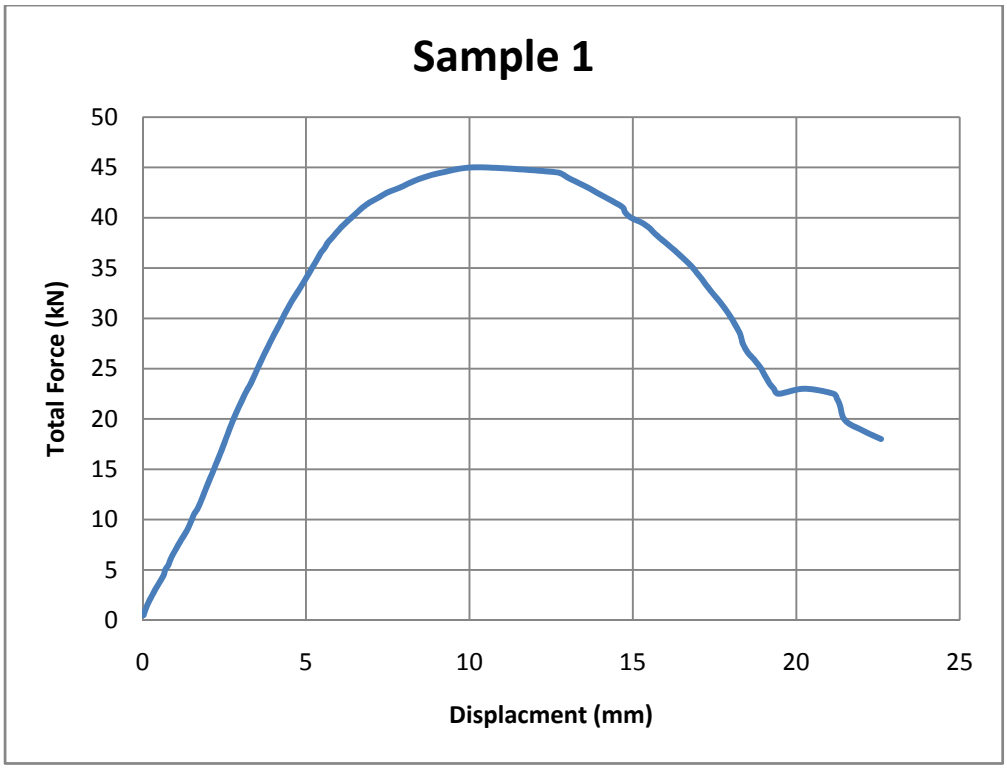

Figure 4-36: Sample-1 Force vs. Displacement curve

The above (Figure 4-36), is similar to that in Wohlfahrt 1996 (Figure 4-37) [14]. The channel lip starts to yield which leads to increase in the distance between both lips and the hammer bolt was pulled from the channel as show in (Figure 4-38) and (Figure 4-39). Another failure that was not predicted was in the hammer head bolt itself, as it exerted bending due to cantilever action in the bolts head as show in (Figure 4-40).

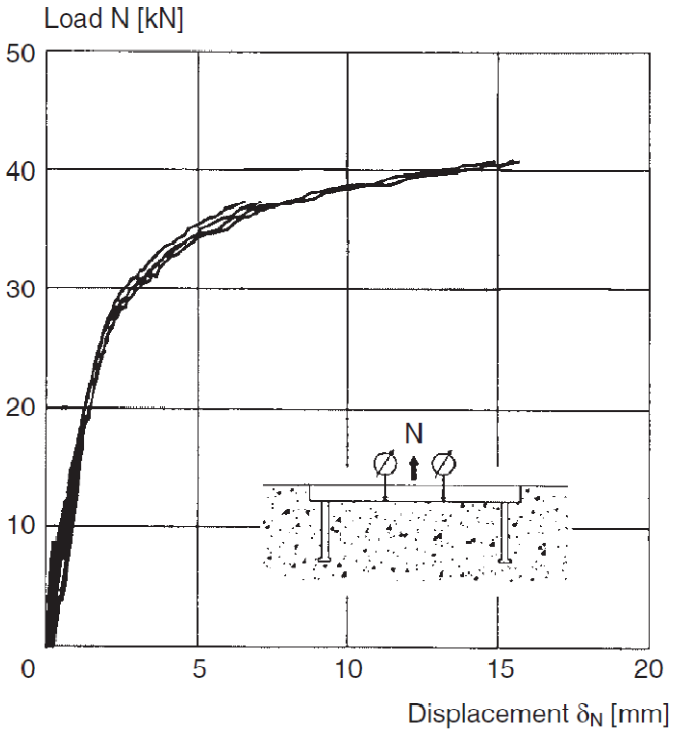

Figure 4-37: Load-displacement curves of channels with Load-displacement curves of channels with two anchors; failure was caused by flexural yielding of the channel followed by distortion of the channel flanges or rupture of the connection between anchor or channel [14].

Figure 4-38: Hammer bolt pulling out of the channel causing yield in channel lip.

Figure 4-39: Lip failure in sample-1

Figure 4-40: Hammer Bolt bending in head.

From above test results, it can be seen that the concrete surrounding the cast in channel had a major impact in confining the channel, which forced the failure to happen in the channel lip. The whole lip did not bend completely only part of it that is above the hammer head bolt yielded and the bolt went out of the channel. This confinement also lead to diagonal failure as shown in (Figure 4-39) and (Figure 4-41). This kind of failure was not predicted, and it was not symmetric, it could be due to the diagonal strut appearing in the edge of the channel as the whole lip was trying to bend while the concrete was confining it. In addition, it could be due to the edge distance was not enough to absorb such a force.

Figure 4-41: Diagonal Failure at channel edge.

4.6.2 Sample 2

Second sample did not have reinforcement bars welded to observe any anchorage failure that might occur before the lip fails (Figure 4-42). The load vs. displacement was recorder same way as sample-1.

The sample had the same behavior as sample-1 and it had same failure pattern and load.

The channel lip failed before any anchor failure appears, and the maximum load reached was 45 kN (Figure 4-41).

The diagonal concrete breakout at channel edge (Figure 4-44) happened in a similar manner as that of sample-1 (Figure 4-41), and it was at one side only in an un-symmetrical manner. However, in this test the hammer head bending did not happen like that of sample-1.

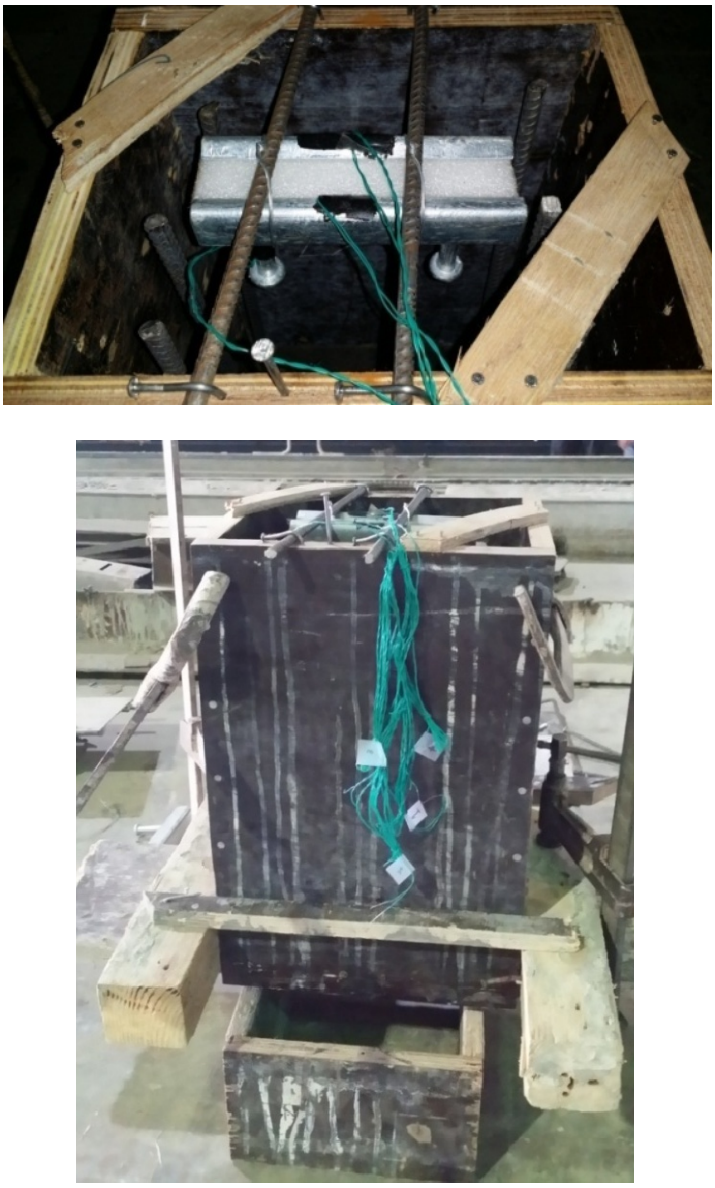

Figure 4-42: Sample-2 during casting.

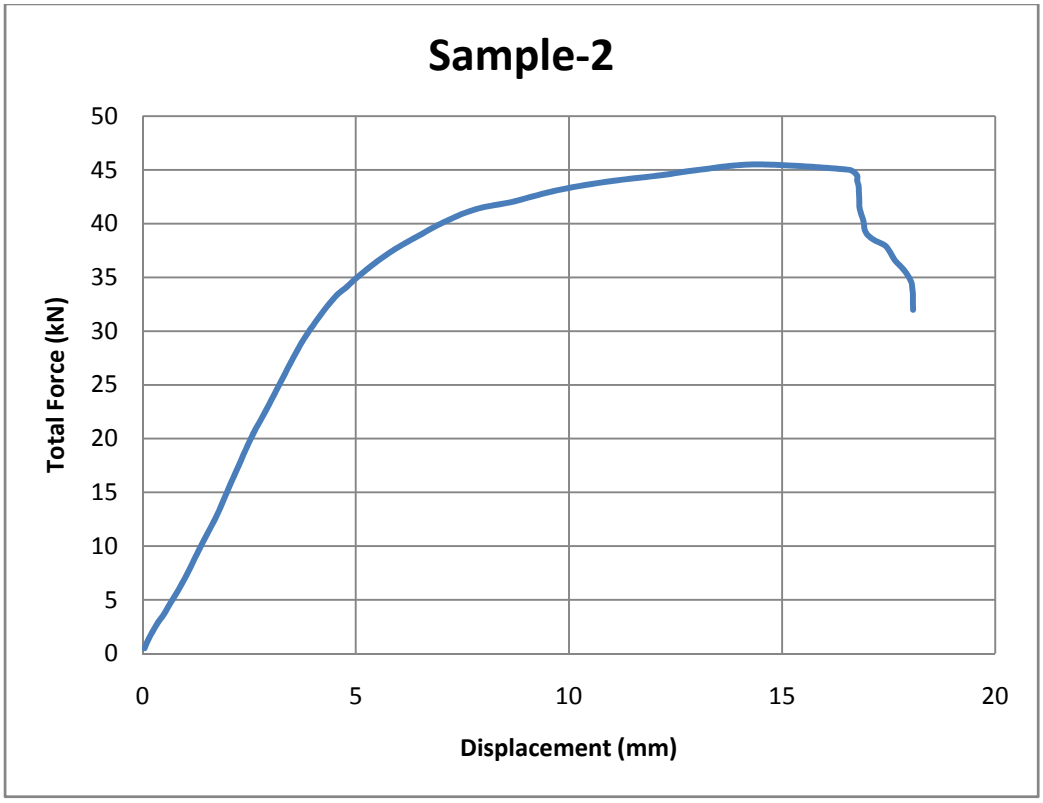

Figure 4-43: Sample-2 Force Vs Displacement.

Figure 4-44: Sample-2 Failure

4.6.3 Sample 3

This sample strain gauges was attached in same location as it was suppose in sample-2, but the difference between this sample and previous ones, is that this sample size was reduced (Figure 4-2) and (Figure 4-6) in order to be able to handle it and observe cracking of concrete and failure of channel during test more easily. The anchor length was reduced because of the failure load of the first sample was less than half that the actual capacity of the sample.

Four strain gauges were attached to the surfaces of the channel. The type of strain gauges used is shown in Figure 4-45 that was for steel elements. These gauges head had two sides, one the small wires are visible and the other not, the visible side of the gauge was glued with a special type of adhesive (Figure 4-46) to the cast in channel and was held for one minute until the glue get hardened.

Gauge#1 was placed in the middle of the channel in the right side lip, gauge # 2 was place in the middle of the channel at the bottom side, and gauges # 3 & 4 were placed in the anchor stud (Figure 4-48).

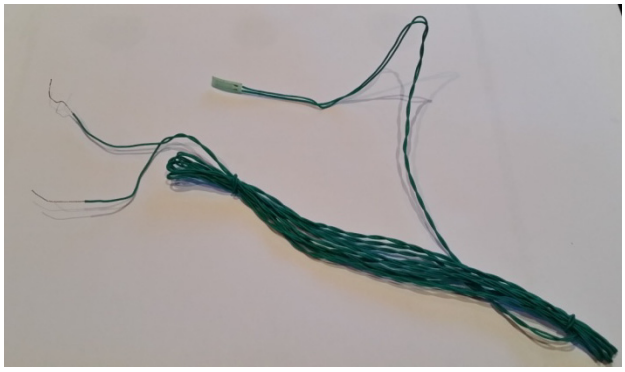

Figure 4-45: Strain gauge for steel.

Figure 4-46: Adhesive used to glue the strain gauge to the cast in channel.

The gauge was covered by waterproof (Figure 4-47) to protect it from water and moisture during casting of concrete.

Figure 4-47: Sample-3 with strain gauges attached to it.

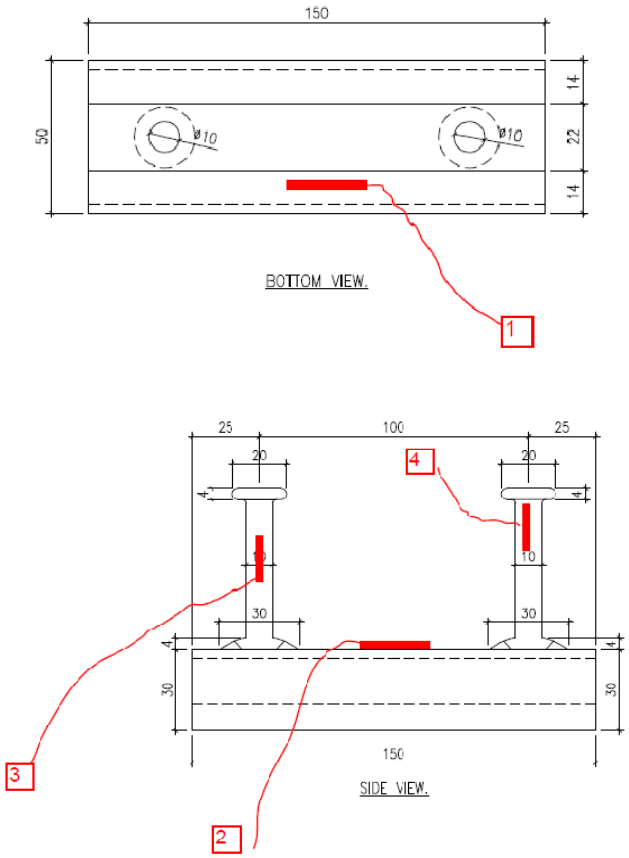

Figure 4-48: Sample-3 Strain gauges

Later these gauges were connected to a data logger (Figure 4-49), to record the force vs. displacement for each strain gauge attached.

Figure 4-49: Data logger

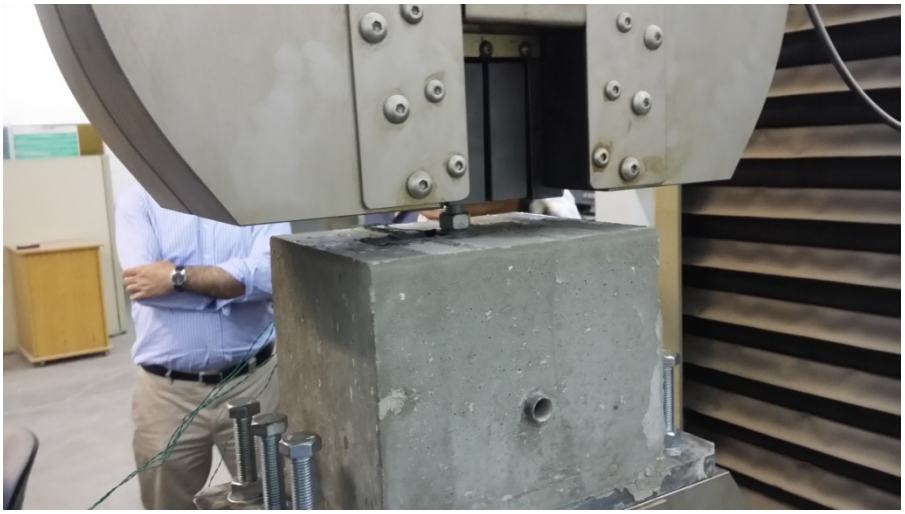

Figure 4-50: Sample-3

It was observed that the sample failed same way as previous samples, with lip yielding before any anchorage failures appear. The strain gauge # 1 was damaged as it was too close to the hammer head bolt location. The force vs. displacement is presented in Figure 4-51 and Figure 4-52.

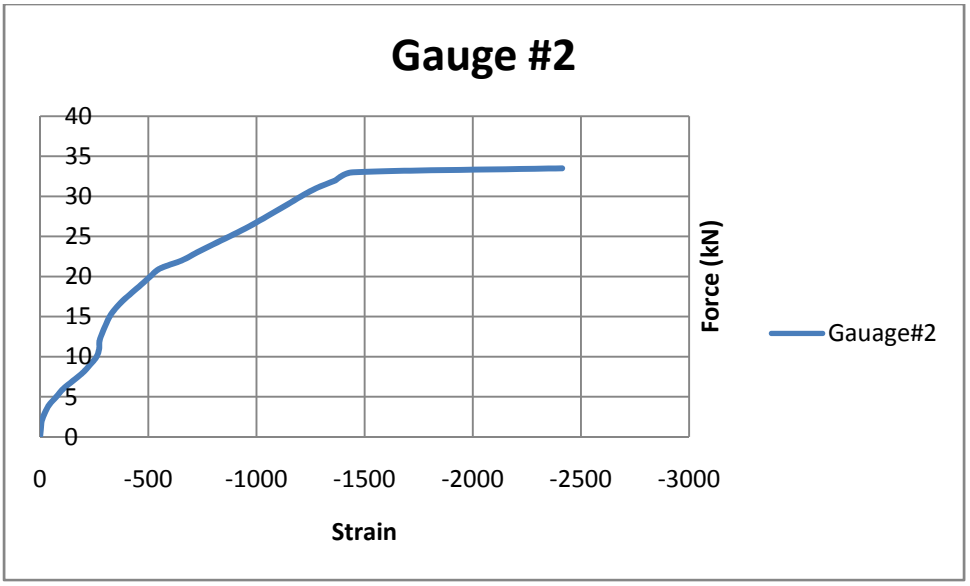

Figure 4-51: Sample-3 Force Vs Displacement for gauge#2.

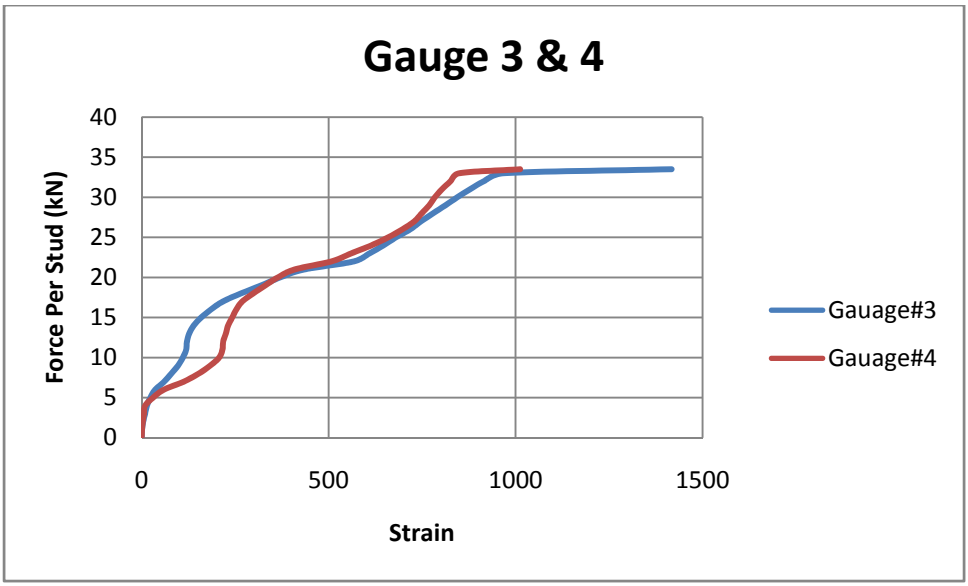

Figure 4-52: Sample-3 Force Vs. Displacement for gauge#3 & 4.

The strain is measured in micrometer (μm), and the negative sign in gauge#2 (Figure 4-51) indicates that channel is under compression, while the positive sign for gauge#3 & 4 (Figure 4-52) indicate tension. As can be seen that both figures reach the same constant force while strain increased, indicating that the channel started to yield at a value of 33 kN.

4.6.4 Sample 4

Since there were not any anchorage failures in previous sample, this sample was made to observe an anchorage failure before the channel local failure. The channel in this sample was cast with the anchor studs only being embedded in concrete as shown in (Figure 4-53) and (Figure 4-54).

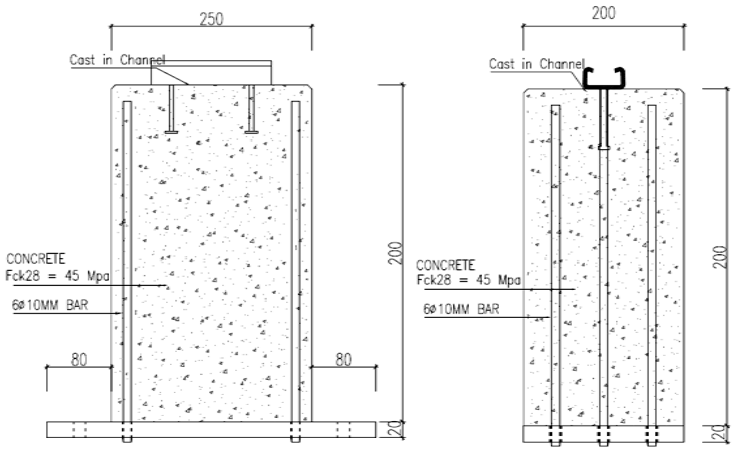

Figure 4-53: Schematic Drawings of Sample-4

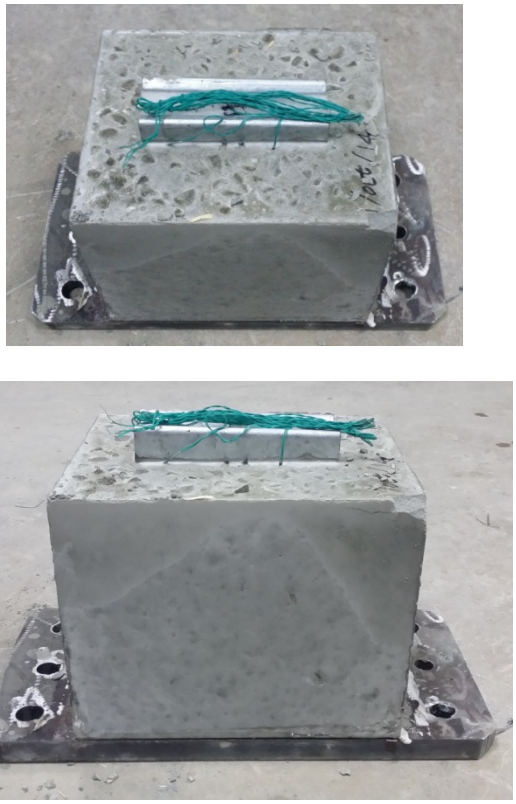

Figure 4-54: Sample-4 with channel being projected and only the stud anchors are embedded in concrete.

This sample also was the reduced size one and the remaining three tests were made with same reduced size as in (Figure 4-2) and (Figure 4-6).

Two strain gauges were attached to the sample anchor studs to measure the force vs. displacement.

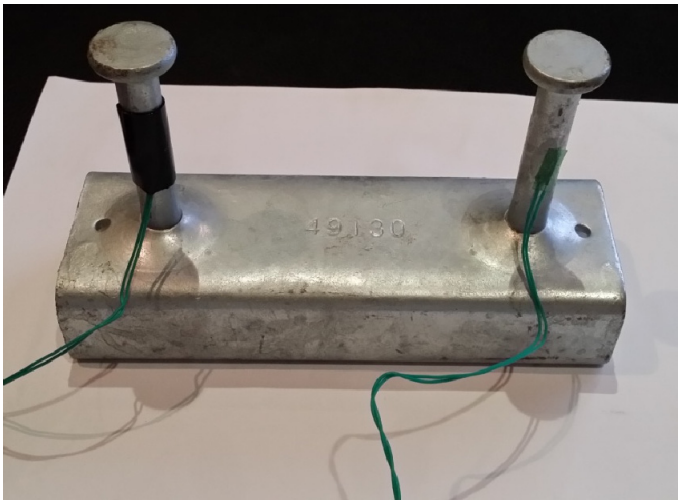

Figure 4-55: Sample-4 strain gauges location.

Figure 4-56: Sample-4 during casting.

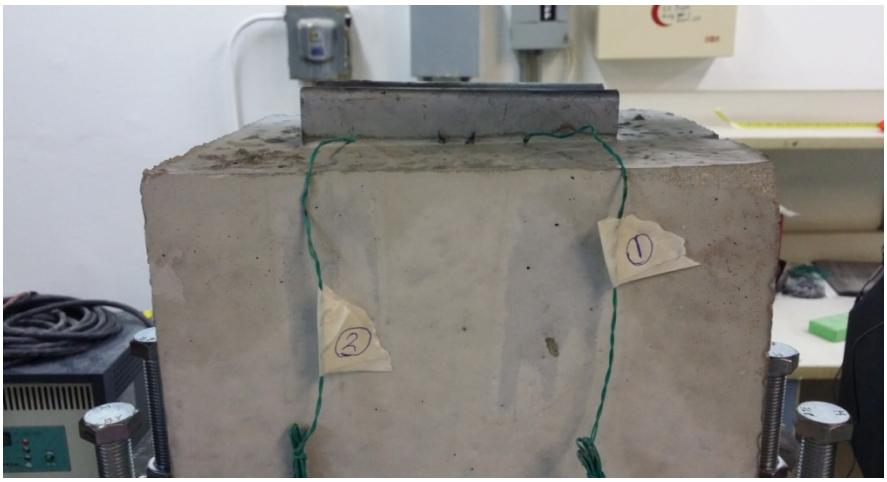

Figure 4-57: Sample-4 on the test machine.

The test results of sample-4 was recorded based on strain gauges reading and the test machine readings from the hammer bolt and channel as a whole (Figure 4-58).

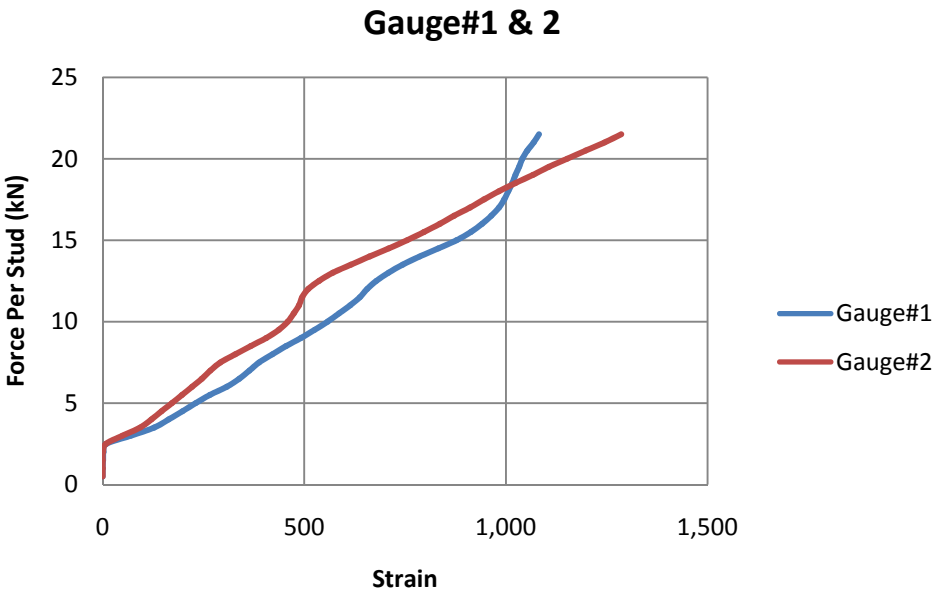

Figure 4-58: Force vs. Displacement curve reading for sample-4

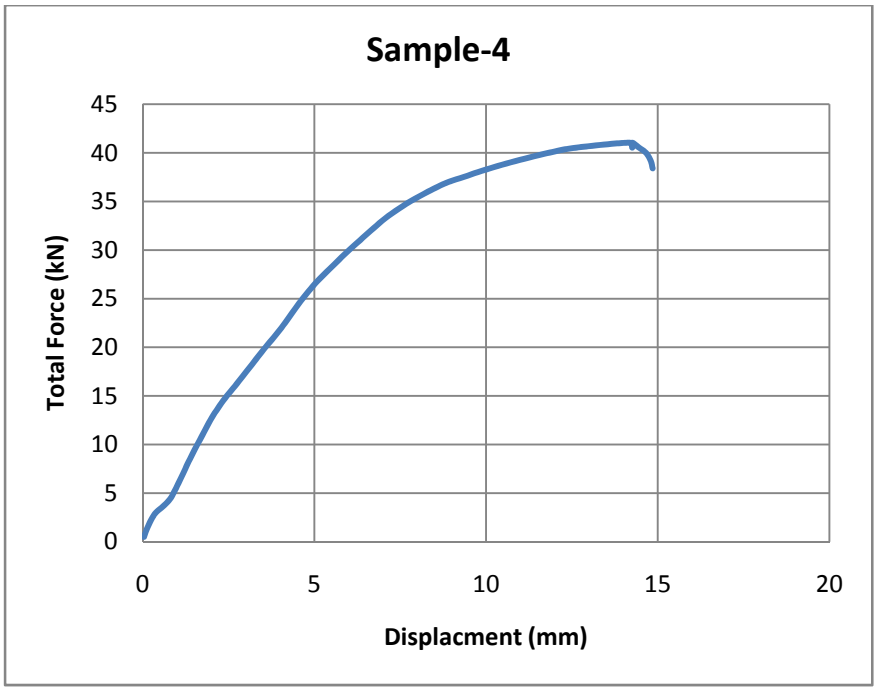

Figure 4-59: Force Vs Displacement curve of sample-4.

The sample had less capacity than samples 1, 2, and 3. The sample failed at 41 kN in comparison with 45 kN, the force vs. displacement curve in (Figure 4-59) has different slope than other samples. This could be due to the sample unconfined by concrete. In addition, in this sample no anchorage failure occurred, meaning that still the channel local failure govern the channel capacity more than the anchorage failure.

Figure 4-60: Sample-4 local channel failure.

4.6.5 Sample 5

It was observed from pervious test that there were not anchorage failure and pulling of the channel from concrete occurred. Therefore, the channel in this sample was cast without anchorage studs (Figure 4-61) to see the impact of removing the studs in the capacity of the assembly.

Two strain gauges were attached to the lip, and they are perpendicular in direction to each other as show in (Figure 4-62). The force vs. displacement is shown in Figure 4-63.

Figure 4-63, is showing maximum force of 11.5 kN in comparison with 45 kN that was achieved in previous sample, this shows how anchorage stud have a huge impact on channel capacity.

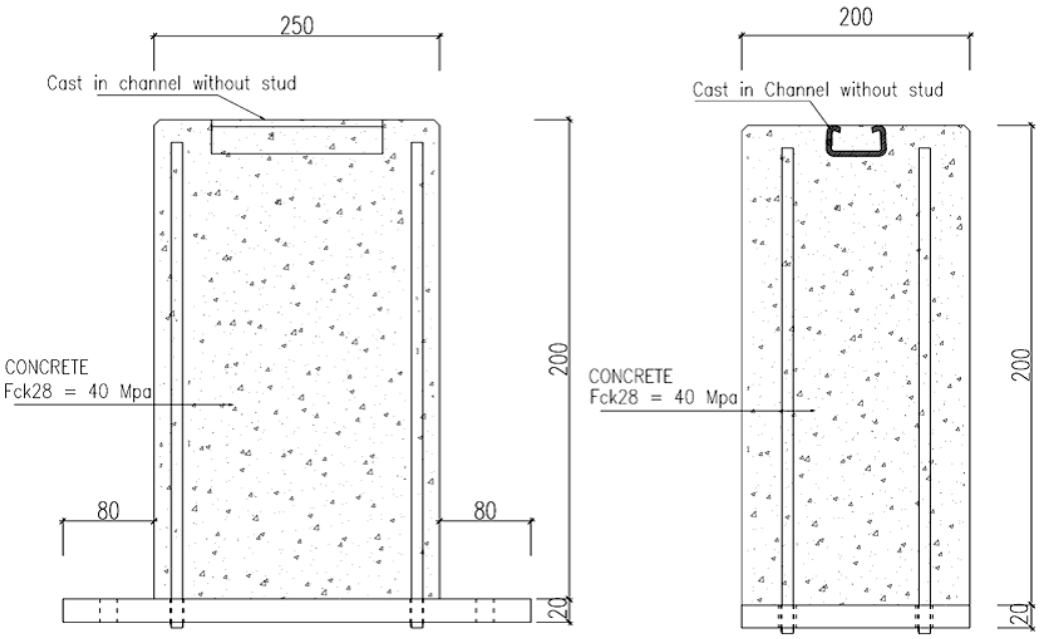

Figure 4-61: Schematic of sample with cast in channel without stud.

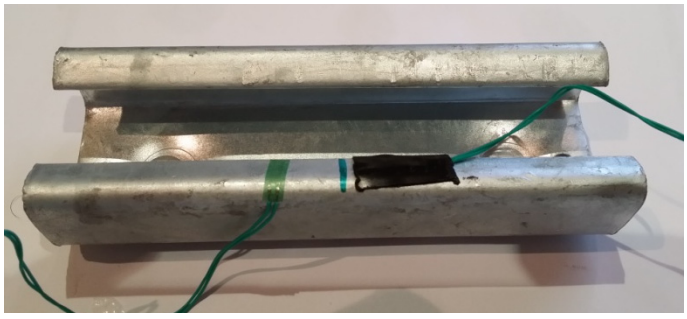

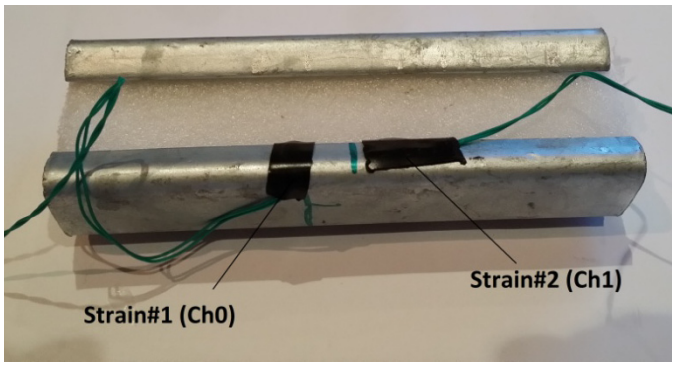

Figure 4-62: Sample-5 strain gauges location and numbering.

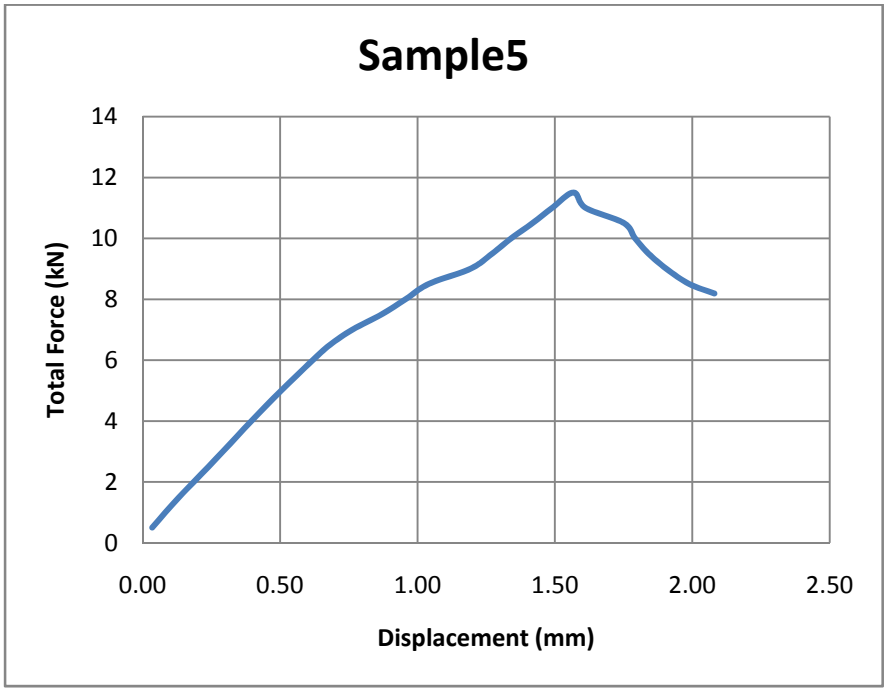

Figure 4-63: Sample-5 force Vs displacement curve.

Figure 4-64: Sample-5 after testing.

4.6.6 Sample 6

It was observed in previous samples that the shape of failure took place in the channel lip. Therefore, to improve the channel capacity, the stress needs to be distributed along larger area. However, due to hammer bolt limitation in size and difficultly in inserting mechanism of head in the channel, the hammer bolt head cannot be increased. Another approach proposed is by increasing the washer size that was placed below the nut, this sample was constructed with a bigger washer as shown in (Figure 4-65). The washer was

made of a steel plate of grade A36 and had a size of 80 mm x 80 mm x 8 mm thickness. The force vs. displacement is shown in Figure4-66.

From (Figure 4-66), the slope up to 15 kN had a different shape, the change happened because of the washer effect, but the effect start to decrease because of bolts elongation and the nut start to move away from the washer, leaving the washer lose and not attached with the channel as can be seen in (Figure 4-67).

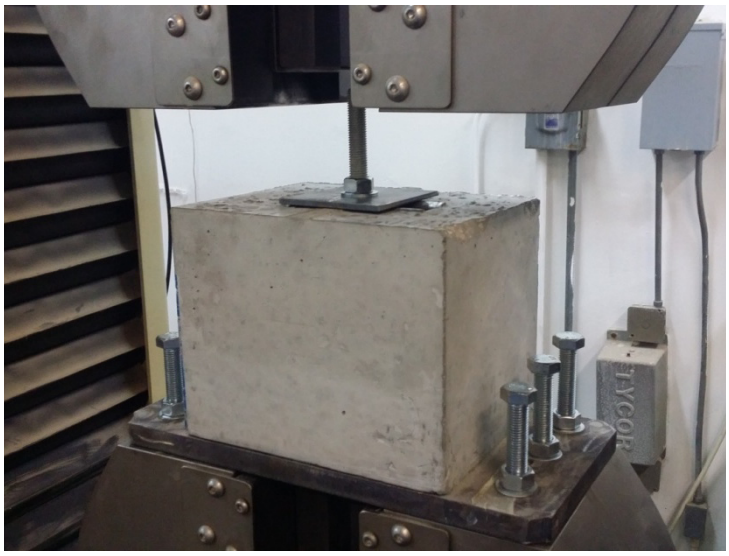

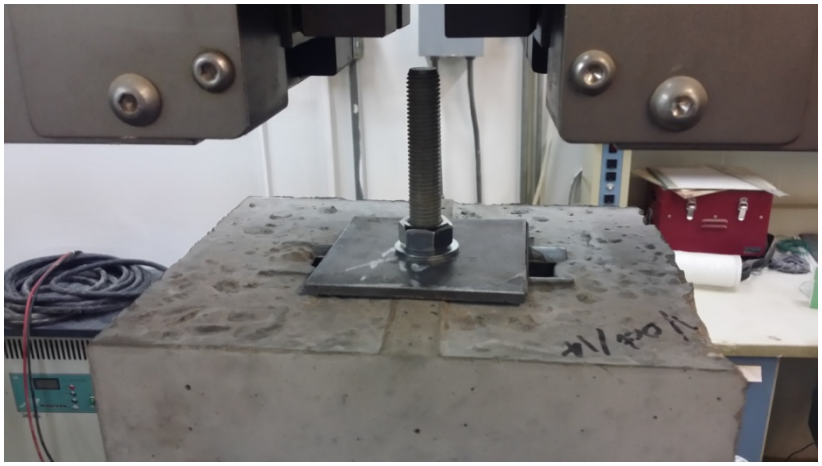

Figure 4-65: Sample-6 with a wider washer.

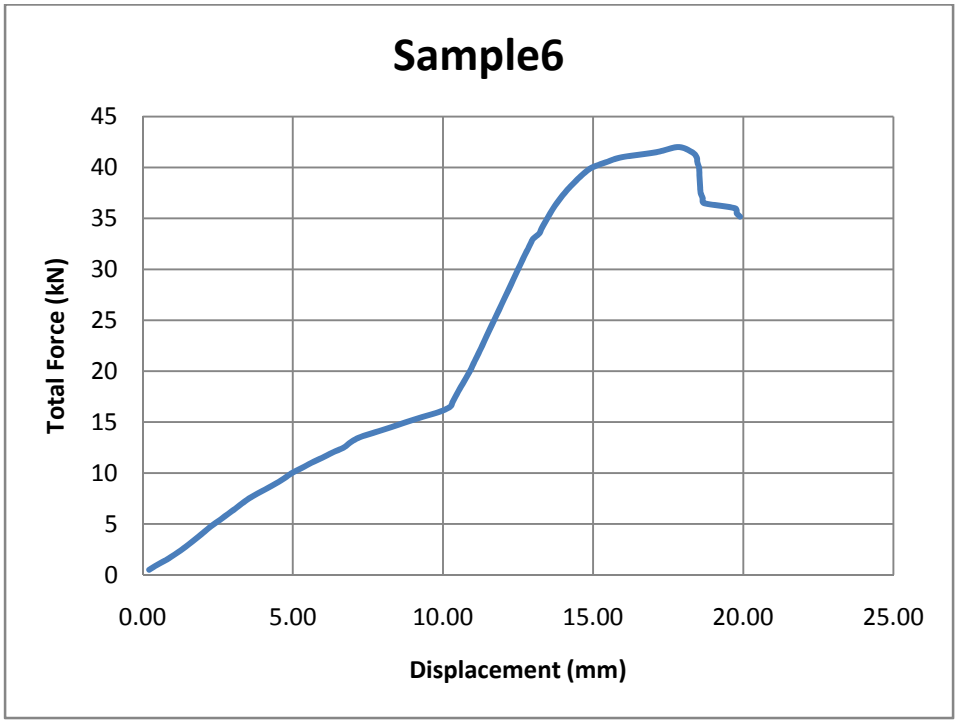

Figure 4-66: Sample-6 Force Vs. Displacement curve.

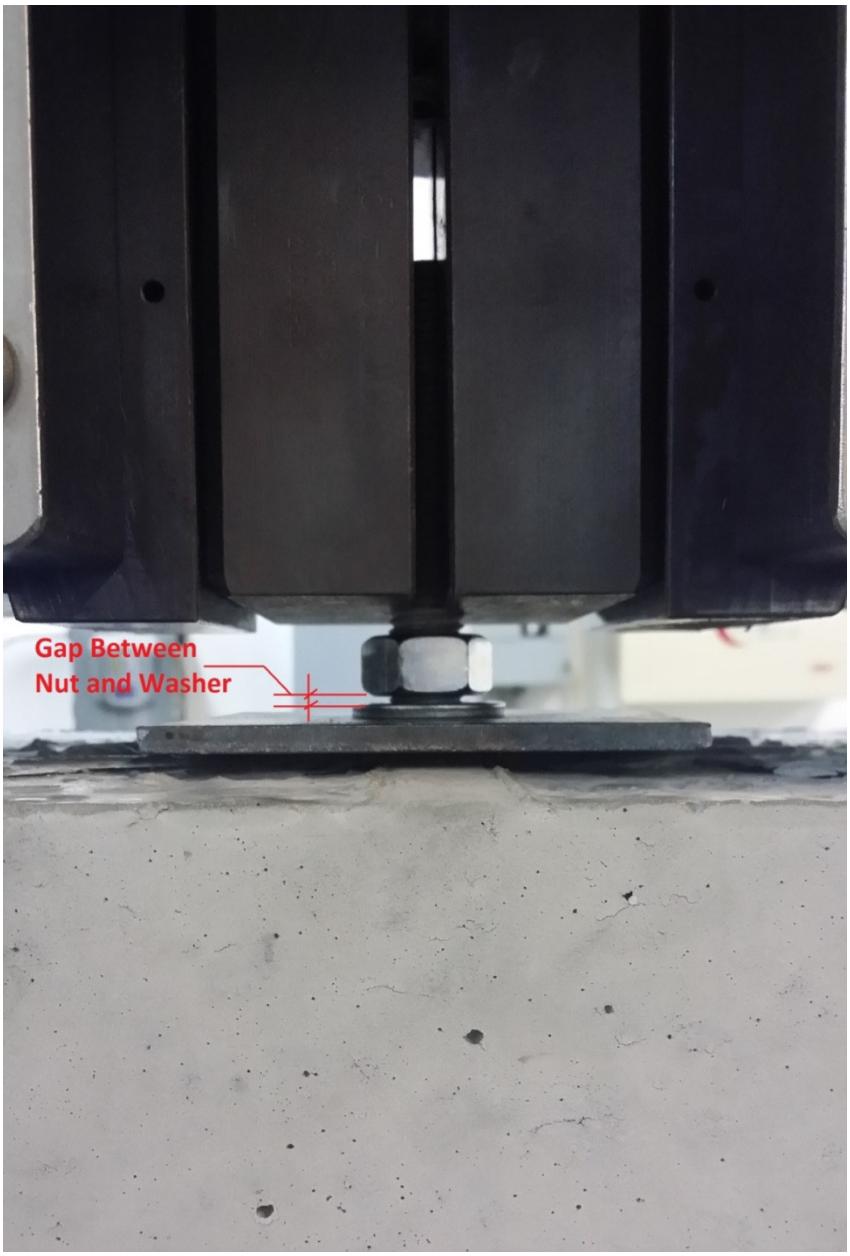

Figure 4-67: Sample-6 gap between nut and washer.

Figure 4-68: Sample-6 failure after test.

Sample 6 had similar capacity as the other samples, but different force vs. displacement curve was obtained (Figure 4-66). It is found that the washer had an effect as was predicted, but the nut separation from washer was not predicted and expected. Therefore, another sample has to be made with a washer attached to the channel by welding.

4.6.7 Sample 7

Based on the results achieved from sample 6, sample 6 was repeated but with the washer tag welded to the channel. The washer plate was the same size and material grade as that of sample 6. The washer was welded at the shop, the difference between this washer and the other washer in sample 6, is that this washer had a slot type of hole (Figure 4-69) to

enable inserting the hammer head bolts into the cast in channel. The washer was welded in four points with the channel lip (Figure 4-70), with a tag type of weld, as these four point had an easy access for the welding rod. The welding will ensure that the washer is well attached to the channel, this improvement of adding the channel, is economical and practical and may increase channel capacity. Figure 4-71 shows the force-displacement readings and curve recorded by test machine.

Figure 4-69: Sample-7 large washer with a slot hole.

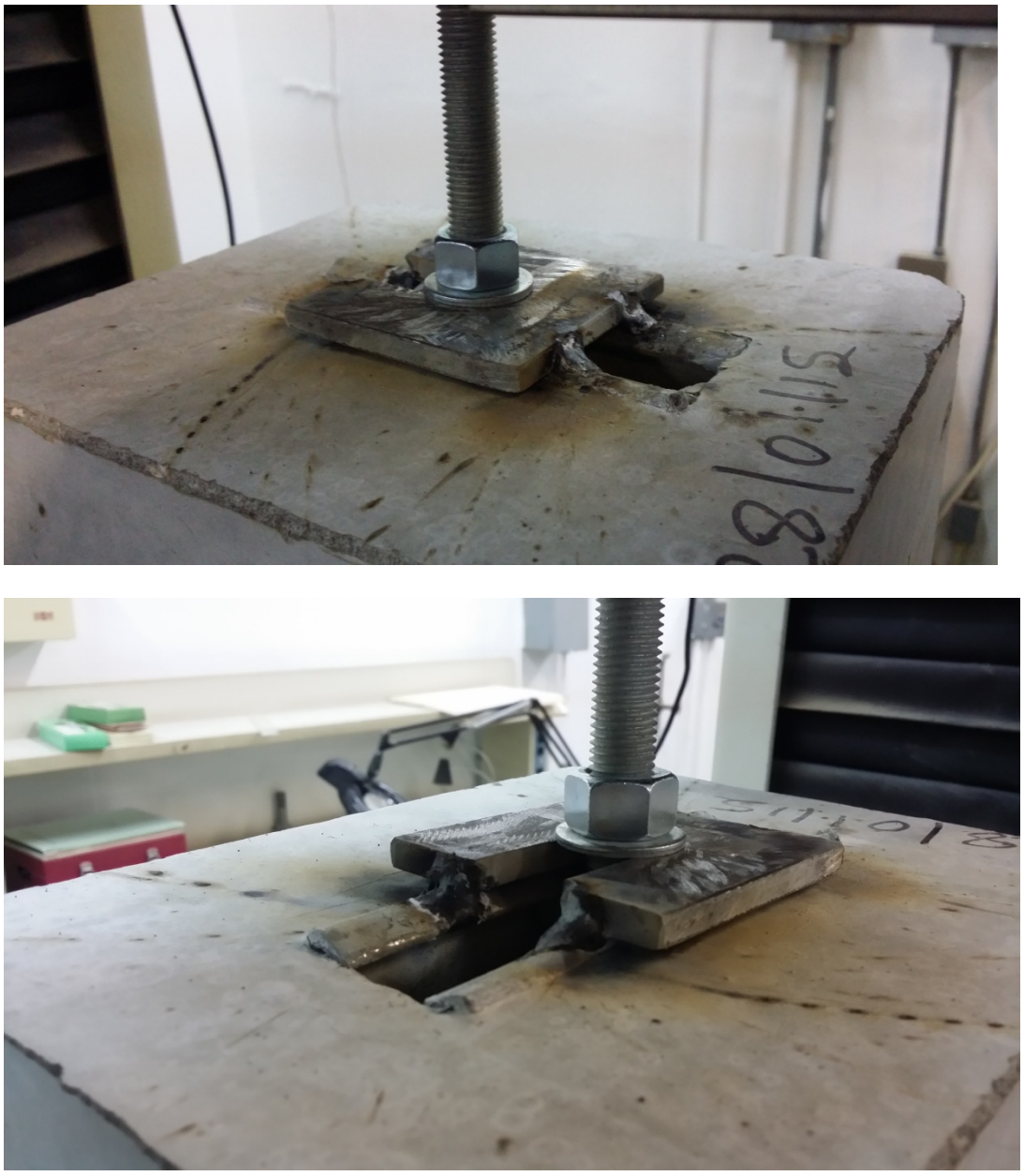

Figure 4-70: Sample-7 large washer with tag weld.

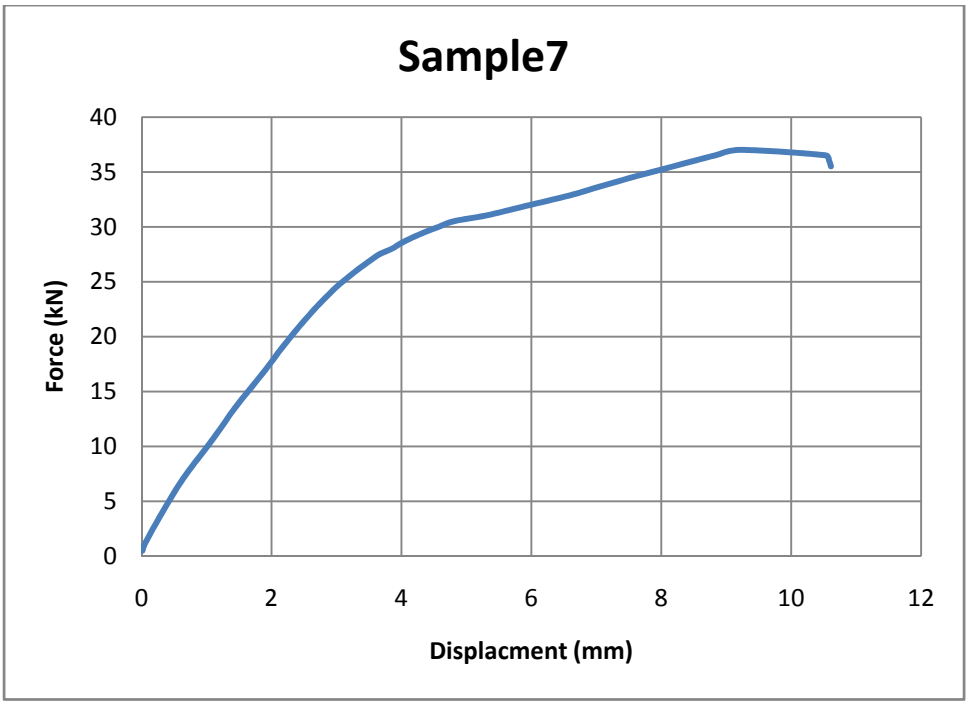

Figure 4-71: Sample-7 Force Vs. Displacement curve.

The maximum load capacity in this sample was 37 kN, and a sudden concrete breakout failure appear suddenly, which can be presented in the sudden drop in (Figure 4-71). The lip in this sample did not exhibit any local failure, although the capacity did not increased as was predicted, but there was no local failure in the lip, and the whole channel was out of the concrete by 1 cm (Figure 4-72).

Figure 4-72: Sample-7 channel projection after test.

CHAPTER 5

ANALYTICAL APPROACH

5.1 Failure Modes

As explained in Chapter 2, there are two major failure modes, one related to steel, and the other to concrete.

The major components of failure modes of the channel system are shown in (Figure 5-1).

The capacity of each component was computed. these components are as follow:

- Hammer Head Bolt.
- Cast in Channel.
- Anchorage Studs.

Every component has different failures that can be summarized in chart shown in Figure 5-2.

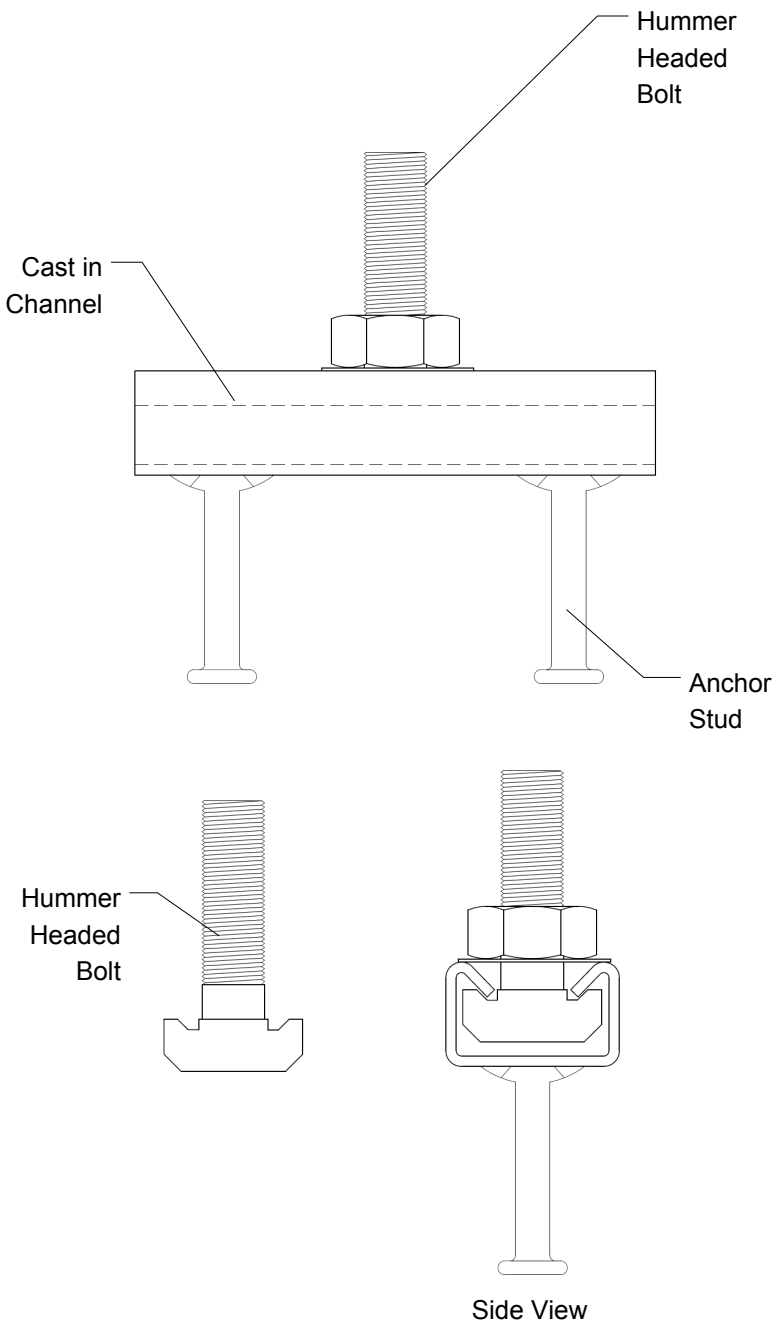

Figure 5-1: Cast in channel component

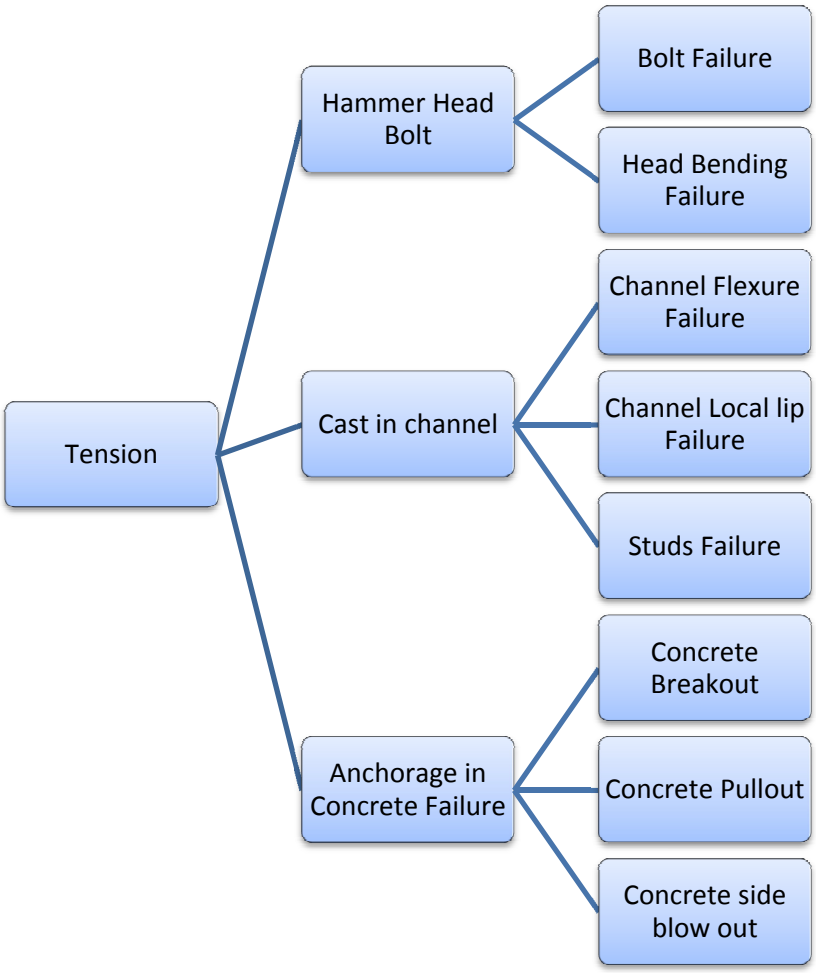

Figure 5-2: Chart showing cast in channel failure modes in tension.

The minimum value computed from all expects failure shown in Figure 5-2 is the governing failure mode. As mentioned earlier only tension will be computed in order to compare it with test results, which was made considering tension only. In addition, the shear needs to be computed but it is out of the scope of this report.

5.2 Hammer Headed Bolt Failure Modes

5.2.1 Bolt Failure

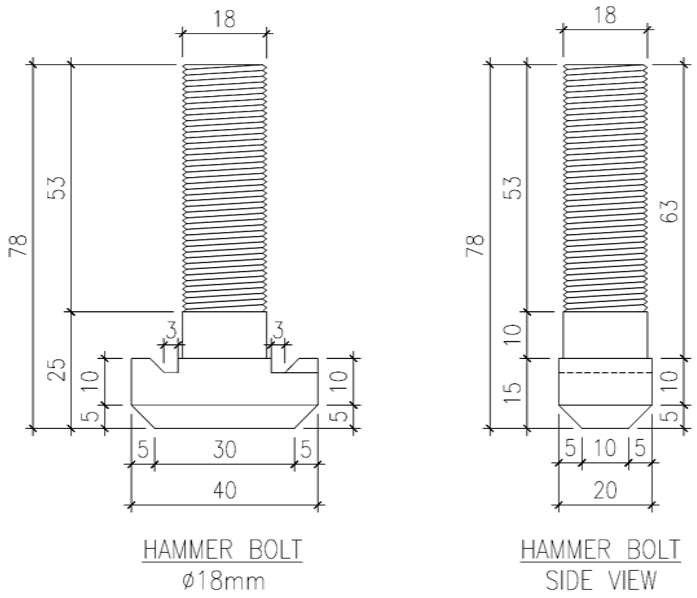

Figure 5-3: Hummer Head Bolt

The bolt used is 18 mm diameter with a head shape like a hummer or T (Figure 5-3), the bolt is of grade 4.6

As per AISC [5], the bolts capacity in tension:

$R_n = F_n A_b$ (5.1)

$R_n = 300 \times 254 =$ **76,200 N**

Where:

$F_n = 0.75 F_u = 0.75 \times 400 = 300$ N/mm^2

$F_u = 400$ N/mm^2 (58 ksi)

$A_b = 254$ mm^2 (stress area of threaded part)

5.2.2 Head Bending Failure

This failure appeared in the head of the bolt as shown in Figure 5-4;

Figure 5-4: Bending of bolts head

The bolts head was assumed to act as a cantilever beam with uniform load acting on the contact area between the channel lip and the head. Figure 5-6 shows the free body diagram of such an action.

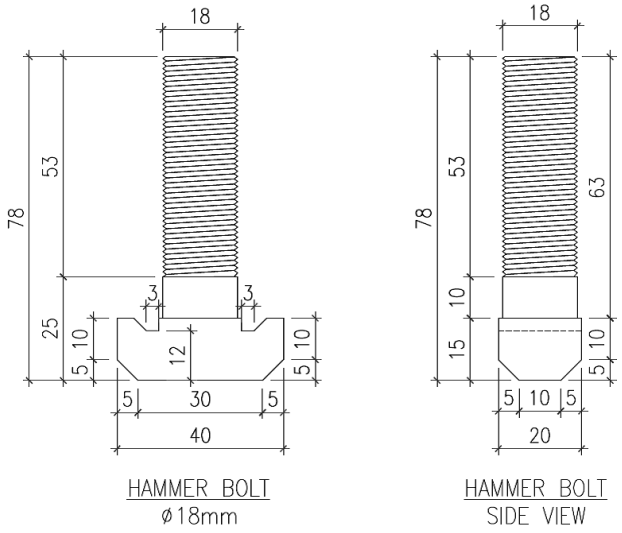

Figure 5-5: Hammer Headed Bolt Geometry

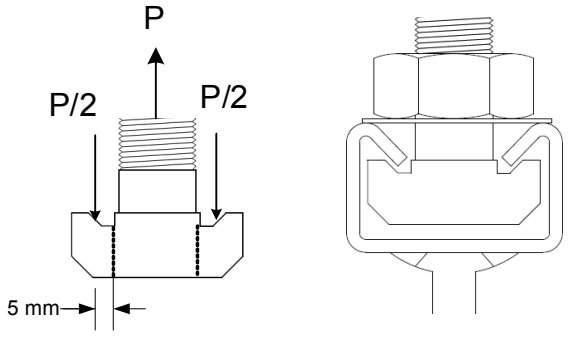

Figure 5-6: Free Body Diagram of Force acting on the bolts head

$M = (P/2)x5 = 5P/2 \rightarrow P = 2M/5$ (5.2)

$P = (2x212,400)/5 =$ **84,960 N**

The flexure capacity (M_n) is for solid rectangular cross section having a width of 20 mm and depth of 12 mm (Figure 5-5).

As per AISC [5], two limit states need to be checked, yielding and lateral-torsional buckling.

Yielding:

$\frac{L_b d}{t^2}$ = (10x12)/(20^2) = 0.3 < $\frac{0.08E}{F_y}$ = (0.08x200,000)/295 = 54 → Therefore only the limit state of yielding is govern.

$M_p = F_y Z$ = 295 x 720 = 212,400 N.mm

$Z = \frac{20 \times 12^2}{4}$ = 720 mm^3

M_e = 1.6 $F_y S$ = 1.6 x 295 x 480 = 226,560 N.mm

$S = \frac{20 \times 12^2}{6}$ = 480 mm^3

M_n = 212,400 N.mm

5.3 Cast in Channel Failure Modes

5.3.1 Flexure Failure

Since the channel is loaded in tension, the contact surface between the bottom of the channel and the concrete is under tensile stress. Furthermore, since concrete has low tensile strength, it shall be ignored and the channel can be studied as a simple supported beam with studs modeled as hinge support. Figure 5-7 shows the single line diagram of the channel system.

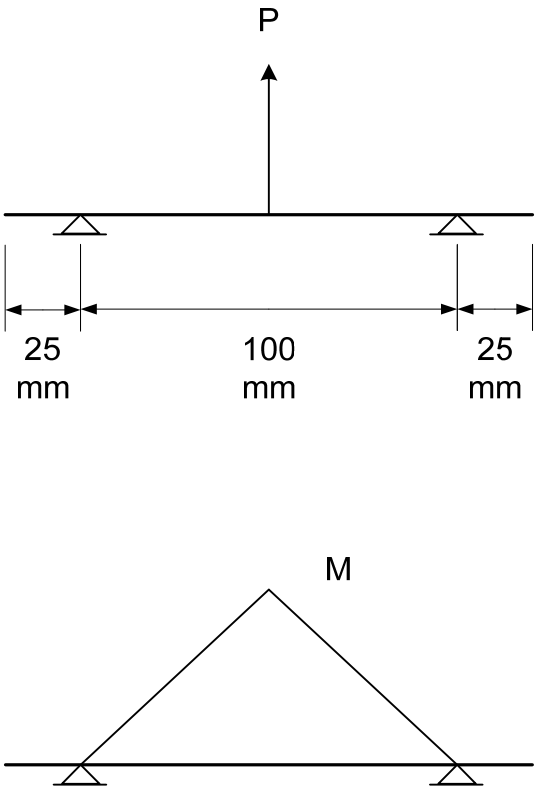

Figure 5-7: Single line diagram of the cast in channel.

Therefore, the channel flexure was computed as per the AISC [5], and the load P was determined by equating the flexure capacity (M_n) to the moment from analysis (M),

$$M = \frac{P \times 100}{4} = 25\ P \rightarrow P = M/25 \quad (5.3)$$

The channel is bended on the minor axis. Therefore, yielding and flange local buckling failure need to be checked as per the AISC [5].

Yielding:

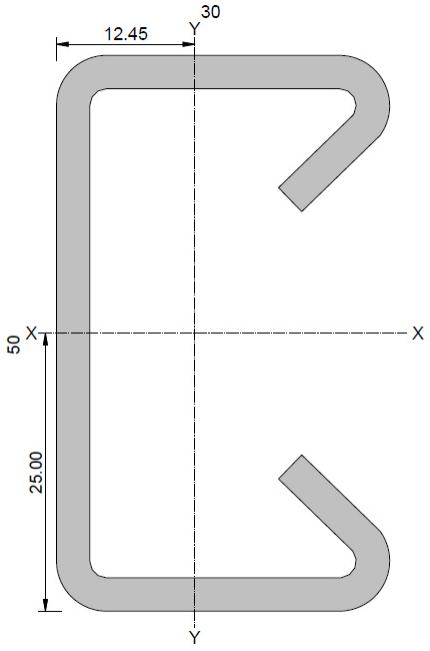

Figure 5-8: Channel local axis definition for geometrical properties computation

$S_{y\ (\text{min elastic section modulus})}$ = 2,351.8 mm^3

$Z_{y\ (\text{Plastic section modulus})}$ = 3,616.9 mm^3

$M_e = 1.6\ F_y\ S_y$ (5.4)

M_e = 1.6 x 235 x 2,351.8 = 884,276.8 N.mm

$M_p = F_y\ Z_y$ (5.5)

M_p = 235 x 3,616.9 = 849,971.5 N.mm

Flange local buckling:

λ = b/t = 30/3 = 10

$\lambda_{pf} = 0.38\sqrt{\frac{E}{F_y}} = 0.38\sqrt{\frac{200{,}000}{235}} = 11.1 > b/t$

$\lambda_{rf} = \sqrt{\frac{E}{F_y}} = \sqrt{\frac{200{,}000}{235}} = 29 > b/t$

Therefore the flange is compact

M_n is the minimum of Eq (5.4), & (5.5) = 849,971.5 N.mm

Substituting above result in Eq(5.3) yields:

P = 849,971.5 /25 = **33,999 N = 34,000 N**

5.3.2 Local Lip Failure

This failure was the most governing failure in the experiment work, yield line (YL) approach is used to compute this failure.

In most references, yield line is an approach used for concrete slabs, but it can be used also for steel plates [15].

YL is an upper bound solution and it give the collapse load (ultimate load) [16]. There are two approaches to calculate the ultimate load carrying capacity, one by using virtual work and the other is by using equilibrium method [17]. In this study, the virtual work method was used.

A yield line pattern is assumed and it is form a collapse mechanism around the bolts head as can be seen in Figure 5-9 and Figure 5-10.

Figure 5-9: Local lip failure-1

Figure 5-10: Local lip failure-2

The virtual work approach is based on the following [17]:

External work = Internal work

External work is load multiplied by the displacement at the centroid of this load and internal work on the other hand is the value of the moment multiplied by the angle of rotation [17].

Figure 5-11 shows the proposed yield line pattern.

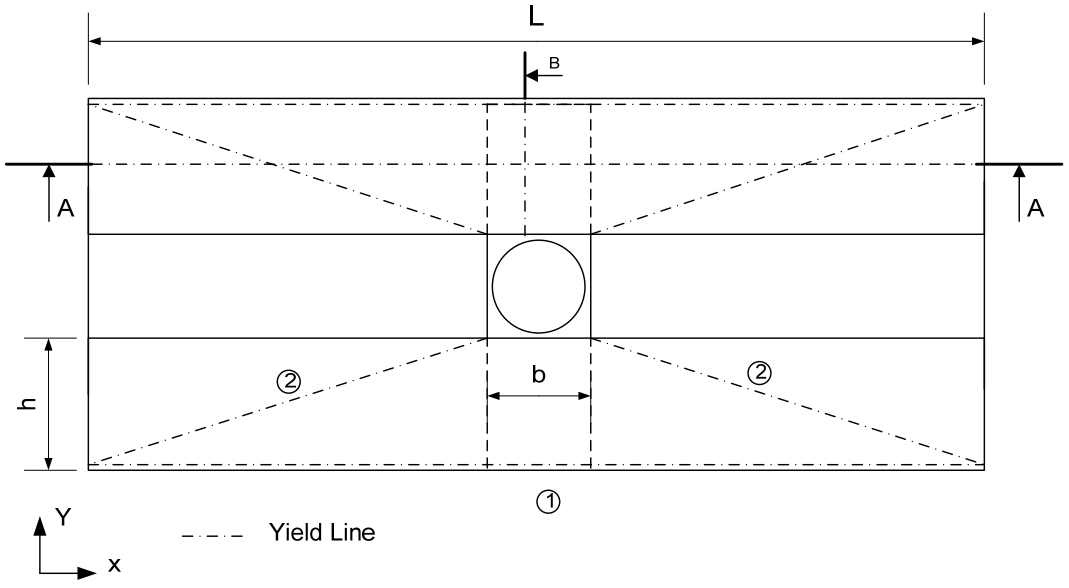

Figure 5-11: Top view of the channel and bolt with proposed Yield Line on the channel lip.

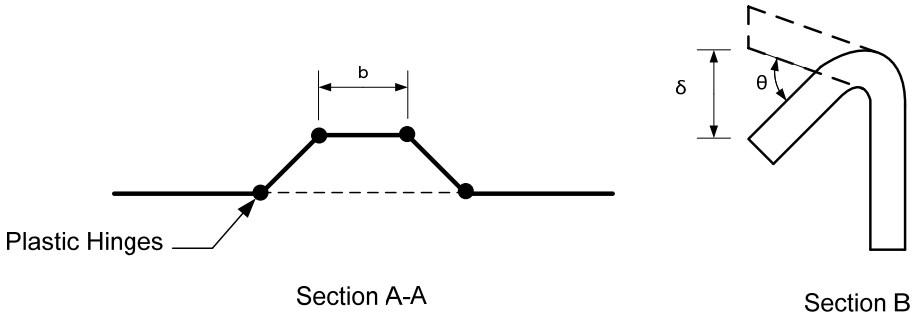

Figure 5-12: Section A-A, and section B.

h : Lip length.

b : Hammer head width.

L : Channel length.

1 & 2 : Yield line patterns.

δ : Displacement.

θ : Rotation angle.

f : Yield strength of steel.

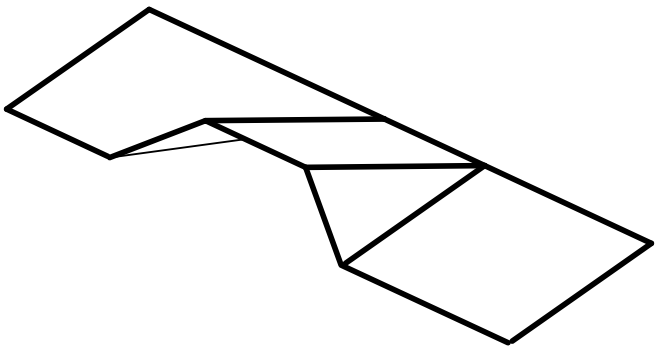

Figure 5-13: Isometric view of the proposed failure mechanism.

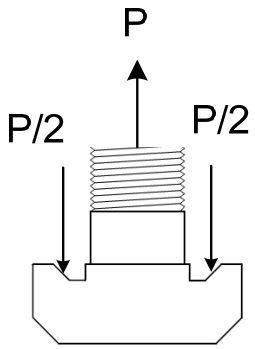

Figure 5-14: Tension Load Acting on the bolt

External work (per unit length):

External work = $\int_0^h w.\delta(x).dx = \int_0^h w.x.\theta.dx = \frac{w.h^2.\theta}{2}$ *substituting below equations yield:*

$\delta = h \cdot \theta$ & $w = P/2h$

$$\frac{w.h^2.\theta}{2} = \frac{P.h^2.\theta}{4.h} = \frac{P.h.\delta}{4.h} = \frac{P.\delta}{4}$$

External work = $\frac{P.\delta}{4}$

Internal work (per unit length):

From (Figure 5-11), three yield lines are proposed; the projection of yield line 3 was taken about x-axis and y-axis.

Internal Work = $\int_1 M.\theta_y.dx + 2\int_2 M.\theta_y.dx + 2\int_2 M.\theta_x.dx$

= $M.L.\theta_y + 2.M.\frac{(L-b)}{2}.\theta_y + 2.M.h.\theta_x$

$$\theta_x = \frac{\delta}{(L-b)/2}$$

$\theta_y = \frac{\delta}{h}$

M = Plastic moment capacity per unit length = $\frac{f.t^2}{4}$

Substituting above equation yields:

$= M.L. \frac{\delta}{h} + 2.M. \frac{(L-b)}{2}. \frac{\delta}{h} + 2.M.h. \frac{\delta}{(L-b)/2}$

$= M.\delta.(\frac{L}{h} + \frac{(L-b)}{h} + \frac{4.h}{(L-b)})$

$= \frac{f.t^2.\delta}{4} (\frac{L}{h} + \frac{(L-b)}{h} + \frac{4.h}{(L-b)})$

Internal work = $\frac{f.t^2.\delta}{4} (\frac{L}{h} + \frac{(L-b)}{h} + \frac{4.h}{(L-b)})$

Setting External work = Internal Wok

$\frac{P.\delta}{4} = \frac{f.t^2.\delta}{4} (\frac{L}{h} + \frac{(L-b)}{h} + \frac{4.h}{(L-b)})$

$P = f . t^2 . (\frac{L}{h} + \frac{(L-b)}{h} + \frac{4.h}{(L-b)})$

Substituting above with below values:

f = 235 N/mm^2

t = 3 mm

b = 20 mm

L = 14 mm

P = **43,211 N**

5.3.3 Studs Failure

The nominal strength of a single or group of anchors in tension shall not exceed [4] :

$N_{sa} = n\ A_{se,N}\ f_{uta}$ (5.6)

$N_{sa} = 2 \times 78.54 \times 490 =$ **76,969 N**

n: number of anchors in group = 2

$A_{se,N}$: effective cross sectional area of the threaded part.

$A_{se,N} = 10^2 \times \frac{\pi}{4} =$ 78.54 mm^2

f_{uta}: ultimate tensile strength.

$f_{uta} = 490\ N/mm^2 < 1.9\ f_{ya} = 1.9 \times 295 = 560.5\ N/mm^2$ & $< 860\ N/mm^2$

$f_{uta} =$ 490 N/mm^2

5.4 Concrete Anchorage Failure Modes

It is important to know the edge distance to center of studs, spacing between studs, and stud anchor length to compute concrete anchorage failure. Figure 4-1& Figure 5-15 show the geometry of the sample and the previously mentioned data.

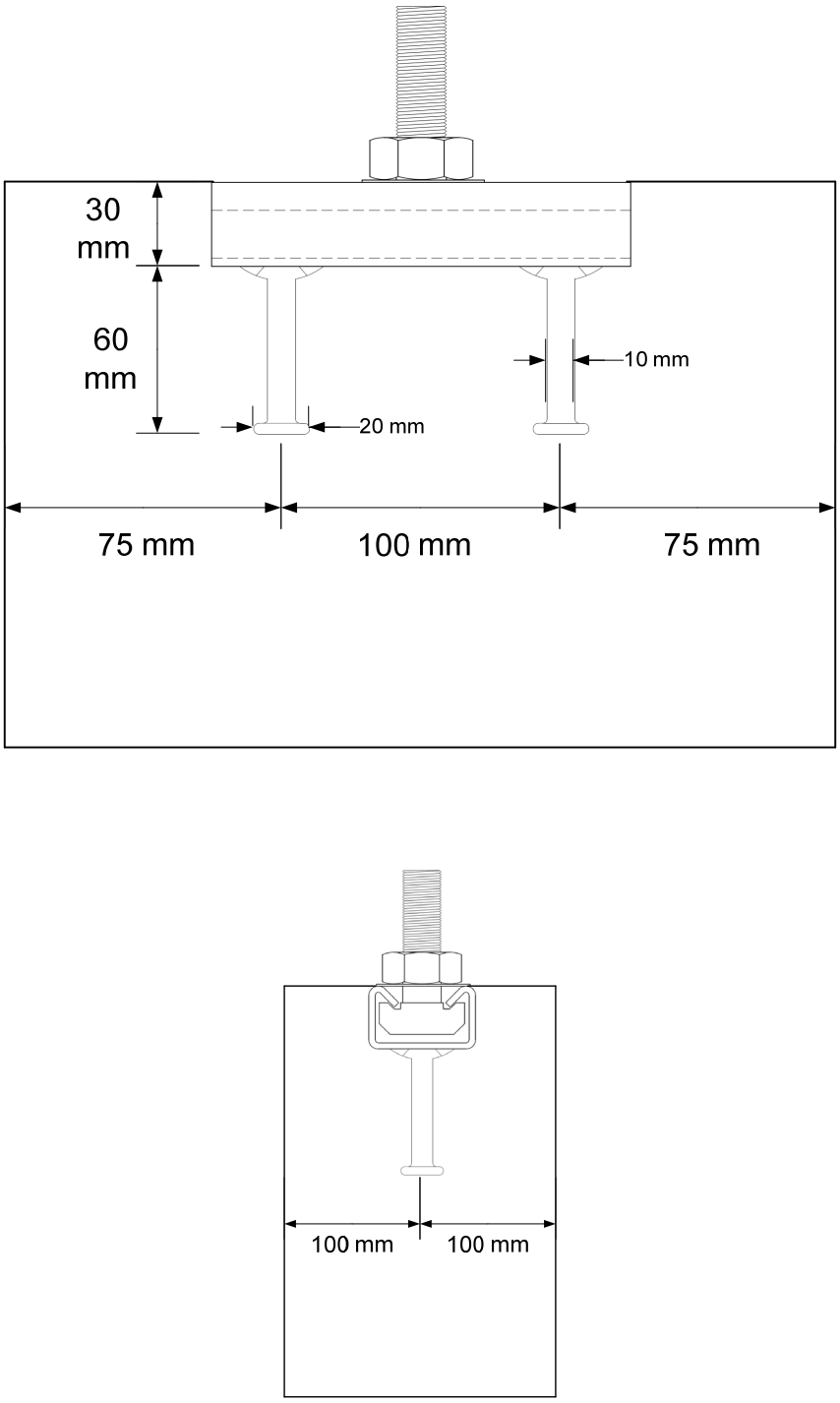

Figure 5-15: Geometry of cast in channel in the concrete test sample.

5.4.1 Concrete Breakout

As explained in section 2.3.1.1, and as shown in Figure 5-16, the nominal concrete breakout strength [4], where h_{ef} is the anchor embedment length not considering the channel depth of 30 mm (Figure 4-24), because the cone failure will reach the surface therefore it shall have a depth of (30+60 = 90mm) as shown in (Figure 5-17).

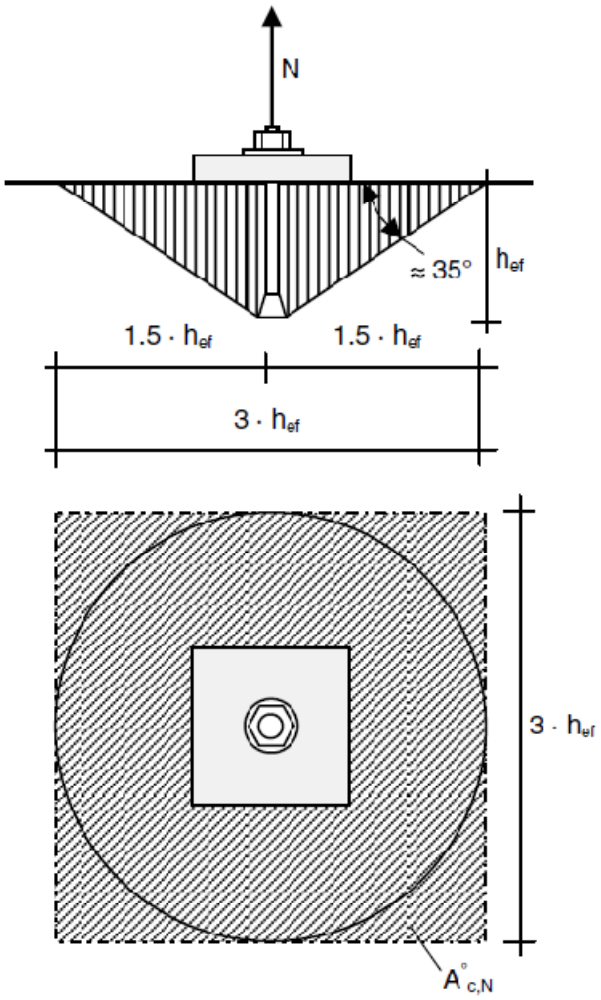

Figure 5-16: Schematic presentimg h_{ef}

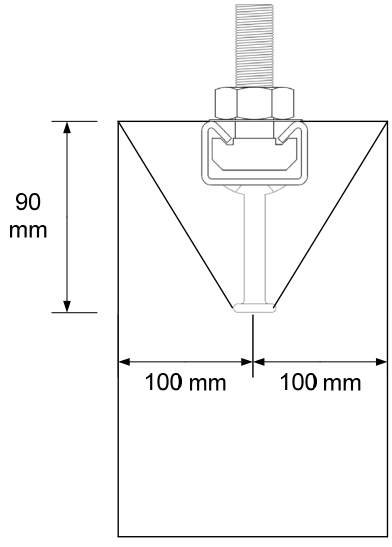

Figure 5-17: Breakout failure of cast in channel.

For a group of anchor:

$$N_{cbg} = \frac{A_{Nc}}{A_{Nco}} \psi_{ec,N} \psi_{ed,N} \psi_{c,N} \psi_{cp,N} N_b \quad (5.7)$$

N_{cbg} = (13,500/6,750) x 1 x 0.95 x 1.25 x 1 x 29,394 = **69,810 N**

A_{Nc} : projected concrete failure area of a single anchor or group of anchors (Figure 2-9).

1.5 h_{ef} = 1.5 x 60 = 90 mm

c_{a1} = 75 mm < 1.5 h_{ef} → 75 mm will be used

c_{a2} = 100 mm > 1.5 h_{ef} → 90 mm will be used

A_{Nc} = (75 + 100 + 75) x 180 = 45,000 mm^2

nA_{Nco} = 2 x 6,750 = 13,500 mm^2 < A_{Nc} therefore nA_{Nco} will be used

A_{Nco} : projected concrete failure area of a single anchor with an edge distance ≥ 1.5 h_{ef}.

A_{Nco} = 75 x 90 = 6,750 mm^2

$\psi_{ec,N}$: modification factor for anchor groups loaded eccentrically in tension.

$\psi_{ec,N}$ = 1.0

$\psi_{ed,N}$: modification factor for edge effects.

$c_{a,min}$ = 75 mm < 1.5 h_{ef} = 90 mm

$\psi_{ed,N}$ = 0.7 + 0.3 (75/90) = 0.95

$\psi_{c,N}$: modification factor to account for cracked or un-cracked concrete.

Concrete is non-cracked since it is not loaded.

$\psi_{c,N}$ = 1.25

$\psi_{cp,N}$: factor to consider and control splitting in concrete.

Since the channel is embedded before concrete casting,

$\psi_{cp,N} = 1.0$

N_b : basic concrete breakout strength.

$$N_b = k_c \lambda \sqrt{f_c'}\, h_{ef}^{1.5} \quad (5.8)$$

$N_b = 10 \times 1 \times \sqrt{40} \times 60^{1.5} = 29{,}394$ N

$k_c = 10$ (cast-in anchors)

5.4.2 Concrete Pullout

The pullout strength of a single anchor in tension is shown in Figure 2-10:

$$N_{pn} = \psi_{c,P}\, N_p \quad (5.9)$$

$N_{pn} = 1.4 \times 75{,}398 = 105{,}557$ N

For both studs the pullout strength is:

$\phi N_{pn} = 105{,}557 \times 2 =$ **211,114 N**

$\psi_{c,P}$: modification factor to account for cracked or un-cracked concrete.

$\psi_{c,P} = 1.4$ (Un-cracked concrete)

$$N_p = 8\, A_{brg} f_c' \quad (5.10)$$

$N_p = 8 \times 235.6 \times 40 = 75{,}398$ N

A_{brg} : net bearing area of the head of stud.

$A_{brg} = (20^2 - 10^2)\frac{\pi}{4} = 235.62$ mm^2

5.4.3 Concrete Side-Face Blowout

$h_{ef} = 60$ mm $< 2.5 \times 75 = 187.5$ mm therefore side-blow out will not occur, as the anchor is not deeply embedded [4].

5.5 Summary

Below (Table 5-1) is summary of all failure loads with the critical failure load is highlighted:

Table 5-1: Summary of failure loads on cast in channel

Failure Type	**Failure Value (kN)**
1) Bolt	76.2
2) Bolt Head Bending	84.96
3) Channel Flexure	**34**
4) Channel Local Lip	**43.21**
5) Studs	76.97
6) Concrete Breakout (cone)	69.81
7) Concrete Pullout	211
8) Concrete side blowout	N/A

As shown from Table 5-1, the governing failure capacity is the channel local lip failure, which is same result that was achieved from most of the failure in the experimental work.

CHAPTER 6

COMPUTATIONAL MODEL

6.1 Introduction

As explained in literature review, more than one failure modes is expected to happen. Therefore, finite element modeling (FEM) approach was used to develop and simulate the cast in-channel to estimate and observe the failures modes and compare it with the real experiment work.

The sample was composed of cast in-channel embedded and confined in concrete. In FE, the concrete can be modeled by using different approaches. These two approaches are concrete smeared cracking model and concrete damage plasticity (CDP) model [18].

In this study, the (CDP) model is used to predict the failure load and cracking patterns of the assembly.

There is a wide variety of commercial and research FEM software such as ANSYS, ABAQUS and DAINA. ABAQUS was used in this study to simulate the failure modes.

6.2 Modeling Approach

ABAQUS was used to simulate the specimens and input parameters for concrete and steel have to be entered. These parameters are stress-strain diagram for concrete and steel.

C3D8R 8-node linear brick, reduced integration, and hourglass control element is used in modeling of all parts of the model (concrete, C-channel, nuts, bolts, and steel studs).

The interaction between the walls of C-Channel and the concrete is modeled by using general concrete with coefficient of friction of 0.75 and limit of shear stress of 1.33 MPa (as measured) whereas the interaction between the two studs and the concrete was assumed to be perfect bond.

Three specimens were simulated as follow:

- Model (SP1) with cast in-channel fully embedded in concrete (Sample 1, & 2).
- Model (SP2) with cast in-channel studs only embedded in concrete (Sample 4, Figure 4-54).
- Model (SP3) with washer plate tag welded to cast in channel (Sample 7, Figure 4-70).

As mentioned earlier, (CDP) model is used in ABAQUS. Table 6-1 shows the concrete parameters in (CDP) model.

Table 6-1: Concrete parameters for plastic damage model.

Young's Modulus MPa	Poisson's Ratio	Dilation Angle ψ Degree	Eccentricity ε	f_{bo}/f_{co}	K
30000	0.18	36	0 .1	1.16	0.67

Another important parameter is the damage factor, that is measured beyond the elastic region which is at stress approximately 30% [19] of the maximum concrete compressive

strength (f'_c). It can be calculated from the slope of the cyclic curve generated from loading and unloading the concrete cylinder samples.

This factor was taken at every strain point for the cyclic curve and all points was added to ABAQUS along with the stress vs. strain points of the concrete compressive diagram.

The cyclic curve can be generated from test by loading and un-loading a concrete cylinder or can be estimated from analytical procedure. There are two methods, one is suggested by Saenz (1964) [19], and the other by Tsai [20].

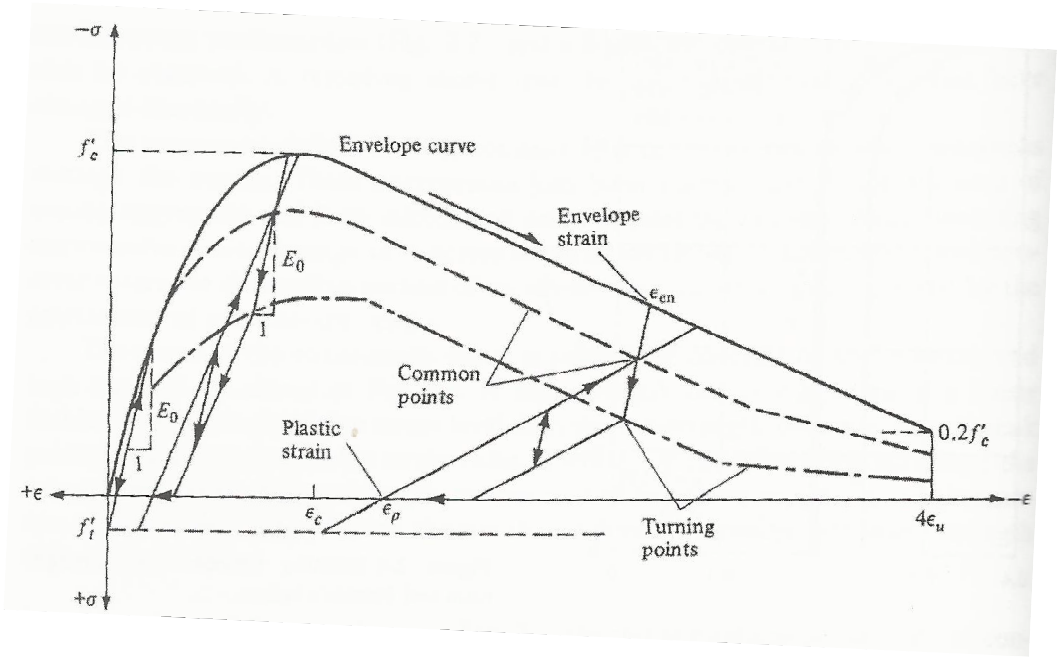

Figure 6-1: Proposed model under cyclic behavior [21].

Saenz analytical model suggests using the following equation [19]:

$$\sigma = \frac{E_0 \epsilon}{1+[(E_0/E_S)-2](\epsilon/\epsilon_C)+(\epsilon/\epsilon_C)^2} \quad (6.1)$$

It is used to describe the ascending branch of the stress-strain curve shown in Figure 6-1, and the falling branch is assumed straight line.

Tsai model is a bit different than Saenz as it is more generalized and the equation tend to control the ascending and descending behavior. In this study, equation 6.2 is used in ABAQUS to input the concrete stress-strain diagram points as shown in Figures 6-2 and 6-3.

$$y = \frac{mx}{1+\left(m - \frac{n}{n-1}\right)x + \frac{x^n}{n-1}} \qquad (6.2)$$

Where

$y = f_c / f'_c$

$x = \varepsilon / \varepsilon_c$

$m = 1 + (17.9/f'_c)$ (MPa)

$n = (f'_c/6.68) - 1.85 > 1$ (MPa)

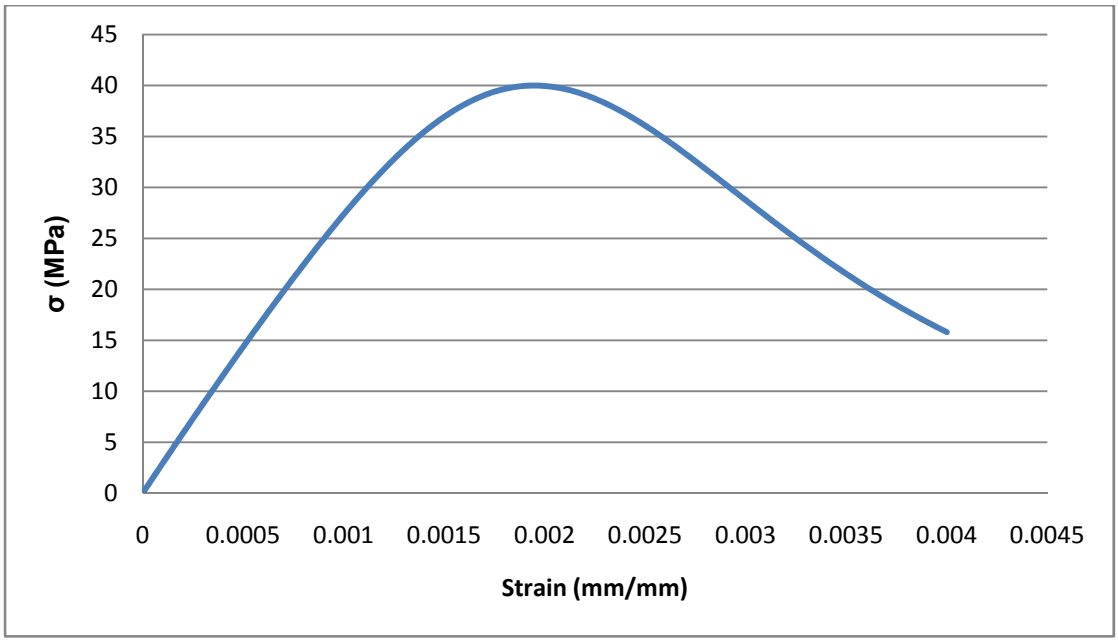

Figure 6-2: Stress-Strain diagram of concrete with 40 MPa using Tsai (Eq6.2).

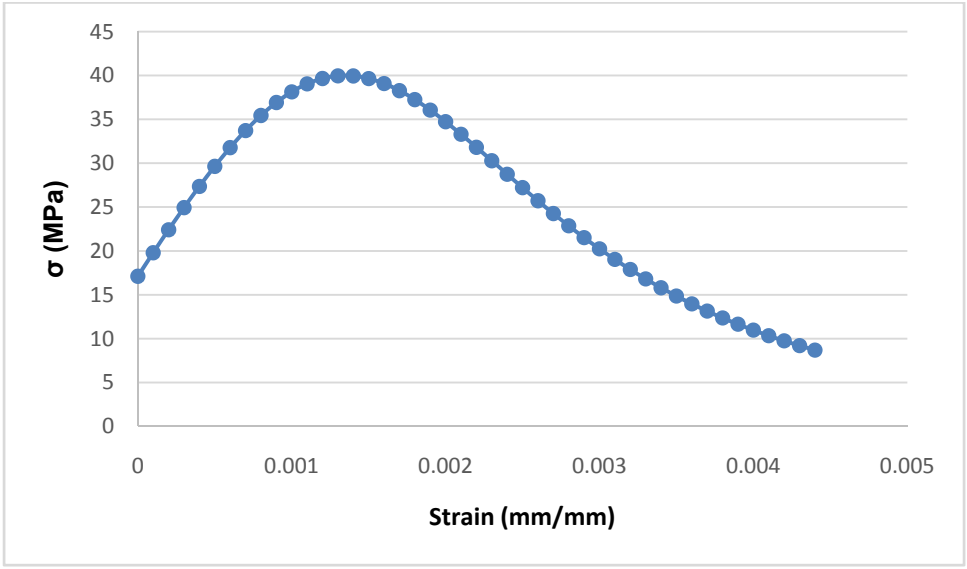

Figure 6-3: $0.4f'_c$ curve for damage factor.

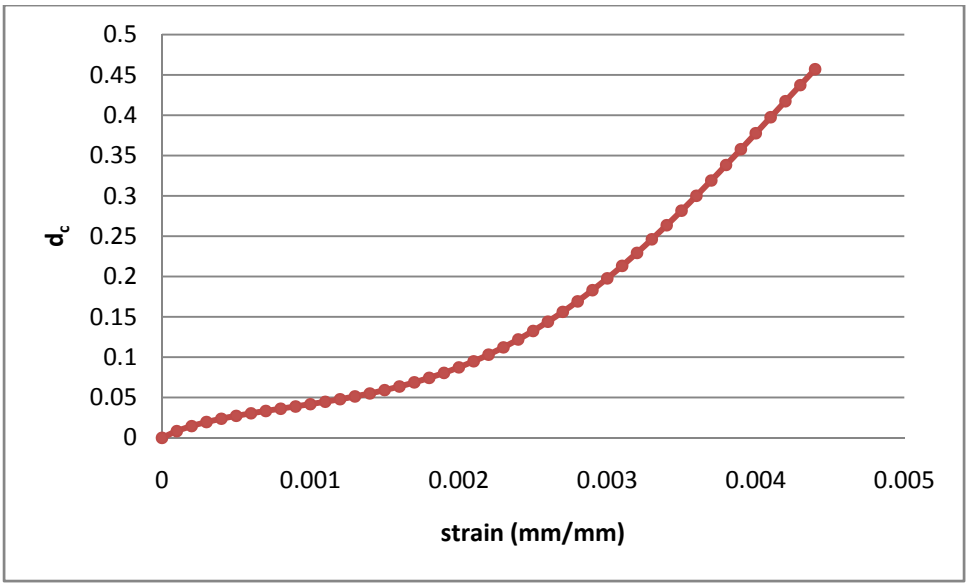

Figure 6-4: Damage factor (d_c) Vs. Strain Diagram.

Figure 6-4 shows the damage factor for concrete in compression used in ABAQUS to capture the cracking failure in concrete. It is estimated by using Eq (6.3) [22].

$$d_c = 1 - \frac{\sigma_c E_c^{-1}}{\varepsilon_c^{pl}\,(1/b_c - 1) + \sigma_c E_c^{-1}} \qquad (6.3)$$

For steel, also the hardening curve was inserted in ABAQUS model to capture the plastic behavior of the cast in channel as shown in Figure 6-5.

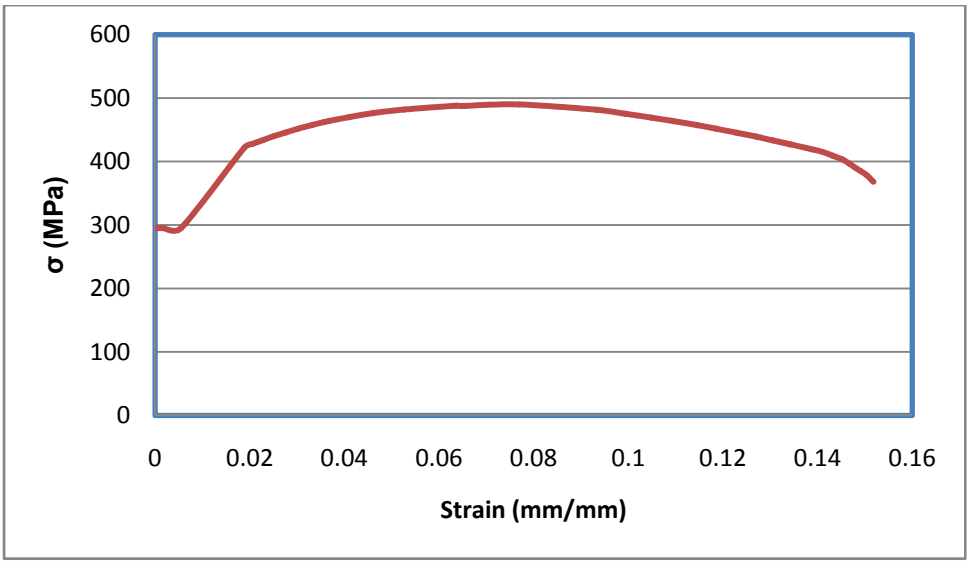

Figure 6-5: Stress Vs Strain diagram for St50-2 steel grade used in cast in channel.

For both concrete and steel, elastic region is inserted as linear lines by inputting the modulus of elasticity for concrete and steel as well as Poisson's ratio and material density.

6.3 Model SP1

This model as mentioned above is a simulation of sample 1 (Figure 4-30), and sample 2 (Figure 4-42). The details of the finite element model of the C-channel, and concrete and its meshing is shown in (Figure 6-6) and (Figure 6-7). Figure 6-8 shows the force-displacement curve obtained from FE model of sample #1. It can be seen that excellent agreement is found between the failure load from FEM and experimental work that is 45 kN. In addition, it can be observed from Figures 6-9 and 6-10 that the failure modes of the specimen and the cracking pattern of concrete due to the uniaxial tension load in the experimental work and finite element analysis are almost similar.

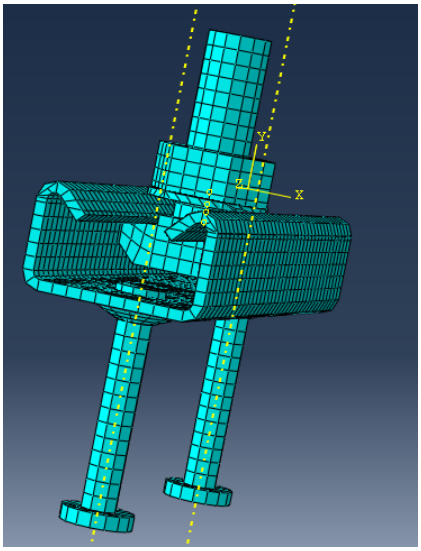

Figure 6-6: ABAQUS meshed model of the cast in channel.

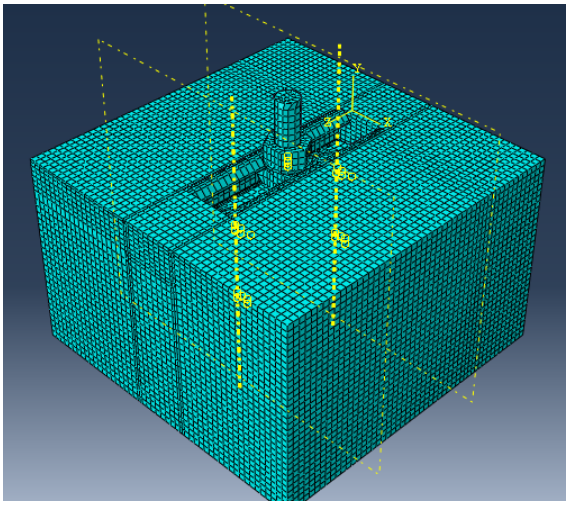

Figure 6-7: ABAQUS meshed model of the complete SP1.

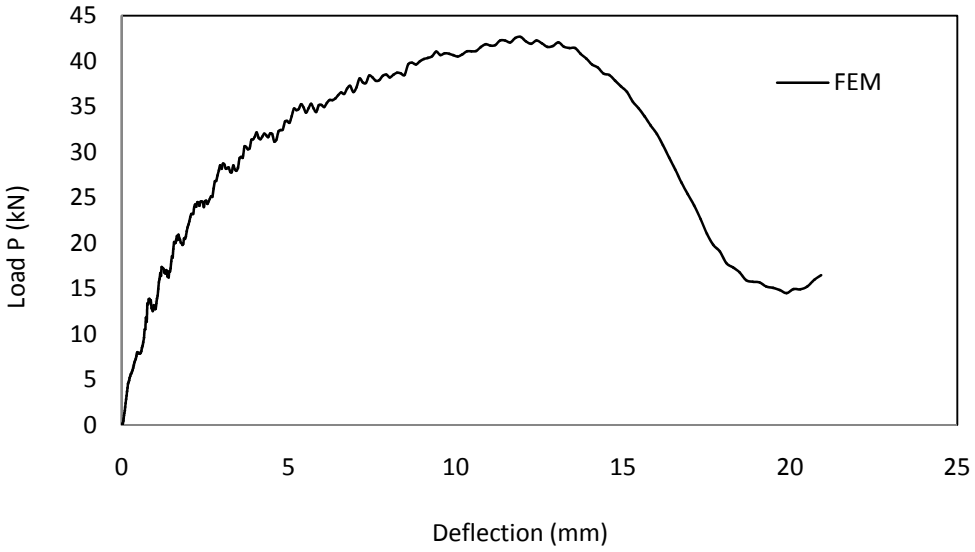

Figure 6-8: Force Vs Displacement curve of model SP1.

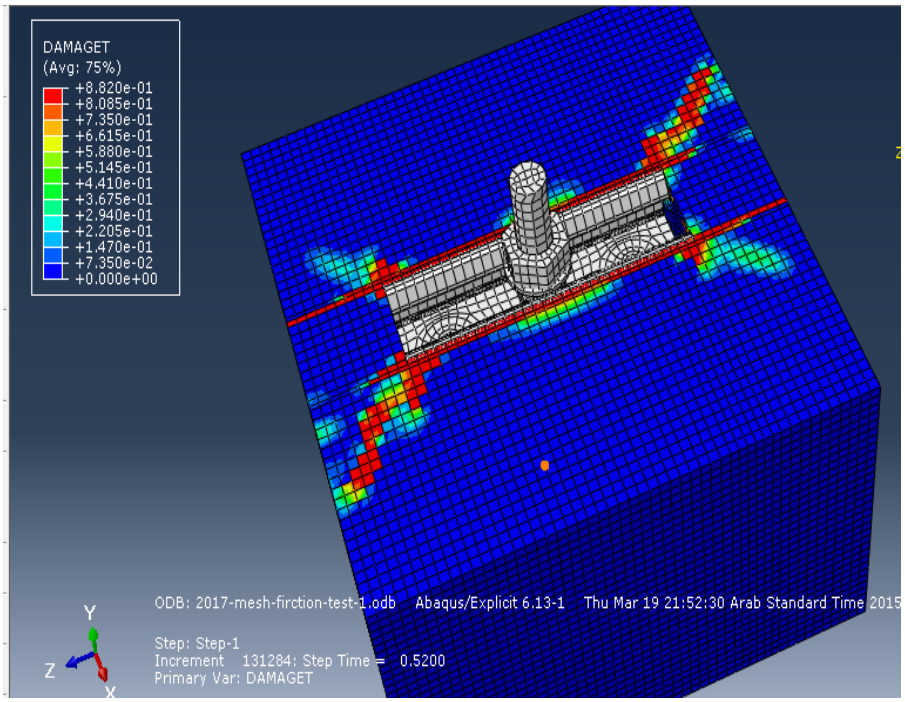

Figure 6-9: Model SP1 damage result.

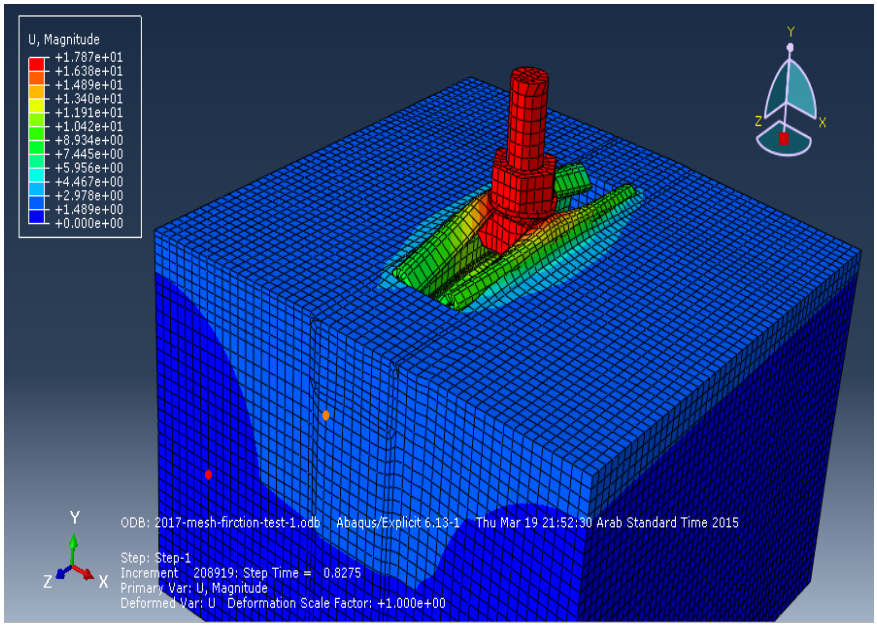

Figure 6-10: Model SP1 bolt slipping from channel.

6.4 Model SP2

SP2 is a simulation of sample 4.Figure 4-54 shows sample with cast in-channel studs embedded in concrete. The maximum load computed is 40 kN as shown in Figure 6-14 .

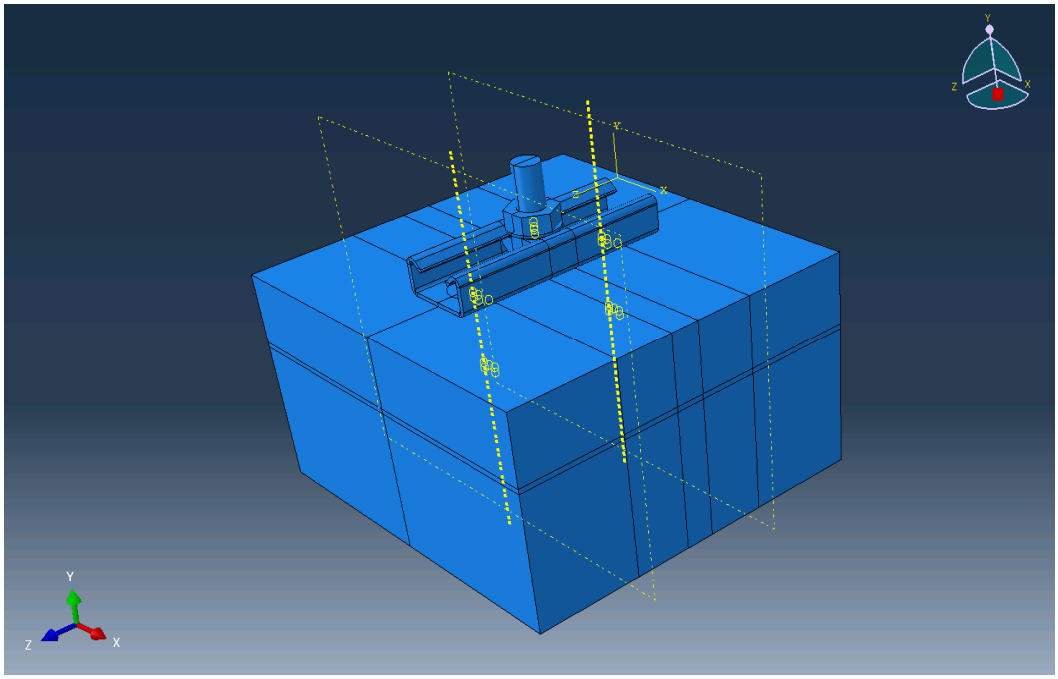

Figure 6-11: Model SP2 before meshing.

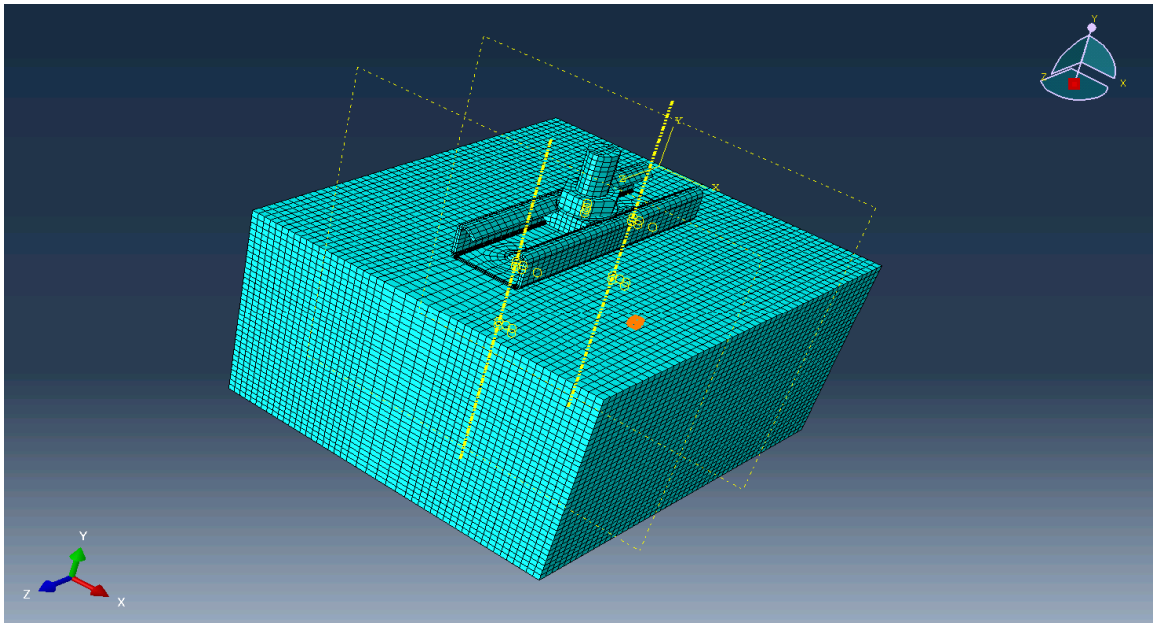

Figure 6-12: Meshed view of SP2.

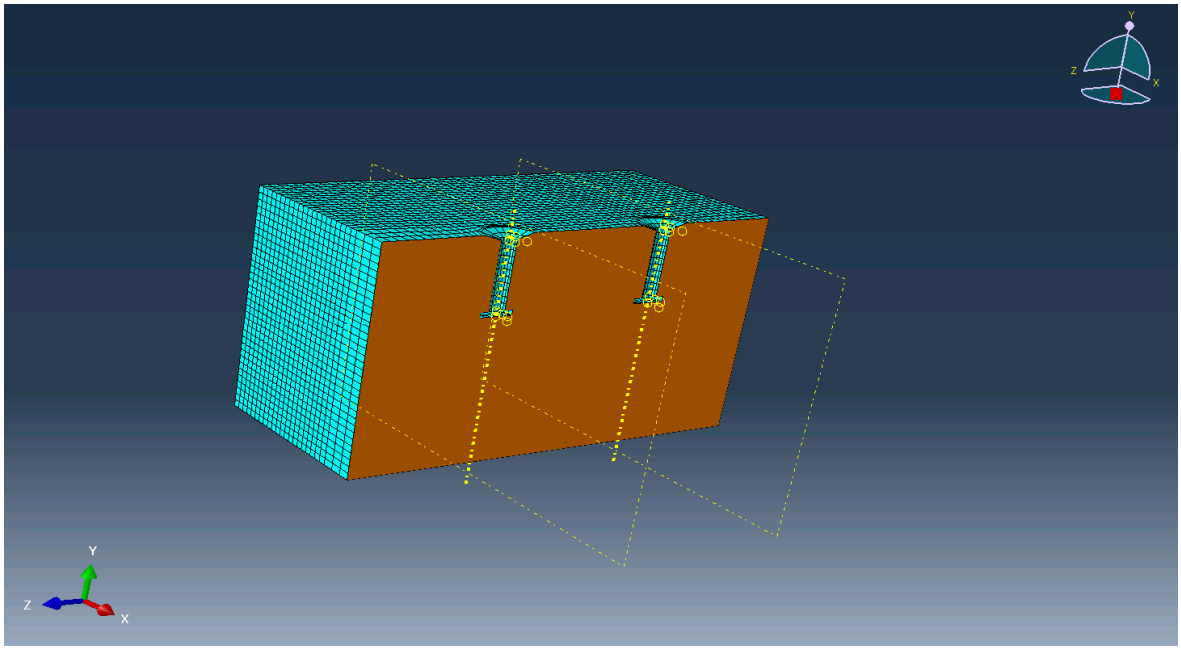

Figure 6-13: Cross section meshed view of SP2.

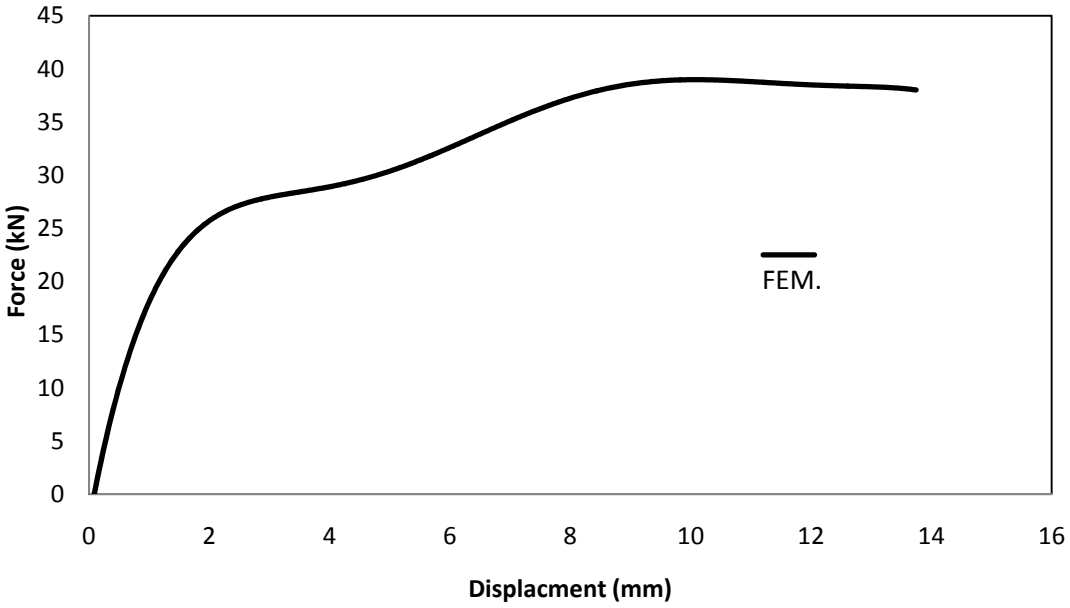

Figure 6-14: Force Vs. Displacement for model SP2.

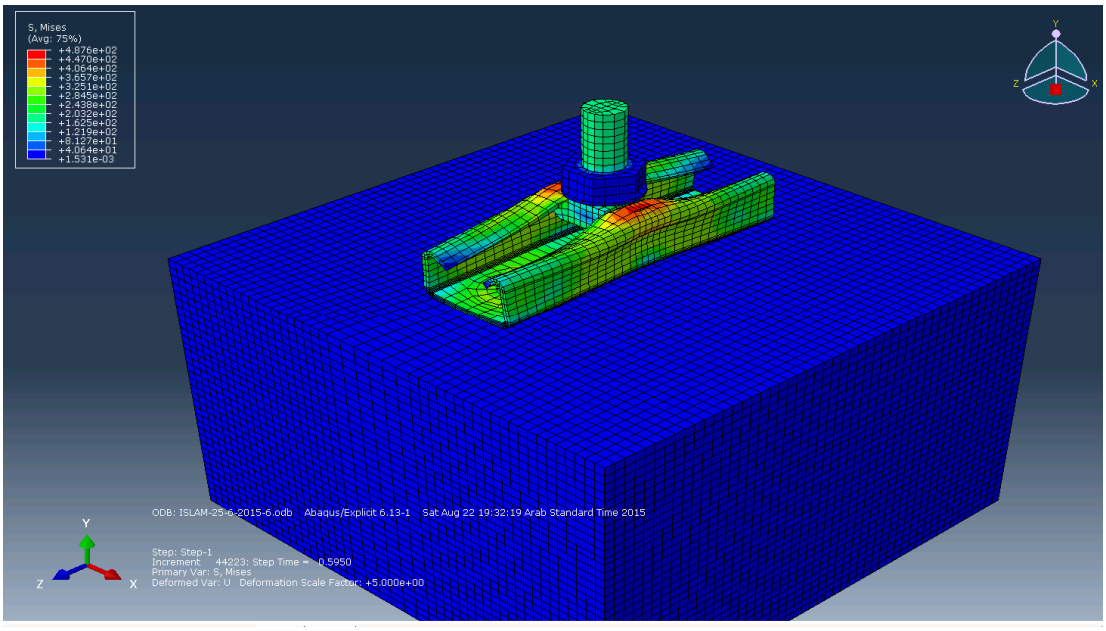

Figure 6-15 : Local lip and channel failure in SP-2 ABAQUS model.

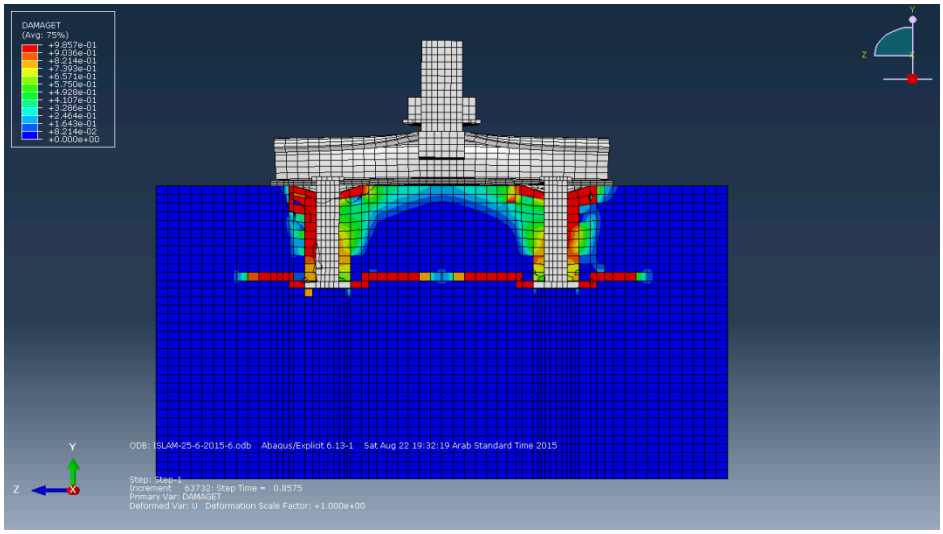

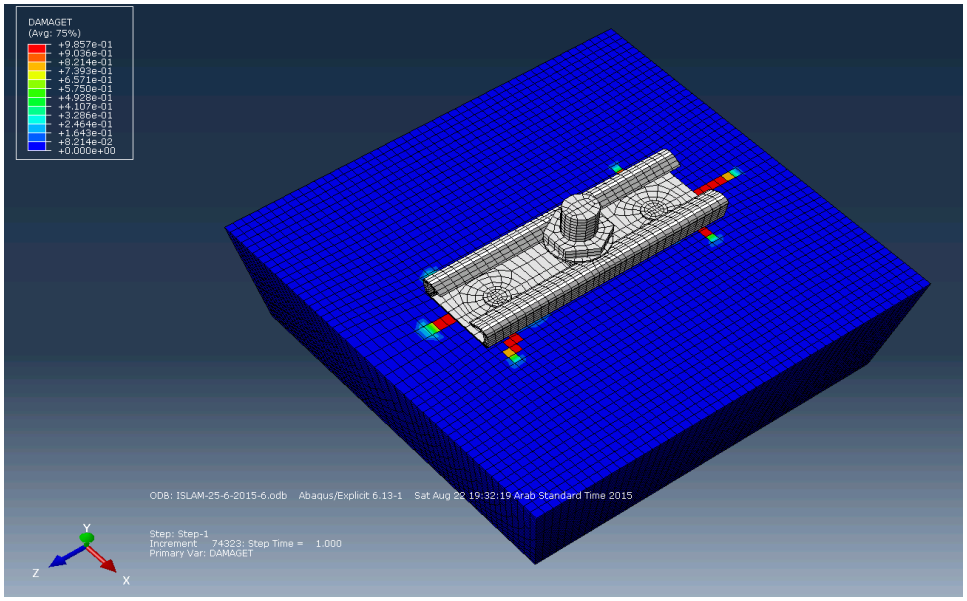

Figure 6-16: Concrete failure in SP-2 ABAQUS model.

CHAPTER 7

DISCUSSION OF RESULTS

7.1 Experimental work

Table 7-1 shows the seven samples that were tested along with the capacity of each sample. It can be seen that samples 1, 2, & 3 had similar conditions, as they were embedded and confined by concrete, whereas samples 6 & 7 were stiffened by the wide washer plate on top.

Table 7-1: Summary of tested samples

Sample	Description	Failure load (kN)
1	First sample to be tested.	45
2	Second sample and was made without welded rebars.	45
3	Same as sample 2 but with strain gauges attached to the channel.	33.5
4	Studs only were embedded in concrete in order to capture the concrete anchorage failure.	41

5	Studs were removed from channel to monitor the anchorage capacity of channel without the studs.	11.5
6	Same as sample 2 but using wider washer plate to strengthen the channel lip.	42
7	Same as sample 6 but using wider washer plate and welded to the channel lip.	37

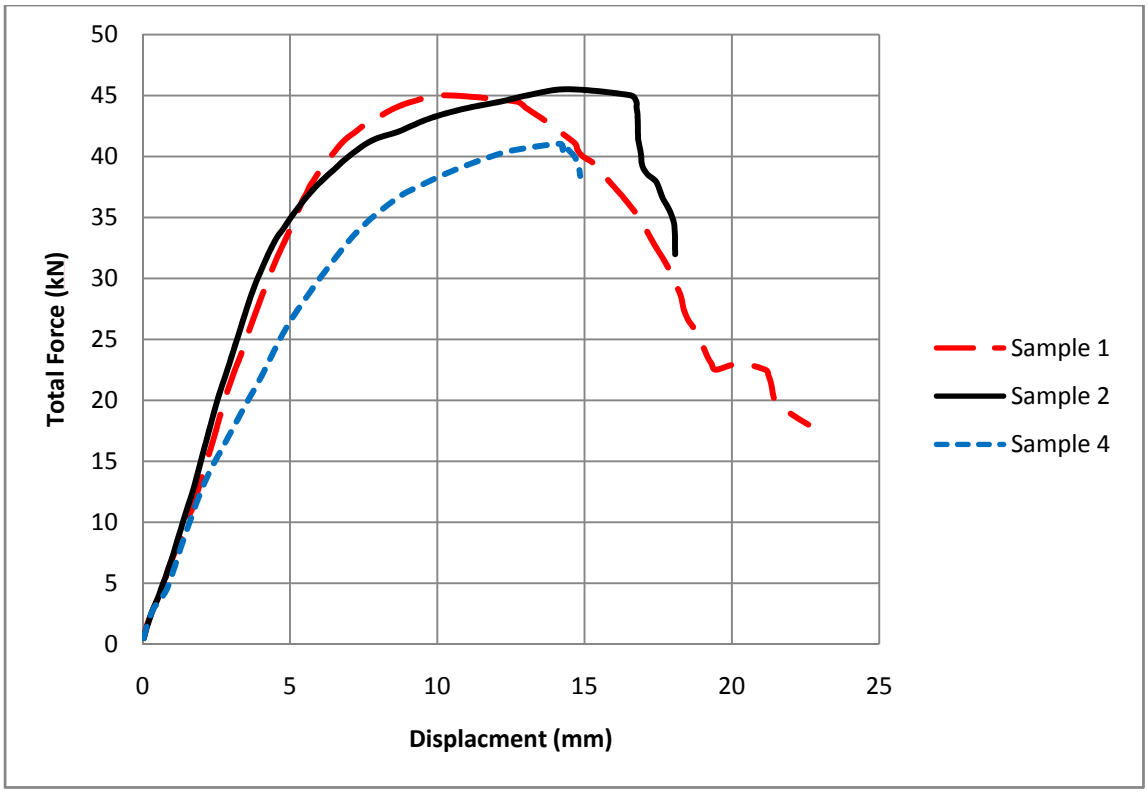

Figure 7-1: Comparison of sample 1, 2, & 4.

It was observed that samples 1, 2, 3, & 4 had a local plastic failure deformation in the channel. Figure 7-1 shows force vs. displacement diagram for samples 1, 2 and 4. It can be noted that sample 1 appears to have more deformation and ductile kind of behavior due to the reinforcement rebar welded at the bottom of the cast in channel (Figure 4-29). However, samples 2 and 4 had a less ductile behavior but with more displacement, as the failure were concentrated locally in the channel and lip itself (Figure 4-39, Figure 4-44, & Figure 4-60), while no anchorage failure was observed.

Figure 7-2: Diagonal Crack.

Diagonal crack (Figure 7-2) was observed in samples 1, 2, 3, 6, & 7; such crack appeared as a secondary effect. This could be due to the restraining from the concrete confinement that has resulted in a shear for on the edge of the channel causing an edge shear breakout. The above crack had a depth of 30 mm (Figure 7-3) and an angle of Tan-1 (30/50) = 31^{o}, where the 50 mm is the edge distance from the channel to the concrete sample.

Figure 7-3: 30 mm deep diagonal crack.

Sample 5 was made to get the bond capacity between the sides of the channel and the concrete.

The value of the bond stress is computed as follow:

Failure tension load = 11.5 kN (Figure 4-63)

Sides area = 2 (30x150) = 9,000 mm2 (Figure 4-24)

τ = 11,500 / 9,000 = 1.3 MPa.

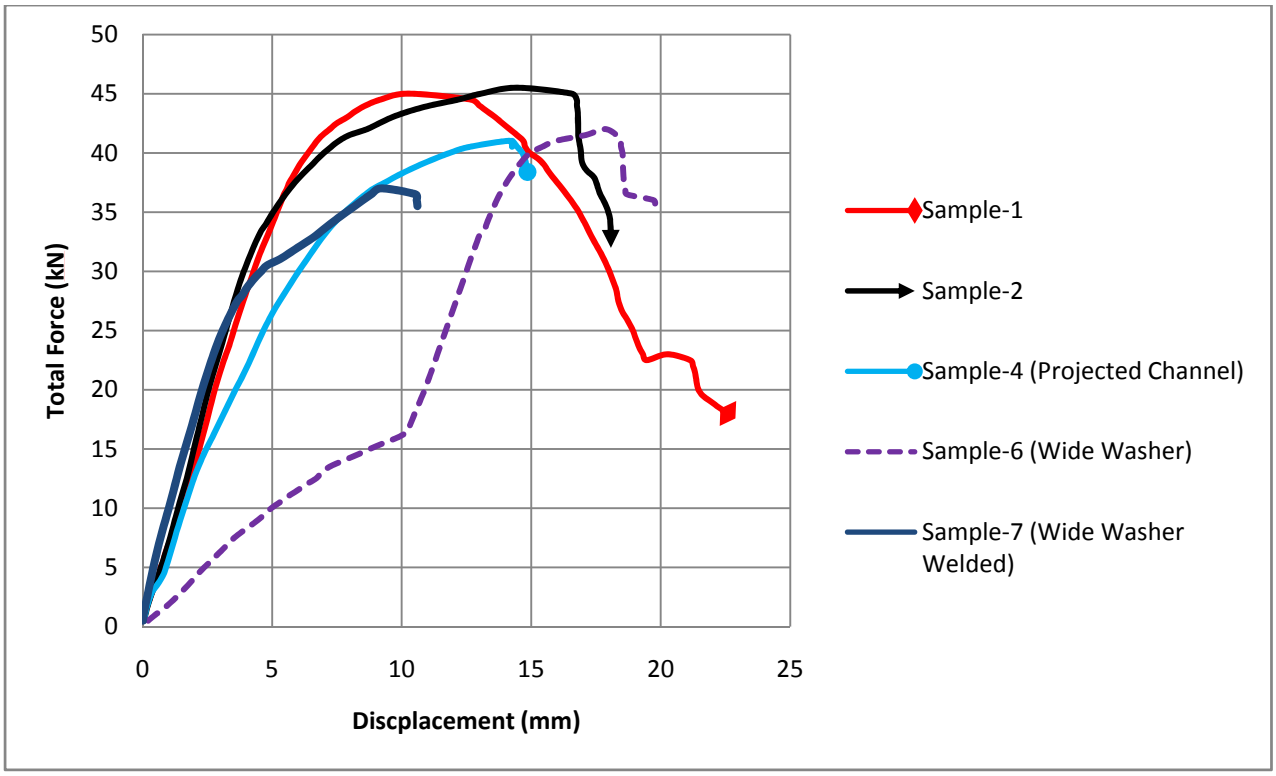

Figure 7-4: Force Vs Displacement curves for Sample 1, 2, 4, 6, & 7.

Figure 7-4 shows comparison of force vs displacement for the samples 1, 2, 4, 6, & 7.Samples 6 & 7 are the sample with stiffened washer. Although, the capacity is less than other samples but the maximum displacement of sample 7 is much less than the other samples, which shows an improvement in the channel behavior and during the experiment the whole sample start to get out of the concrete specimen did not happen in the previous samples.

The average capacity of the channel from above samples in Figure 7-4 is **41 kN.**

7.2 Mechanistic Model

Eight failure modes were calculated, and tabulated in Table 7-2:

Table 7-2: Summary table of the eight failures that have been computed.

Failure Type	Failure Value (kN)
1) Bolt	76.2
2) Bolt Head Bending	84.96
3) Channel Flexure	**34**
4) Channel Local Lip	**43.21**
5) Studs	76.97
6) Concrete Breakout (cone)	69.81
7) Concrete Pullout	211
8) Concrete side blowout	N/A

As can be seen from above table the minimum value was for that of channel flexure and the second minimum value is the local lip failure. Regarding the channel flexure failure, it was assumed that the channel is work as a simple support beam neglected concrete confinement around the channel that have an effect in increasing the channel capacity. Since, the channel tends first to de-bond from the surrounding concrete after that the channel is work as a simple supported beam. Therefore, such a failure needs further study to include the concrete contribution to the channel capacity.

The value of **43.21 kN** achieved from yield approach was very close to that of the experimental work.

7.3 Computational Model

Figure 6-9 shows the secondary effect that was exactly similar to that of the experimental work. In addition, the lip deformation in Figure 6-10 was similar to that of experimental work.

As for model SP-2, Figure 6-16 shows that the channel start to deform before the diagonal damage similar to that of the concrete breakout (cone) failure appeared.

Model SP-1 had a maximum load of **42 kN** (Figure 6-8) & model Sp-2 was **40 kN** (Figure 6-14).

7.4 Comparison between Experimental, Mechanistic, & Computational Model

In summary below figures show a comparison between the experimental and the FEM approach.

A comparison of the experimental and numerical results for load-deflection curve of the specimen is shown in Figures 7-5 and 7-8. The FE results displayed a good agreement with experimental ones. It can be seen that the difference between the finite element failure load of the specimen and experiment failure load is less than 5%. It can be observed from Figures 7-6, 7-7 and 7-9 that the failure modes of the specimen and the cracking pattern of concrete due to the uni-axial tension load in the experimental work and finite element analysis are almost similar.

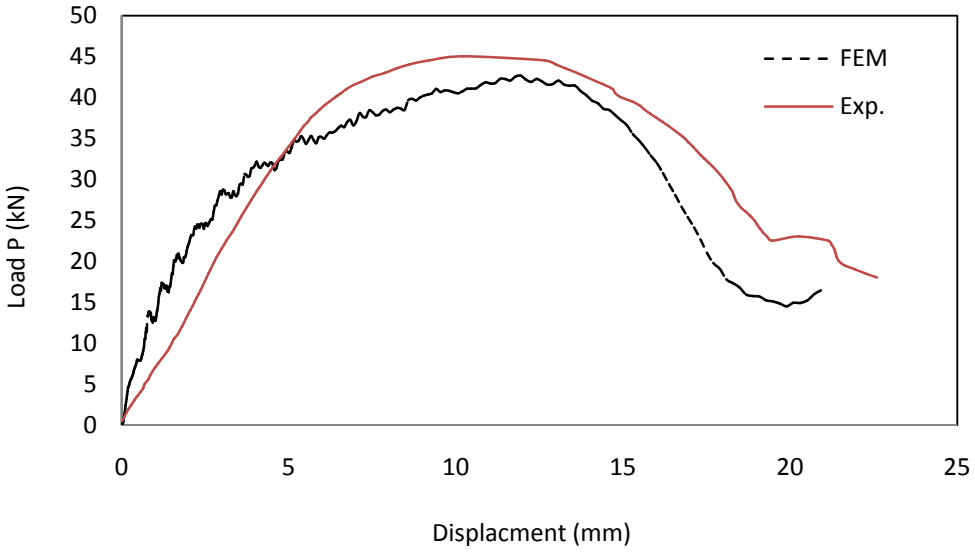

Figure 7-5: Sample 1 & Model SP-1 Force Vs Displacement diagram.

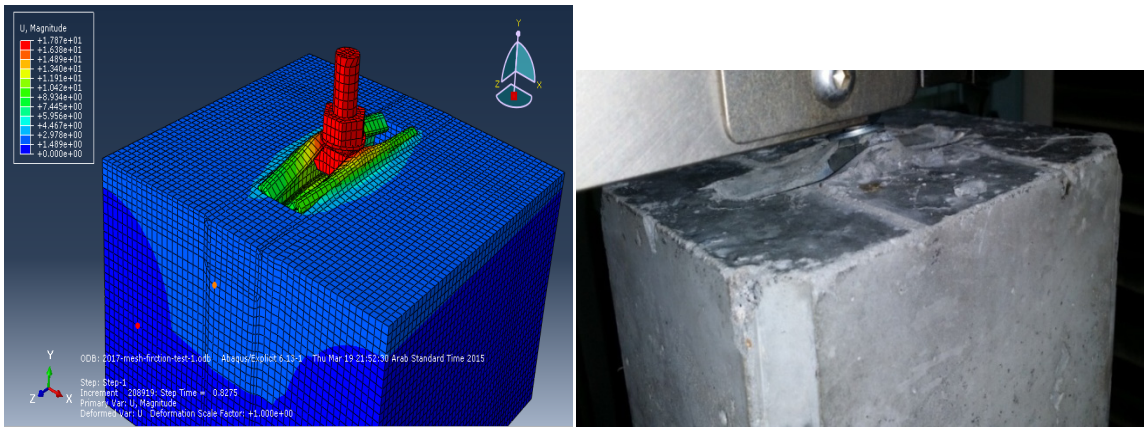

Figure 7-6: Local lip failure FEM SP-1 (left) & Sample 1 (right)

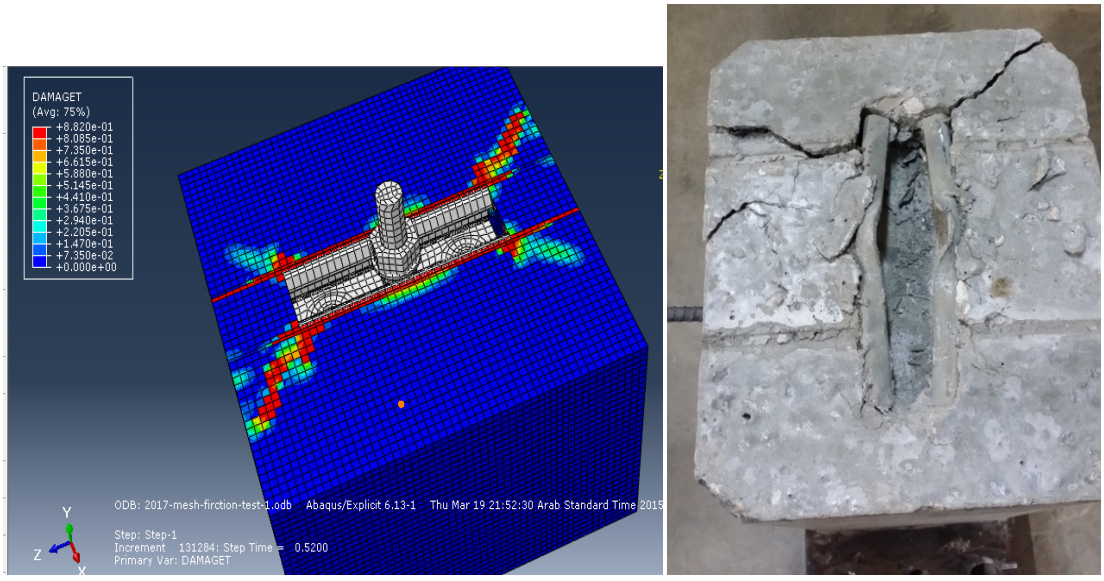

Figure 7-7: Diagonal crack due to secondary effect from FEM SP-1(left) and experiment (right).

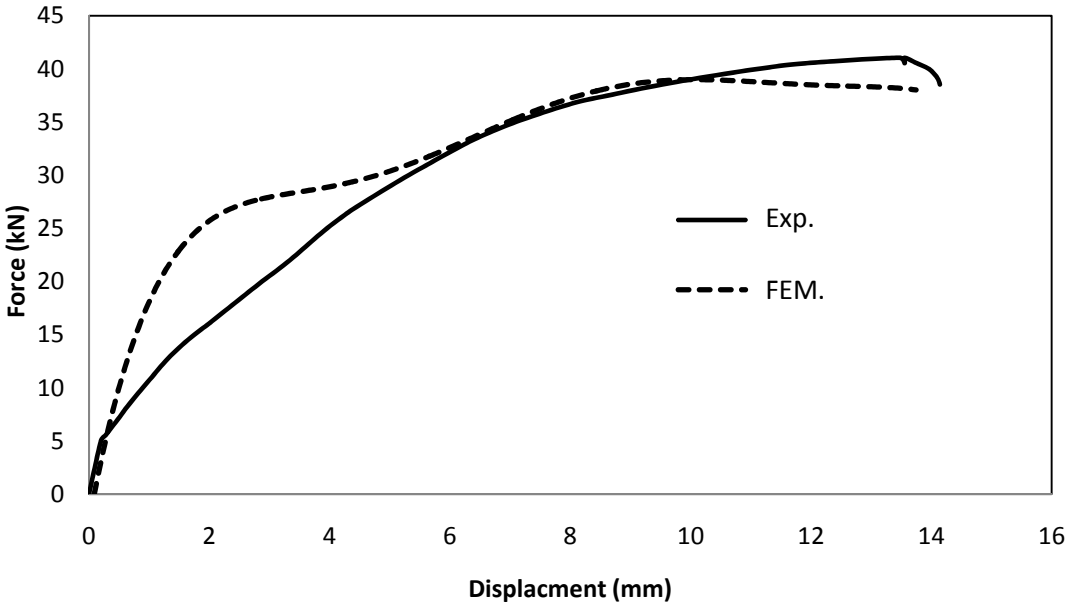

Figure 7-8: Force Vs displacement curves for sample4 & model SP-2

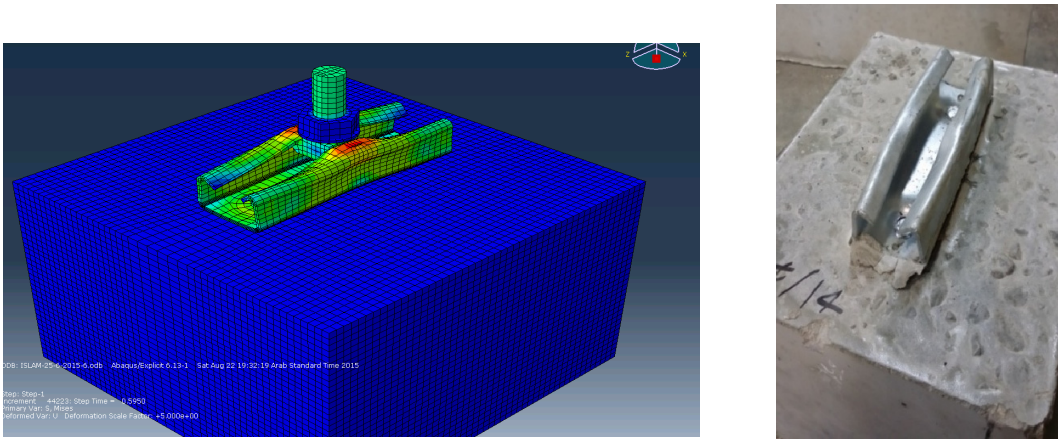

Figure 7-9: Channel plastic deformation FEM SP-2 (left) Sample 4 (right).

Table 7-3 shows a comparison between failure load of the average value of sample 1, 2, & 3, FEM model SP-1, and the local lip failure value from the analytical approach.

Table 7-3: Comparison table of the channel capacity between experiment, analytical, and computational model.

	Experiment	Analytical	FEM (ABAQUS)
Tension capacity (kN)	**41.6**	**43.21**	**42**

CHAPTER 8

CONCLUSION

8.1 Conclusion

In this research, the objective was to experimentally investigate the ultimate capacity of cast-in C-channel under uni-axial tension and compare its ultimate load capacity and failure mode with 3-D finite element model and by analytical approach. 7 samples were made to capture the different failure modes of the channel, and to see the effect of the confinement of the concrete on the channel capacity and behavior, as well as the effect of the studs to anchor the channel and how to strengthen such channels in an economical and simple way. Out of the seven samples, five samples were with the channel embedded in concrete, three of them had a failure in the channel itself and no anchorage failure observed. This indicated that the governing failure was always in the channel itself especially in the lip. This is due to low bearing area between the bolts head and the channel lip, which lead to high stress at this area. Therefore, the channel at lip needs to strengthen by increasing the thickness of the lip, increasing the material grade, increasing the hammer head dimension; all of the previous suggestion was not possible due to following reasons:

- Increasing the thickness would increase the cost of the channel and since the channel is cold formed, it required a specific machine to bend the plate, the machine had a certain capacity and could not bend more than 3 mm.

- Increasing the material grade was not possible due to the availability of the steel grades in the market and it is limited mainly to A36 (f_y = 248 N/mm^2 Vs f_y = 295 N/mm^2 of the channel)
- Increasing the head of the bolt will not make it possible to insert the bolt into the channel.

Therefore, the simplest way was to increase the area on the top of the channel by using a wider washer plate.

After testing sample #6, it was observed that due to bolt elongation, the washer was separated away from the channel. However, the curve had a different and better slope than other samples until the point that the washer went away from the channel. Therefore, another sample was made (sample #7) and the washer was tag welded to the channel, and this approach leaded that the lip did not deform and the failure was concentrated in other modes.

The other two different samples were made to study and try to capture the anchorage failure, one sample had the stud only embedded and another one had the channel embedded only without the studs, and there was a big difference in capacity in both samples as the stud had increase the channel capacity much more than the sample without stud.

A FEM was conducted using ABAQUS software and the output was compared to the experimental results, using such, approach simplifies the study of such channel and would save the time and resources of making a physical experiment. In addition, it will help in studying in details the channel and the techniques of improving the channels without making a physical sample.

From the experimental work and finite element simulation the following conclusion can be drawn:

- The channel local failure governed the capacity in the experimental work.
- Anchorage failure was not observed in the experimented samples.
- Local channel capacity was much less than concrete anchorage capacity.
- All samples with whole channel+stud embedded got secondary failure in concrete edge.
- Additional steel rebars parallel to the channel need to be added to prevent such diagonal crack due to the secondary effect as shown in (Figure 8-1)

Figure 8-1: Additional Steel parallel to channel to prevent the edge diagonal cracking.

- The wide plate increased the stiffness of the whole channel system, although the capacity value in tension did not increase but the displacement decreased.
- Damage-plasticity model for concrete developed by (Lubliner et al) and elasto plastic model for steel developed by Von Mises in ABAQUS is found to be acceptable in modeling the behavior of the cast-in C-channel embedded in the host concrete.
- The channel was modeled by using non-linear constitutive law.
- The proposed finite element modeling of C-channel embedded in the concrete was predicted the failure load with a reasonable accuracy and can therefore serve as an acceptable analytical tool for estimation of failure load as well as the failure modes, including cracking at the edges and related slip of channel with respect to concrete. Local yielding of C-channel lips was also predicted.
- Mechanistic model predicted eight failure modes, and the governing failure was the channel lip, although the lip capacity was very low compared to experimental and FEM. However, it can be used as design guide for such channels as a lower bound value indicating the first yielding value of the channel lip.
- The result of having the lip as the governing failure mechanism was similar to that of experimental work and FEM. A mechanistic model was made to study every failure modes separately and calculating the capacity

of each mode. It is found that the values are very close to both experimental work and FEM approach.

8.2 Recommendations for Future Works

This study was conducted for the channel under un-axial tension force. Therefore, it can be extended to study the channel under shear force and bending moment as the channel can be considered as a fixed support system.

Another area to be studied is the channel behavior under dynamic (cyclic) loading that can appear due to seismic forces, impact, or blast loading, or any other type of dynamic force that can act on a structure.

The sample was un-reinforced; therefore, another study could be made by reinforcing the sample and welding the washer plate.

The finite element modeling can be extended in the future to cover more key parameters and to be used to develop design guidelines of the cast-in C-channel systems.

References

[1] JORDHAL. [Online]. **http://www.jordahl-group.com/en/266/company/history/**

[2] ACI Committee 355, *ACI 355.1R-91 STATE-OF-THE-ART REPORT ON ANCHORAGE TO CONCRETE*.: ACI , 1991.

[3] European Committee for Standarization (CEN/TS 1992-4-3), *Design of Fastenings for use in Concrete - Part 4-3*.: CEN , 2009.

[4] ACI COMMITTEE 318, *BUILDING CODE REQUIRMENTS FOR STRUCTURAL CONCRETE AND COMMENTARY (ACI 318M-08)*. Farmington Hills: American Concrete Institute, 2008.

[5] *AISC*., 2005, vol. 13th Edition.

[6] Rolf Eligehausen, Werner Fuches Rainer Mallée, *Design of Fastenings for Use in Concrete - the CEN/TS 1992-4 Provisions*. Berlin , Germany: Ernst & Sohn, 2013.

[7] Rainer Mallée, John F. Silva Rolf Eligehausen, *Anchorage in Concrete Construction* , 1st ed. Berlin, Germany: Ernst & Sohn, 2006.

[8] Forschungs, "Tests with Anchor channels in non-cracked and cracked concrete," Stuttgart, 25-18547-2, 1995.

[9] Donald F. Meinheit Neal S. Anderson, "Pryout Capacity of Cast-In Headed Stud Anchors," *PCI Journal* , vol. 50 , no. 2 , March-April 2005.

[10] PCI industry Handbook Committee, *PCI DESIGN HANDBOOK* , 7th ed. Chicago, USA: PCI, 2010.

[11] Louay Abdel-Razek Aboul-Nour, FRACTURE AND PERMEABILITY CHARACTERISTICS OF THERMALLY DEGRADED CONCRETE, June 1988, M.S. Thesis.

[12] ASTM C470/C470M, *Standard Specification for Molds for Forming Concrete Test Cylinders Vertically*. USA: ASTM, 2003.

[13] Y. and Chen, J. Tao, "Concrete Damage Plasticity Model for Modeling FRP-to-Concrete Bond Behavior," *Journal of Composites for Construction*, vol. 19, no. 1, February 2015.

[14] R Wohlfahrt, "Behaviour of Anchor Channels without Supplementary Reinforcement ," Universitat Stuttgart , Stuttgart, Doctor Thesis 1996.

[15] Holger Falter A. Salam Al-Sabah, "Finite element lower bound “yield line” analysis of isotropic slabs using rotation-free elements," *Engineering Structures*, vol. 53, pp. 38-51, August 2013.

[16] Werner Wagner Jochen Wust, "Systematic prediction of yield-line configurations for arbitrary polygonal plates," *Engineering Structures*, vol. 30, no. 7, pp. 2081-2093, July 2008.

[17] T.H.G. Megson, *Structural and Stress Analysis*., 2005.

[18] Anas Mohammad Ibahim Al-Khatib, STUDY OF HIGH STRENGTH REINFORCED CONCRETE EXTERIOR BEAM-COLUMN JOINT UNDER CYCLIC LOADING, MAY 2015, MS Thesis.

[19] Wai-Fah Chen, *Plasticity in Reinforced Concrete*.: J.ROSS, 2007.

[20] Wan T.Tsai, "Uniaxial Compressional Stress-Strain Relation of Concrete," *Journal of Structural Engineering*, vol. 114, no. 9, pp. 2133-2136, September 1988.

[21] Darwin and D.A. Pecknold, "Analysis of RC Shear Panels under Cyclic Loading," *ASCE* , vol. 102, pp. 355-369, February 1976.

[22] V. Birtel and P. Mark, "Parameterised Finite Element Modelling," Institute for Reinforced and Prestressed Concrete Structures, Bochum, Germany, 2006.

[23] RUUKKI, "Standard Steel Grades, Coparison, Designations, and Codes,".

Vitae

Name	:	Islam Sayed AbouHamdah
Nationality	:	Egyptian
Date of Birth	:	7/2/1985
Email	:	islam.sayed.85@gmail.com
Address	:	Khobar, Saudi Arabia
Academic Background	:	**MS** in Civil Engineering, King Fahad University of Petroleum and Minerals, Dhahran, Saudi Arabia (2015) **BS** in Architectural Engineering, King Fahad University of Petroleum and Minerals, Dhahran, Saudi Arabia (2007)